

Abnormal Formation Pressures in the Navarin Basin, Bering Sea, Alaska

OCS Report
MMS 91-0034

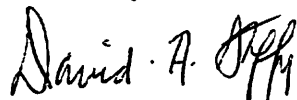


U.S. Department of the Interior
Minerals Management Service
Alaska OCS Region

Abnormal Formation Pressures in the Navarin Basin, Bering Sea, Alaska

OCS Report
MMS 91-0034

By David A. Steffy



Library of Congress Cataloging-in-Publication Data

Steffy, David A.

**Abnormal formation pressures in the Navarin basin, Bering Sea,
Alaska / by David A. Steffy.**

p. cm. -- (OCS report)

"MMS 91-0034."

1. Geology—Navarin basin. 2. Reservoir oil pressure—Navarin basin.

I. United States. Minerals Management Service. Alaska OCS Region.

II. Title. III. Series.

QE350.42.B45S74 1991

553.2'8'0916451—dc20

91-17777

CIP

Available from the National Technical Information Service, 5285 Port Royal Road,
Springfield, VA 22161, Order Number PB 91-172239.

*Any use of trade names is for descriptive purposes only and does not constitute
endorsement of these products by the Minerals Management Service.*

Contents

Abbreviations	vii
Abstract	1
Introduction	3
1. Location and Geologic Setting	7
2. Methods of Investigation	9
A. Direct Pressure Measurements	9
B. Indirect Pressure Measurements	9
(1) Shale Velocity	9
(2) Shale Conductivity	10
(3) Shale Bulk Density	10
(4) Drilling Exponent	11
3. ARCO COST No. 1 Well	13
4. Navarin Basin Exploratory Wells	17
A. Amoco Nicole No. 1 Well	17
B. Amoco George No. 1 Well	21
C. ARCO Packard No. 1 Well	24
D. Exxon Redwood No. 1 Well	29
E. Exxon Redwood No. 2 Well	33
F. Amoco Nancy No. 1 Well	36
G. Amoco Misha No. 1 Well	40
H. Amoco Danielle No. 1 Well	44
5. Compaction History	49
6. Pore Pressures and Present-Day Stress Directions and Magnitudes	53
7. Abnormal Pore Pressures and Shale Diapirism	57
8. Mechanisms of Abnormal-Pressure Production and Maintenance	59

A. Overpressure Zone 1	59
B. Overpressure Zone 2	63
Conclusions	71
References	73

List of Figures

1. Location of the Navarin basin, Bering Sea, Alaska	3
2. Location of the ARCO COST No. 1 well and the eight exploratory wells in the Navarin basin	5
3. Structure-contour map of a middle Eocene unconformity in the Navarin basin	8
4. Geologic time scale, lithology, wireline-log information, and pore pressures of the ARCO COST No. 1 well	14
5. Pore pressure based on estimates derived from shale velocity by using pressure evaluation curves published by McClure (1977) and pore pressure measured by RFT for the ARCO COST No. 1 well	16
6. Geologic time scale, lithology, wireline-log information, and pore pressures of the Amoco Nicole No. 1 well	18
7. Pore pressure based on estimates derived from shale velocity by using pressure evaluation curves published by McClure (1977) and pore pressure measured by RFT and DST for the Amoco Nicole No. 1 well	20
8. Geologic time scale, lithology, wireline-log information, and pore pressures of the Amoco George No. 1 well	22
9. Pore pressure based on estimates derived from shale velocity by using pressure evaluation curves published by McClure (1977) and pore pressure measured by RFT and DST for the Amoco George No. 1 well	24
10. Geologic time scale, lithology, wireline-log information, and pore pressures of the ARCO Packard No. 1 well	26
11. Pore pressure based on estimates derived from shale velocity by using pressure evaluation curves published by McClure (1977) and pore pressure measured by RFT for the ARCO Packard No. 1 well	28
12. Geologic time scale, lithology, wireline-log information, and pore pressures of the Exxon Redwood No. 1 well	30
13. Pore pressure based on estimates derived from shale velocity by using pressure evaluation curves published by McClure (1977) and pore pressure measured by RFT for the Exxon Redwood No. 1 well	32

14. Geologic time scale, lithology, wireline-log information, and pore pressures of the Exxon Redwood No. 2 well	34
15. Pore pressure based on estimates derived from shale velocity by using pressure evaluation curves published by McClure (1977) and pore pressure measured by RFT for the Exxon Redwood No. 2 well	36
16. Geologic time scale, lithology, wireline-log information, and pore pressures of the Amoco Nancy No. 1 well	38
17. Pore pressure based on estimates derived from shale velocity by using pressure evaluation curves published by McClure (1977) for the Amoco Nancy No. 1 well	40
18. Geologic time scale, lithology, wireline-log information, and pore pressures of the Amoco Misha No. 1 well	42
19. Pore pressure based on estimates derived from shale velocity by using pressure evaluation curves published by McClure (1977) and pore pressure measured by RFT for the Amoco Misha No. 1 well	44
20. Geologic time scale, lithology, wireline-log information, and pore pressures of the Amoco Danielle No. 1 well	46
21. Pore pressure based on estimates derived from shale velocity by using pressure evaluation curves published by McClure (1977) and pore pressure measured by RFT for the Amoco Danielle No. 1 well	48
22. Current stress pattern of the Navarin continental shelf	56
23. Seismic profile, free-air gravity profile, and filtered magnetics profile of a shale diapir	58
24. Scanning electron microscope photomicrograph of the diatom <i>Coscinodiscus marginatus</i> magnified 1,000 times	62
25. Geologic cross section of the Navarin basin depicting overpressure zones and stratigraphy	67
26. Graph showing relationship between depth to top of overpressure zone 2 and its vertical extent	70

List of Tables

1. COST and exploratory well characteristics	4
2. Characteristics of compaction trends	51
3. Results of stress analysis for each well	54
4. Characteristics of abnormal-pressure zone 1	60
5. Characteristics of abnormal-pressure zone 2	64

Abbreviations

Amoco	American Oil Company
ARCO	Atlantic-Richfield Company
B	bit diameter
BHC	borehole corrected (sonic log)
BOL	bottom of log
cm ³	cubic centimeters
COST	continental offshore stratigraphic test
°C	degrees Centigrade
°F	degrees Fahrenheit
d	drilling exponent
DST	drill stem test
d _{xc}	corrected drilling exponent
EMW	equivalent mud weight
Exlog	Exploration Logging of U.S.A., Inc.
FDC	formation density compensated
ft	feet
g	gram(s)
gal	gallon(s)
h'	excess head
hr	hour(s)
ILD	deep induction log
K	potassium
Kb	Kelly bushing
lb	pound(s)
LLD	laterolog deep
LSS	long-spaced sonic (log)
md	millidarcies
mhos	millimho(s)
μm	micrometer(s)
μs	microsecond(s)
N	rotary speed
N _x	normalized exponent
%	percent
p'	transient pore-water pressure
PEF	photoelectric factor
P _l	leak-off pressure
P _o	fluid pressure
ppg	pounds per gallon
psi	pounds per square inch
P _v	overburden pressure
R	penetration rate

RFT	repeat formation test
ρ	density
s	second(s)
σ_1	maximum principal stress
σ_2	intermediate principal stress
σ_3	minimum principal stress
SF	seafloor
S _{HMAX}	maximum horizontal compressive stress
S _{HMIN}	minimum horizontal compressive stress
SL	sea level
S _v	principal stress in vertical direction
TD	total depth
Th	thorium
TOL	top of log
W	weight on bit
USSR	Union of Soviet Socialist Republics

All depth measurements are given as feet below sea level.

Abstract

Two zones of abnormal formation pressure occur in eight exploratory wells and one COST well in the Navarin basin, Bering Sea, Alaska. The shallow zone (zone 1) ranges in depth from 1,264 to 2,415 ft below sea level and is commonly 1,500 ft thick; pressures range up to 14.5 ppg equivalent gradient, which is well above a normal pressure of 8.71 ppg. Wells drilled through zone 1 were typically underbalanced, but casing was set immediately below the bottom seal. In all nine wells, zone 1 appears to be stratigraphically controlled by the presence of late Miocene to late Pliocene microfossil-rich clays. Abnormal pore pressures here are attributed to water that was expressed from shrinking pores within a sequence of impermeable clays that restricted drainage. The bottom seal of zone 1 is attributed to dissolution of the abundant siliceous microfossils and subsequent reduced porosities. Zone 1 terminates upward at permeable late Pliocene sandy mudstones and sandstones, which gradually release the abnormal pore pressures.

In the deeper zone (zone 2), abnormal pressures range from 9 to 16 ppg and are believed to result from the combined effects of compaction disequilibrium, aquathermal pressuring, and the dehydration of smectites. The top of zone 1 ranges in depth from 4,469 to 11,239 ft below sea level; the upper seal occurs at various levels within the impermeable Oligocene claystone found throughout the basin. Where fully penetrated, the vertical extent of zone 2 increases with an increase in burial depth; however, the magnitude of overpressure does not necessarily increase. Zone 2 occurs at greater depths in wells situated within the strike-slip regime (the central Navarin wrench zone) than in wells within the surrounding normal-fault regime. In addition, the source layer for the pre-middle Miocene shale diapirs that occur in the northern flank of the Navarin basin appears to lie within zone 2.

Mud weights in the Navarin wells were considerably less (underbalanced) than those required to balance log-derived pore pressures in both zones 1 and 2. Incursion of formation fluids into the wellbore could have occurred had a highly permeable formation been encountered within either overpressure zone.

Introduction

The purpose of this study is to document the areawide presence of abnormally pressured shales in the Navarin basin (fig. 1), to characterize the appearance of these abnormal pressures on well logs, and to identify mechanisms responsible for the abnormal pressures. The ability to predict abnormally pressured shales in an exploration area will ensure safer drilling operations in the future. Prior knowledge enables the driller to: (1) set casing into the overpressured shale so that overlying, normally pressured strata are not exposed to highly weighted muds; (2) proceed with a lighter mud in the section above the overpressure zone to enhance drilling rates; and (3) anticipate mud weight requirements for drilling the abnormally pressured zone (Hottman and Johnson, 1965).

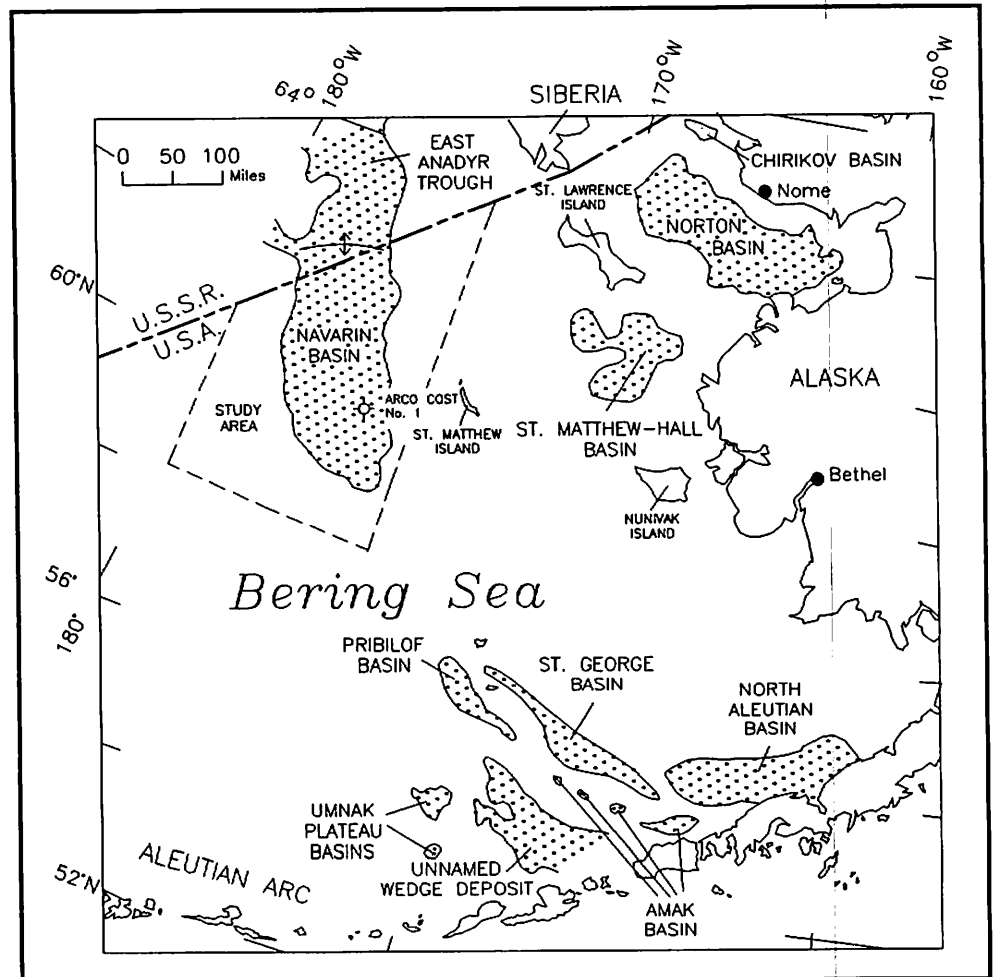


Figure 1. Location of the Navarin basin, Bering Sea, Alaska.

Abnormal formation pressure is the existence of fluid pressure in the rock pores that is in excess of normal hydrostatic pressure, where the normal pressure is the product of an average fluid density, a gravitational constant, and the vertical depth of a column of fluid below sea level. Abnormal formation pressure is also termed geopressure (Exlog, 1980) and surpressure (Fertl, 1976). The presence of abnormal formation pressure in the Navarin basin continental shelf area was first recognized at the ARCO COST No. 1 well and was documented by Sherwood (1984). Results from eight exploratory wells drilled in 1985 indicated that abnormal pressure is a ubiquitous problem in the Navarin basin area (fig. 2; table 1). The analytical techniques used to evaluate these exploratory wells closely follow the procedures used by Sherwood (1984) for the ARCO COST No. 1 well. However, the more spartan suite of geologic and geophysical data from the exploratory wells limited some avenues of investigation.

Table 1. COST and exploratory well characteristics.

Well Name and Operator	Location (degs.)		Water Depth (feet) Below Mean Sea Level	Total Depth (feet) Below Kb	Kb Elev. (feet) Above Sea Level	Corrected Geothermal Gradient (°F/100 feet)
	N. Lat.	W. Long.				
ARCO COST No. 1	60.18	176.27	432	16,400	85	1.78
AMOCO George No. 1	60.85	177.93	480	9,085	86	1.76*
ARCO Packard No. 1	60.37	178.27	541	13,741	86	1.36
EXXON Redwood No. 1	60.33	177.25	483	11,536	86	2.05
EXXON Redwood No. 2	60.40	177.12	481	11,570	86	2.05**
AMOCO Nancy No. 1	59.28	175.42	452	8,708	86	2.14
AMOCO Misha No. 1	59.82	178.48	473	7,962	86	1.25
AMOCO Danielle No. 1	60.78	176.48	393	10,045	86	2.24
AMOCO Nicole No. 1	59.58	175.42	443	11,030	85	2.15

*Estimated from geothermal map.

**Estimated from Redwood No. 1 well.

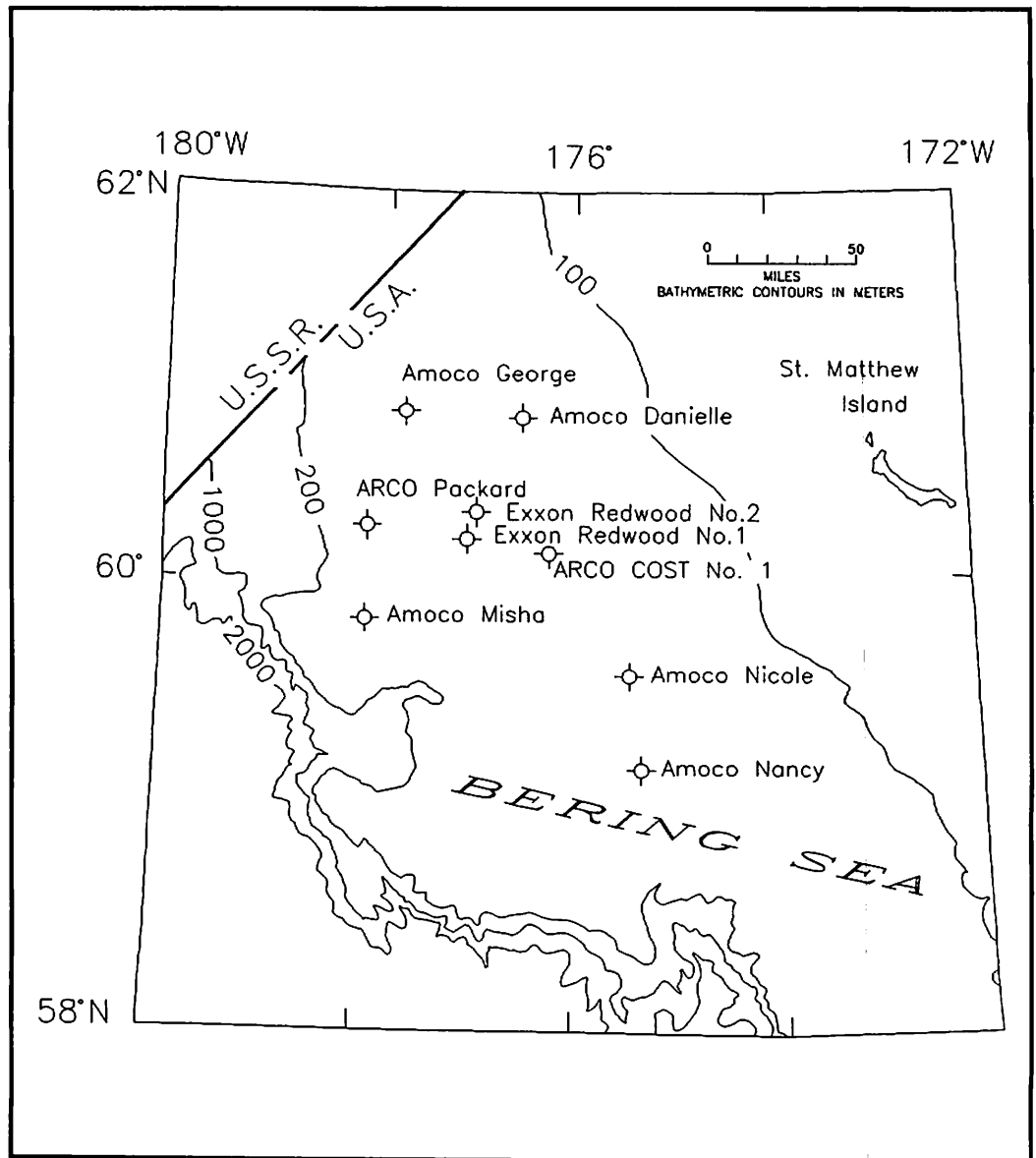


Figure 2. Location of the ARCO COST No. 1 well and the eight exploratory wells in the Navarin basin.

1 Location and Geologic Setting

The Bering Sea lies north of the Aleutian Arc, between western Alaska and the USSR (fig. 1). The northern Bering Sea includes a broad, shallow epicontinental shelf covering an area of approximately 275,000 square miles, where water depths range between 0 and 600 ft. The shelf has a gentle (1-degree) gradient toward the south, with a relatively monotonous, flat seafloor.

The Navarin basin, in the western Bering Sea, consists of three en echelon subbasins each filled with more than 34,000 ft of layered Tertiary sedimentary rocks. Basement rock consists of Early to Late Cretaceous nonmarine clastics and coals and marine clastics and tuffs, and local marine deposits of early Paleogene claystones. These rocks are overlain or interfingered with rocks of the Anadyr-Bristol volcanic belt, a discontinuous, narrow zone of Late Cretaceous to Eocene volcanics and continental rocks. The subbasins started to form in response to extensional subsidence that was associated with strike-slip motion or oblique subduction of the Kula Plate beneath the North American Plate in early to middle Eocene time and is marked by a regional unconformity (fig. 3). Basin axes trend northwestward, parallel to the modern continental shelf break. Fault-bounded ridges and compressional folds segregated the subbasins and isolated their depositional systems. The northwest-trending central Navarin wrench zone bisects the basin and was instrumental in the structural growth of the individual subbasins since the Late Cretaceous.

By late Eocene, movement of the Kula Plate was isolated by subduction along the Aleutian Arc. Subbasin subsidence, in response to structural downdropping, remained active until late Oligocene. Subsequent sedimentation and compaction remained basically uninterrupted until the middle Miocene, although several diastems are present. Basin paleobathymetry deepened rapidly from continental to middle bathyal between Paleocene and early Oligocene. The subbasins received continuous deposits of marine mudstones and siltstones throughout most of the Paleogene and early Neogene.

Cessation of Kula Plate motion by the early Neogene was followed by crustal cooling, which allowed regional subsidence of the shelf. Middle and outer neritic claystones, mudstones, and sandy

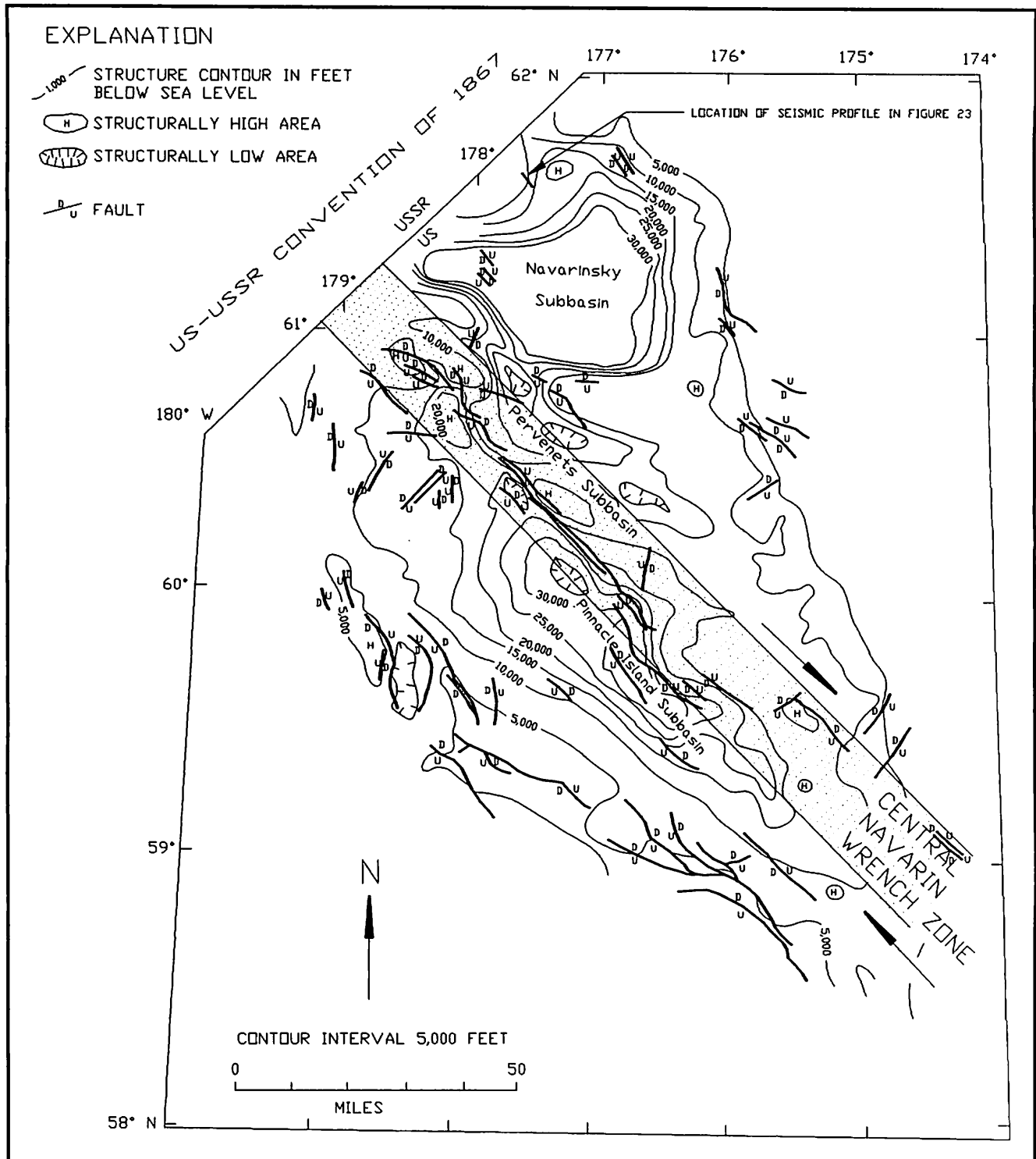


Figure 3. Structure-contour map of a middle Eocene unconformity in the Navarin basin (adapted from Turner and others, 1985).

mudstones were deposited throughout the Neogene. A significant sea-level lowering in the middle Miocene interrupted sedimentation and exposed most of the shelf to erosion and nondeposition. Subsequent sedimentation and deposition were uninterrupted until the Quaternary, when sea-level lowerings exposed a large portion of the Bering shelf and portions of the Navarin shelf to a subaerial environment and the deposition of periglacial material.

2 Methods of Investigation

Direct Pressure Measurements

Formation fluid pressure can be measured directly through conventional drill stem tests (DST's) or wireline devices such as the Schlumberger Repeat Formation Test (RFT). In only two wells were DST or RFT measurements taken within an abnormal-pressure zone.

Sherwood (1984) has calculated a pressure gradient of 8.71 ppg EMW (0.452 psi/ft) for the normally pressured section of the ARCO COST No. 1 well. His calculations utilized the direct pressure measurements taken between the depths of 1,743 and 10,163 ft. These measurements include one DST conducted through perforations over the interval from 6,193 to 6,213 ft and 17 RFT's distributed throughout the remaining part of well. For the present study, this estimate of the normal pressure gradient at the ARCO COST No. 1 well will be considered a standard for comparison in the entire Navarin basin area.

Indirect Pressure Measurements

In the absence of direct formation fluid pressure measurements, wireline well logs may be utilized to obtain an estimate of formation pore pressure. Physical attributes such as electrical resistivity, acoustic velocity, and bulk density of a formation as measured by wireline logs have been reported to progressively increase with depth (Hottman and Johnson, 1965). These changes in physical attributes are a result of tighter particle packing, interparticle bonding, and pore-occluding chemical cements. These processes also lead to decreases in porosity and pore fluid migration. Abnormal formation pressure exists where these processes are disrupted or reversed. Alteration of a formation's physical attributes in an abnormal-pressure zone is reflected in the deviation or reversal of the wireline log response from trends observed in the surrounding normally compacted sediments. This effect is most obvious in shales.

Hottman and Johnson (1965) empirically related the physical properties of overpressured shales to pore pressure. Shale evaluation curves for estimating the amount of overpressuring were published by McClure (1977) and are used in this report.

Shale Velocity

Sonic logs (LSS and BHC), in the opinion of Fertl (1976), are the best indirect source of quantitative information about pore pressure

because the logging device is largely unaffected by hole size, formation temperature, and formation water salinity. Sonic logs measure the travel time of a compression wave between a transmitter and a receiver, and are influenced by degree of compaction, porosity, fluid content, and lithology. Interval travel times (inverse of velocity) are measured in $\mu\text{s}/\text{ft}$.

As clays are buried, they compact and lose porosity with depth, and the measured travel times decrease. If interval travel times for normally compacted shales in a well are plotted with respect to depth on semilog paper, they are arranged on a sloping line which defines the normal compaction curve. If, however, subpressures or surpressures are present in a zone, then plotted travel times for this zone will deflect away from the normal compaction curve.

In this study, shale travel time data were plotted on semilog paper in the manner described above. Pressure evaluation curves published by McClure (1977) were then overlain and matched to the plotted data. Matching consisted of overlaying evaluation curves on data at a common travel time value ($100 \mu\text{s}/\text{ft}$), and then sliding the curves vertically along the $60 \mu\text{s}/\text{ft}$ value parallel to the depth axis until the curve for "normal" compaction (as defined by the 8.71-ppg curve) coincided with the deepest zone that appeared to follow a normal compaction trend. An estimated value of pore pressure was then interpolated for the individual shale velocity-depth pairs.

Shale Conductivity

Conductivity is derived by inverting resistivity. Formation resistivity is dependent upon the amount of water and its salinity, the presence of hydrocarbons, and the distribution of the fluids within the pores (Exlog, 1980). Deep induction logs, such as the Schlumberger ILD and LLD, are designed to be an accurate measure of true resistivity beyond the invaded zone in permeable rock. Resistivity values in normally compacted shales increase with depth. However, a porosity increase in the transition and overpressured zones is reflected by a decrease in resistivity (an increase in conductivity), provided that the pore water salinity has not changed significantly.

Pressure evaluation curves published by McClure (1977) are fitted to plotted resistivity data by sliding the pressure evaluation curves vertically along a 2,000-mmos line until the curve for normal compaction (defined by the 8.71-ppg curve) coincides with the deepest zone that appears to follow a normal pressure gradient.

Shale Bulk Density

Shale densities are obtained from a wireline log (FDC) involving a radioactive source that emits medium-energy gamma rays and a receiver that detects the amount of Compton back-scattering. The amount of back-scattering is directly related to formation electron density, which is in turn proportional to bulk density (Fertl, 1976). As the FDC measurements decrease, porosity increases, which could signify abnormal pressure. Shale density, in the opinion of Fertl

(1976), is the least reliable of the indirect measurements because of mineralogic variations and hole washouts. Because of the poor reliability, pressure evaluation was not performed on the bulk density data. However, trends indicated on the density-versus-depth graphs typically reflect trends found on the conductivity and travel time plots. This resemblance is considered a verification of the other data sources.

Drilling Exponent

The drilling exponent (d-exponent) relates drilling parameters and hole conditions to fluid pressures in the formation. Jordan and Shirley (1966) calculate a normalized rate of penetration (d) that is directly proportional to the rate of penetration in ft/hr (R), diameter of bit in inches (B), weight on bit in pounds (W), and rotary speed in rpm (N):

$$d = \log (R/60N) / \log (12W/10^6B)$$

Generally, d values progressively increase with depth; however, in transitional and overpressure zones, the d values decline because R increases while the other terms remain constant (Fertl, 1976).

Rate of penetration increases (or d declines) in overpressure zones because drilling is aided by greater differential pressure between drilled formation and mud column. Differential pressure is dependent upon mud density; therefore, a corrected d-exponent (d_{xc}) that compensates for changes in mud density is usually calculated.

Exploration Logging of U.S.A., Inc. (Exlog), calculated all of the d-exponent data presented in this paper. Their procedure is to calculate the corrected drilling exponent as soon as drilling starts and to iteratively calculate a new number every 5 to 10 ft. Exlog (1980) estimates the formation pressure from refined d_{xc} values which they term " N_x " (normalized exponent). N_x values compensate for the nonlinear relationship between rate of penetration, tooth efficiency, and rotary speed, which makes N_x values more responsive than d_{xc} to lithologic or pore pressure changes. Drilling-exponent data from Exlog were available for the ARCO COST No. 1 well and for all the exploration wells except the Exxon Redwood Nos. 1 and 2. No d-exponent calculations of any kind were available at the Redwood wells.

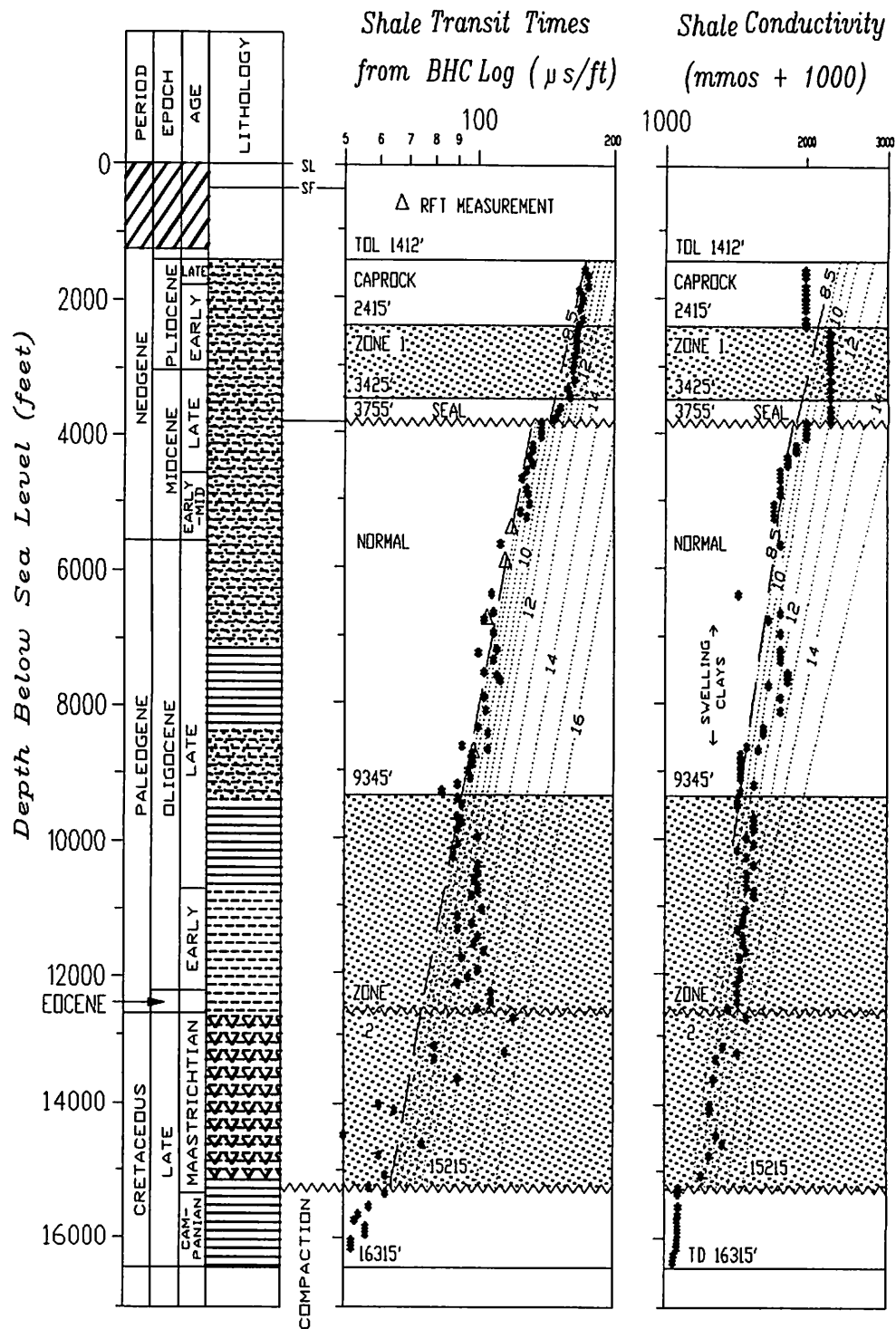
3 ARCO COST No. 1 Well

The ARCO COST No. 1 well, completed in October 1983, was drilled through a thick sequence of relatively flat-lying, undeformed Tertiary marine strata. These strata overlie a Late Cretaceous basement of deep-water marine and nonmarine rocks that form the gentle eastern flank of the Pervenets subbasin (figs. 2 and 3). Sherwood (1984) recognized two zones of overpressuring.

Sherwood (1984) placed the upper zone between 2,415 and 3,755 ft below sea level. This zone occurs within a late Miocene and early Pliocene sequence of poorly consolidated and poorly sorted diatomaceous sandy mudstone and sandy diatomaceous ooze. On the basis of wholesale destruction of siliceous fossils, Sherwood (1984) attributes the shallow zone of overpressuring to collapse of the structural framework of diatomaceous rocks as a consequence of silica dissolution. Potential contribution of excess pore fluids from mechanical compaction of clays or opal dissolution is also recognized. Sherwood's (1984) observations on mechanical dewatering are similar to Burst's (1969) descriptions for the Gulf of Mexico. Isaacs and others (1983) and Hein and others (1978) documented analogous silica diagenesis and an associated porosity reduction in diatomaceous sediments.

For this study, individual compaction trends are evaluated separately for formation pressures, requiring re-definition of "normal" trends within each compaction sequence. Discriminating the compaction history for a basin will provide a more accurate evaluation of the pore-pressure plot (Foster, 1990). Compaction trends are identified for each well based on log responses. Three compaction trends (upper, middle, lower) are correlated to lithostratigraphic breaks in the Navarin basin (a more complete discussion of these trends is given in the Compaction History section).

When the ARCO COST No. 1 well is reinterpreted assuming a multiple compaction history, a slightly different location is obtained for zone 1 (fig. 4). In this reinterpretation, the upper compaction trend is defined to extend from the surface down to 3,755 ft below sea level. Overpressure zone 1 is reinterpreted to be present from 2,415 to 3,425 ft (fig. 5). The overlying seal extends from the top of log (TOL) at 1,412 ft to a depth of 2,415 ft. Based on the pressure plot (fig. 5), a bottom seal resulting from collapse of the silica

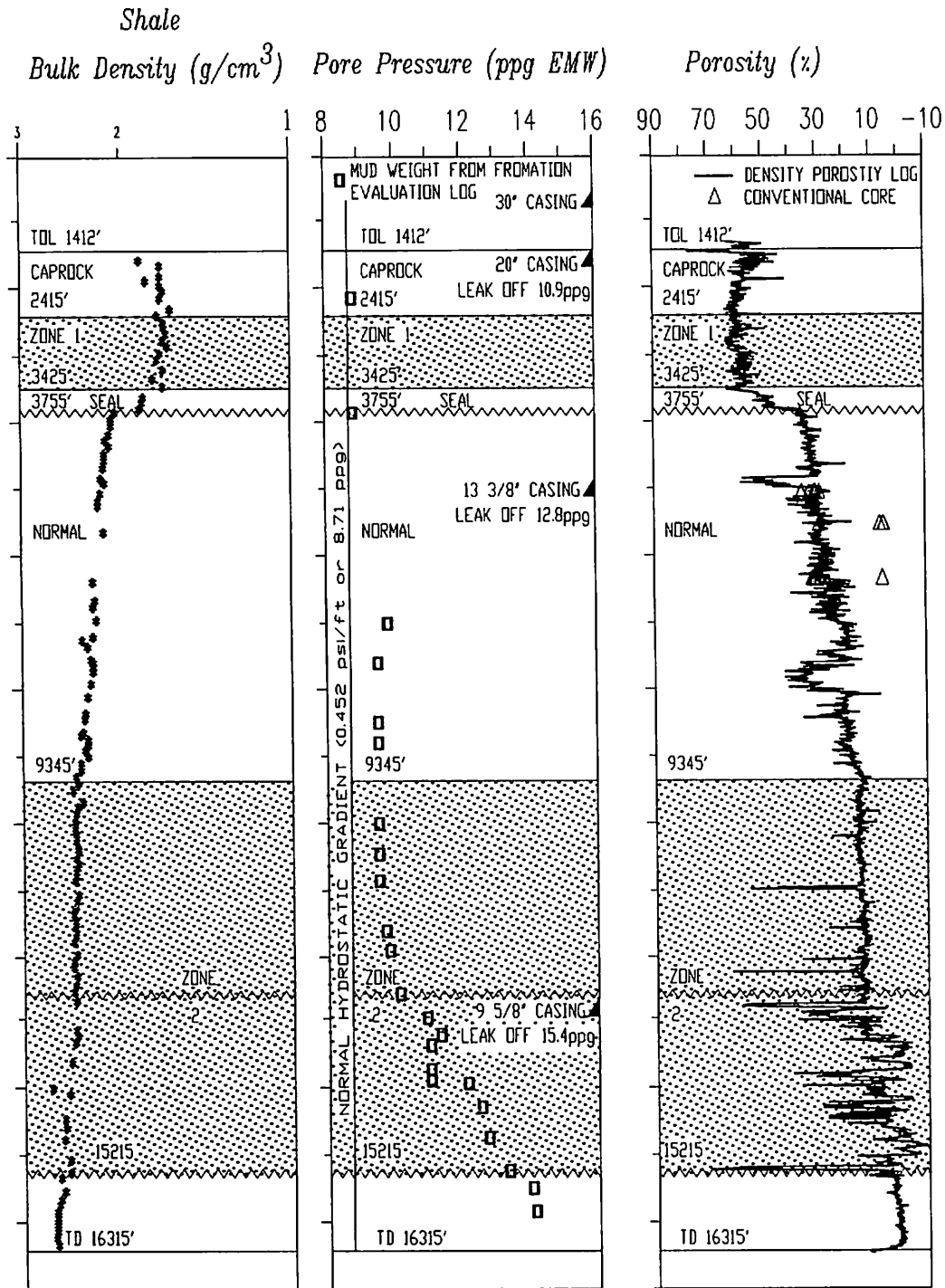


85 feet from Kb to mean sea level. Water depth is 432 feet.

Figure 4. Geologic time scale, lithology, wireline-log information, and pore pressures of the ARCO COST No. 1 well.

framework and having decreasing pore pressure with depth extends from 3,425 to 3,755 ft.

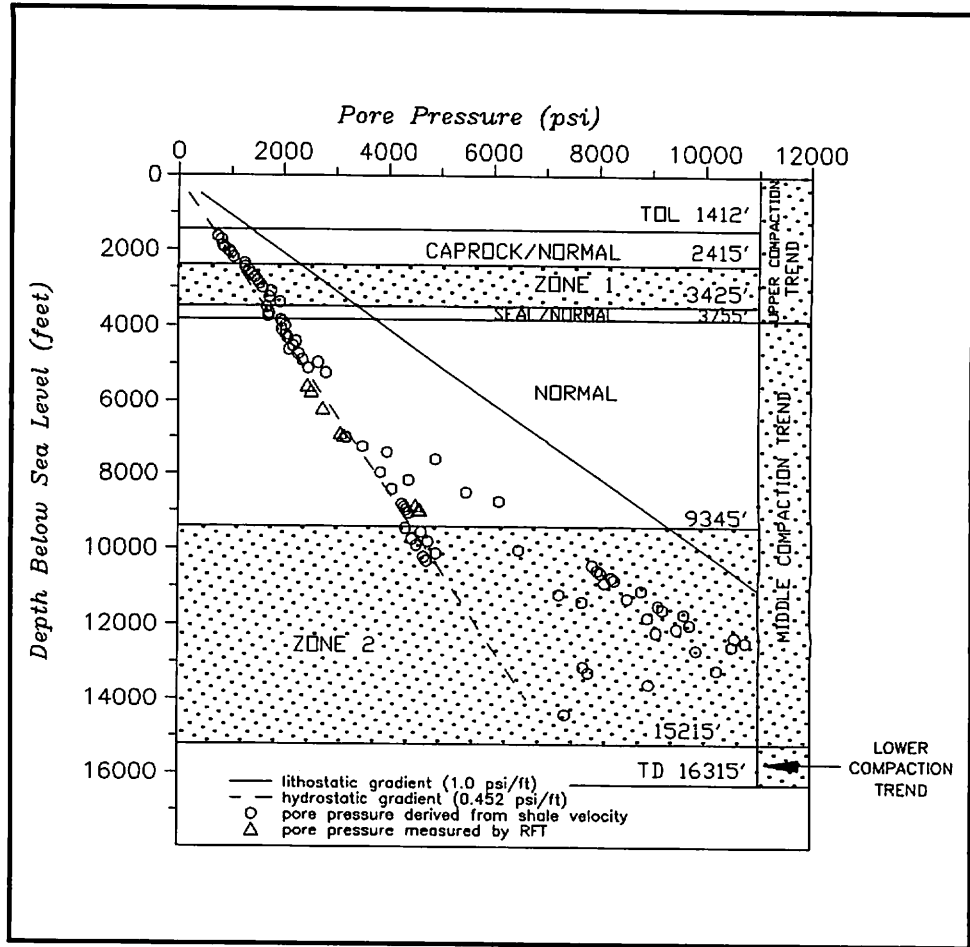
This upper zone (zone 1) has pore pressures that range from 9.0 to 10.7 ppg EMW (0.463 to 0.550 psi/ft) and average 10.0 ppg EMW (0.514 psi/ft), as estimated by shale travel times (fig. 4).



This is higher than the normal pressure gradient of 8.71 ppg EMW (0.452 psi/ft) (Sherwood, 1984).

In both Sherwood (1984) and the present study, the lower zone is placed between 9,345 and 15,215 ft. This zone, which lies within the middle compaction trend, encompasses a complex sequence of late Oligocene marine claystone containing diagenetically altered clays

Figure 5. Pore pressure based on estimates derived from shale velocity by using pressure evaluation curves published by McClure (1977) and pore pressure measured by RFT for the ARCO COST No. 1 well.



(9,345 to 10,715 ft); late to early Oligocene slightly silty marine claystone (10,715 to 12,195 ft); late to middle Eocene marine organic-rich claystone with local limestone (12,195 to 12,695 ft); and Maastrichtian marine fine-grained sandstone, siltstone, mudstone, and coal (12,695 to 15,215 ft). Sherwood (1984) attributes the occurrence of this deeper zone of abnormal pressure to thermochemically controlled structural dewatering of clays. The chief evidence for a relationship between clay diagenesis and overpressure at the ARCO COST No. 1 well is the abrupt loss of smectite between 9,600 and 10,000 ft (Sherwood, 1984, plate 3, diagram F). The principle behind this mechanism is that structural water is expelled during phase transformation of clays (smectites to illites). The expelled water requires 40 to 50 percent more volume in its free state than in structural sites in smectites (Powers, 1967). The expulsion typically occurs over a temperature range of 200 to 300 °F and is associated with an increase in shale bulk density (Burst, 1969).

This lower zone (zone 2) has pore pressures that range from 9.0 to 16.0 ppg EMW (0.463 to 0.822 psi/ft), as estimated by shale travel times (fig. 4). This is higher than the normal pressure gradient of 8.71 ppg EMW (0.452 psi/ft) (Sherwood, 1984).

4 Navarin Basin Exploratory Wells

Amoco Nicole No. 1 Well

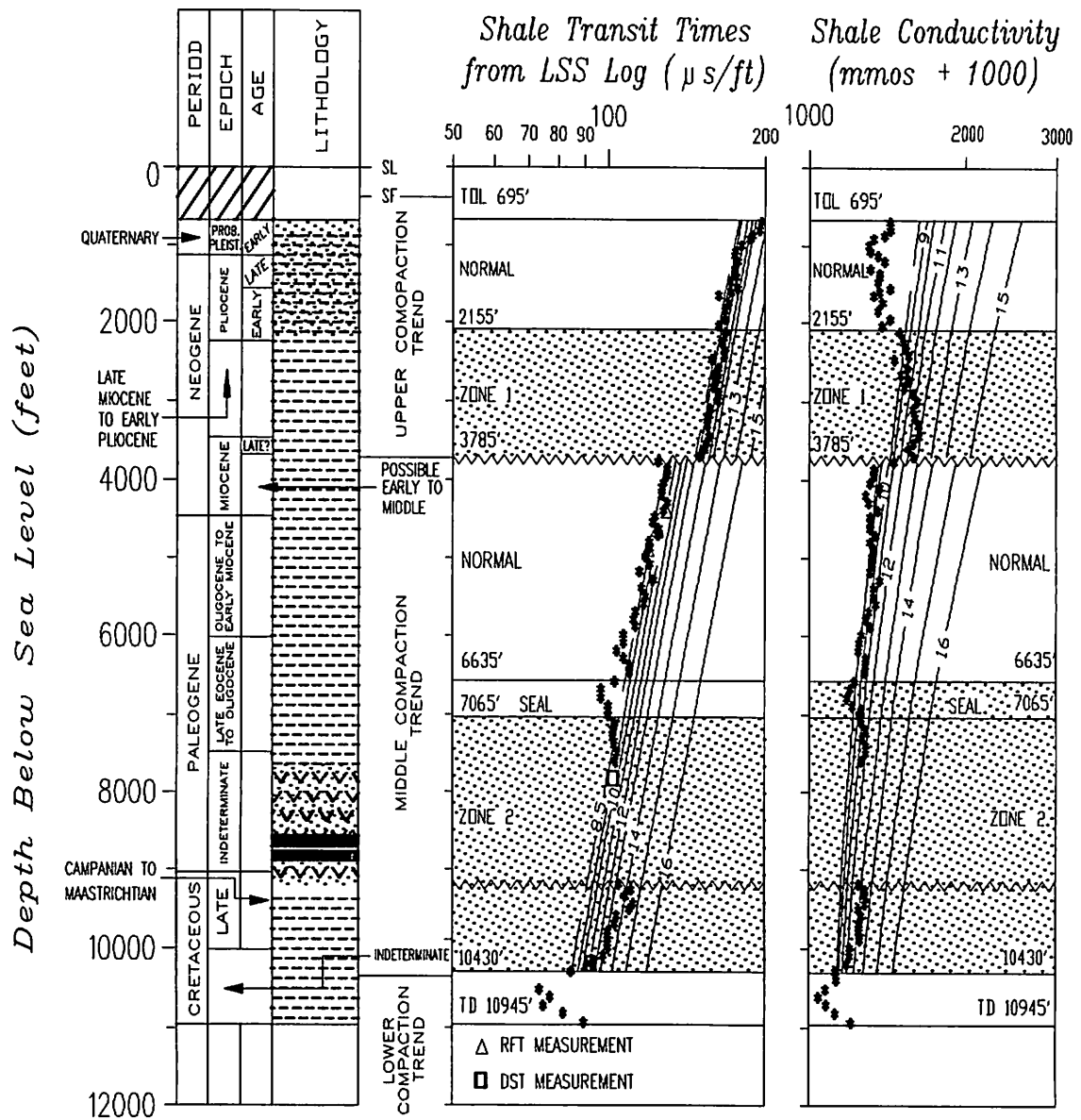
The Amoco Nicole No. 1 well was drilled approximately 50 miles southeast of the ARCO COST No. 1 well (fig. 2). The Nicole well is situated on an isolated basement high that occurs on the gentle southeast flank of the Pinnacle Island subbasin. Tertiary wrench faulting uplifted the basement high and folded the overlying layered marine Tertiary strata.

Two discrete abnormal-pressure zones are present: zone 1 extends from 2,155 to 3,785 ft; zone 2, from 7,065 to 10,430 ft. Zone 1 is best defined in conductivity and density data; zone 2 is most clearly recognized in velocity data (fig. 6). Data between 7,655 and 9,175 ft were not evaluated because the lithology consists of nonmarine volcanic sandstones and siltstones.

Zone 1 occurs in flat-lying marine strata consisting of sandy claystones and siltstones of early Pliocene to late Miocene age. Core Laboratories, Inc. (1985a), performed scanning electron microscope analysis on sidewall cores from the zone (3,475 and 3,691 ft below sea level), and found radiolarian-rich, silty shales, with abundant microporosity in preserved radiolarian tests. The bottom of zone 1 is a sharp break on the wireline data (fig. 6). Shale bulk density within zone 1 typically ranges from 1.59 to 1.72 g/cm³. The bulk density data immediately below 3,785 ft range from 1.95 to 2.01 g/cm³ and fall on or near a normal compaction trend down to a depth of 10,365 ft.

Zone 1 pore pressures range from 8.5 to 11.0 ppg EMW (0.437 to 0.565 psi/ft) and average 10.6 ppg EMW (0.545 psi/ft), as estimated from shale travel times (fig. 6). This is higher than the normal pressure gradient of 8.71 ppg EMW (0.452 psi/ft) (Sherwood, 1984), and higher than the pressure gradient of 8.86 ppg EMW (0.455 psi/ft) measured by the RFT and confirmed by the DST in the normally pressured section below zone 1 (fig. 7).

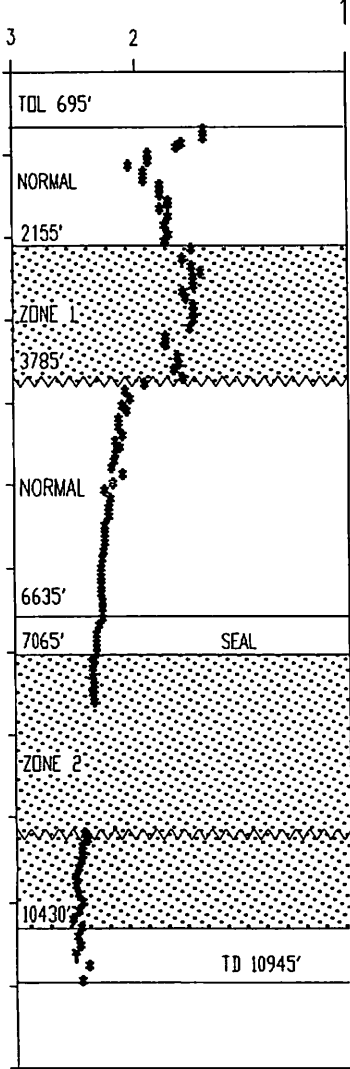
Overpressure zone 1 is overlain by a more permeable section. The presence of the permeable section is most apparent in the conductivity data (fig. 6). The shale travel time data, however, do not indicate the presence of sands (low travel time/high velocity) (fig. 6). The Exlog Formation Evaluation log describes cuttings from this section of strata as being dominated by white-gray, consolidated



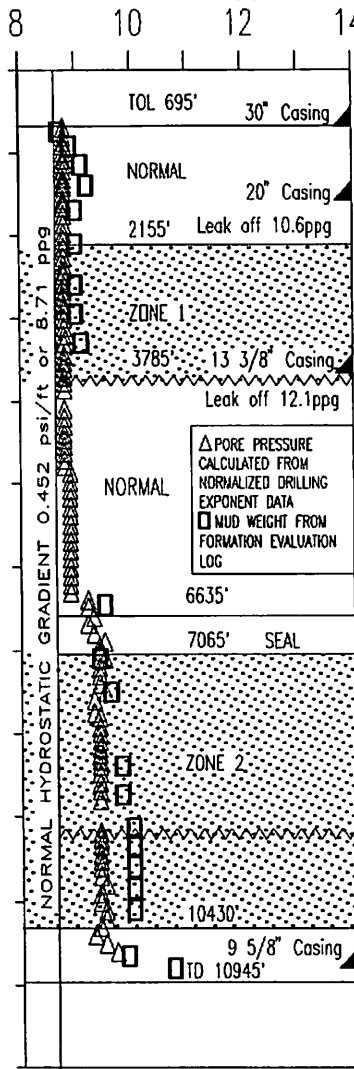
85 feet from Kb to mean sea level. Water depth is 443 feet.

Figure 6. Geologic time scale, lithology, wireline-log information, and pore pressures of the Amoco Nicole No. 1 well.

Shale
Bulk Density (g/cm^3)



Pore Pressure (ppg EMW)



Porosity (%)

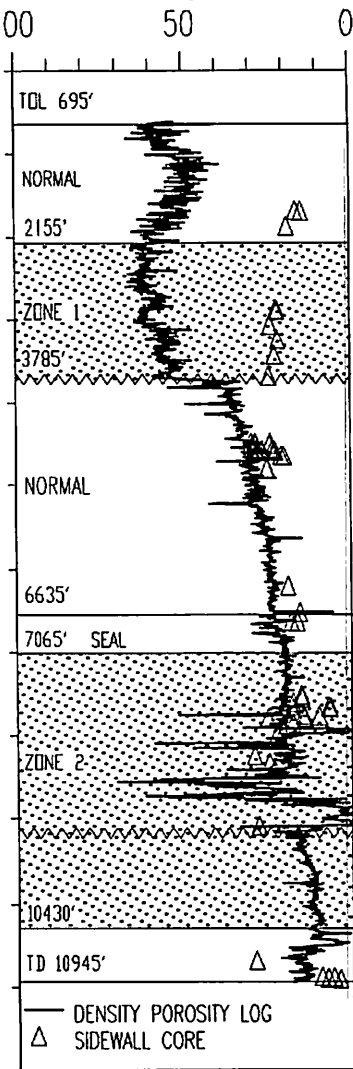
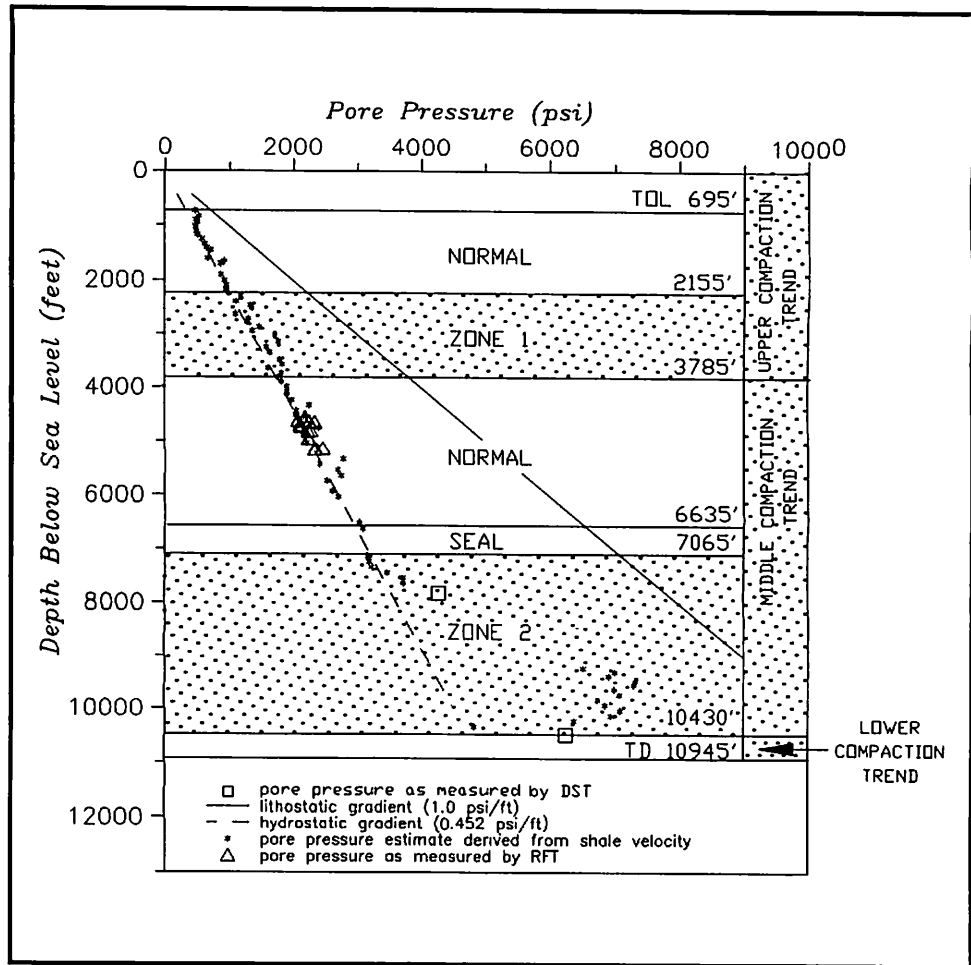


Figure 7. Pore pressure based on estimates derived from shale velocity by using pressure evaluation curves published by McClure (1977) and pore pressure measured by RFT and DST for the Amoco Nicole No. 1 well.



to slightly firm sandstone with subrounded to subangular grains and a clay matrix that contains traces of volcanics, pyrite, and shell fragments. This early Pliocene sandstone is interbedded with an amorphous, sandy, gray-green claystone that is moderately to very sticky.

Zone 2 (7,065 to 10,430 ft) encompasses a 640-foot section of flat-lying, possible late Eocene to Oligocene bathyal siltstones; a 1,470-foot section of nonmarine, fine-grained, volcanic-rich sandstone; and a 1,255-foot section of Cretaceous bathyal shales. Unlike zone 1, zone 2 has no distinct bulk density contrast with the strata above and below. The top of zone 2 is tentatively placed at 7,065 ft, based on a small gradual deviation to the right from the 8.71-ppg McClure curve by shale travel time and conductivity data (fig. 6). The overpressuring apparently continues through the nonmarine volcanic, coal, and clastic sequence between the depths of 7,655 and 9,175 ft, based on a DST measurement at 7,775 ft of 10.8 ppg EMW (0.555 psi/ft) (fig. 6). Zone 2 continues into the Cretaceous marine sequence below 9,175 ft and extends to 10,430 ft. Within the Cretaceous sequence, pore pressure as estimated by shale travel time data ranges from 12 to 14.9 ppg EMW (0.617 to 0.766 psi/ft). This overpressuring is confirmed by a DST measurement at 10,430 ft of 11.8 ppg EMW (0.607 psi/ft) (fig. 7).

Elevated pore pressures in zone 2 were also calculated by Exlog (1985a) using the normalized drilling exponent (fig. 6). Elevated pressures above 9 ppg EMW (0.462 psi/ft) were calculated starting at a depth of 6,405 ft and continuing to 10,615 ft, where a maximum drilling-exponent value of 9.8 ppg EMW (0.504 psi/ft) was calculated.

Amoco George No. 1 Well

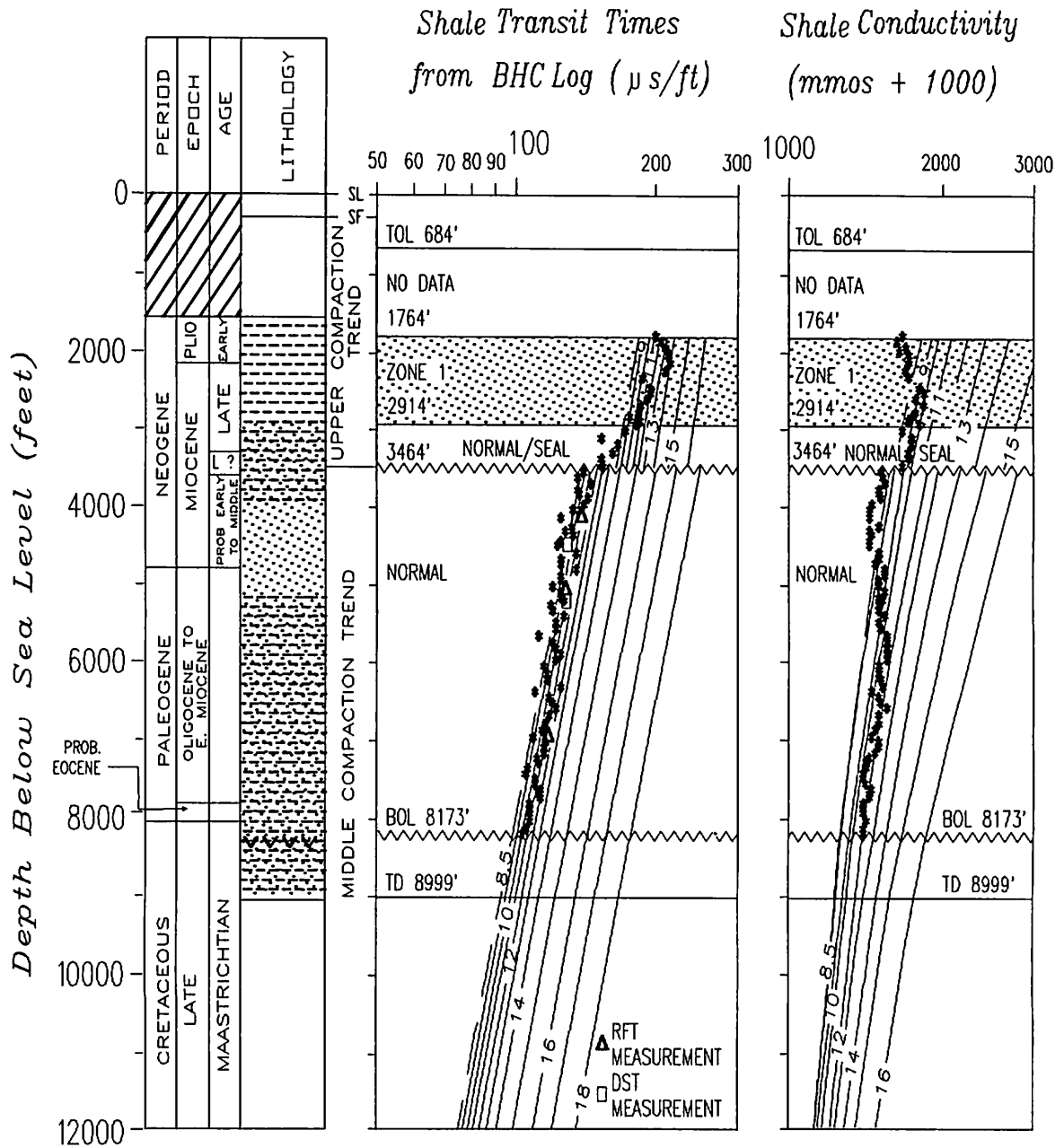
The Amoco George No. 1 well was drilled approximately 80 miles northwest of the ARCO COST No. 1 well (fig. 2). The George well is situated on an isolated basement high that trends northwestward and separates the Pinnacle Island subbasin from the Navarinsky subbasin (fig. 3). Tertiary wrench faulting uplifted the basement high and folded the overlying marine Tertiary strata.

One abnormal-pressure zone is present (fig. 8). Zone 1 extends from the top of log (TOL) at 1,764 ft to a depth of 2,914 ft, as suggested by shale transit time data. The conductivity data indicate that a lithologic change is present between 1,764 and 2,304 ft.

Data between 8,173 ft and TD at 8,999 ft were not evaluated because the lithology consisted of nonmarine volcanic sandstones and Cretaceous basement rocks. Zone 1 occurs in flat-lying marine sandstone, sandy siltstone, and claystone with sparse volcanoclastics of early Pliocene to late Miocene age. Zone 1 occurs within the upper compaction trend, the base of which is a sharp break on wireline logs (table 2, fig. 8). Shale bulk density within zone 1 ranges from 1.55 to 1.85 g/cm³ (fig. 8). The bulk density between 3,464 and 8,173 ft ranges from 1.98 to 2.42 g/cm³.

Zone 1 pressures range from 9.0 to 14.5 ppg EMW (0.463 to 0.745 psi/ft) and average 12.0 ppg EMW (0.617 psi/ft), as estimated by the shale transit times (fig. 8). This is higher than the normal pressure gradient of 8.71 ppg EMW (0.452 psi/ft) (Sherwood, 1984), and higher than the pressure gradient of 10.5 ppg EMW (0.540 psi/ft) measured by the RFT and confirmed by the DST between 4,210 and 6,822 ft in the normally pressured section (fig. 9).

The presence of low conductivity values above 2,304 ft may be due to lithologic changes, such as greater sand content. Cuttings above 2,304 ft were described as being dominated by green-brown-gray, very hard volcanoclastics with compound conchoidal fracturing (Exlog, 1985b). Lithic fragments, calcareous veins, and quartz inclusions were present. These early Pliocene volcanoclastics were interbedded with cream-buff, hard to soft, conchoidally fractured limestone. These limestone layers were typically less than 10 ft thick and were widely spaced. In addition, there were clear to frosted, medium-grained sandstones; gray-green, soft to firm siltstones; and dark green-gray, sticky claystones.



86 feet from Kb to mean sea level. Water depth is 480 feet.

Figure 8. Geologic time scale, lithology, wireline-log information, and pore pressures of the Amoco George No. 1 well.

Shale

Bulk Density (g/cm^3)

Pore Pressure (ppg EMW)

Porosity (%)

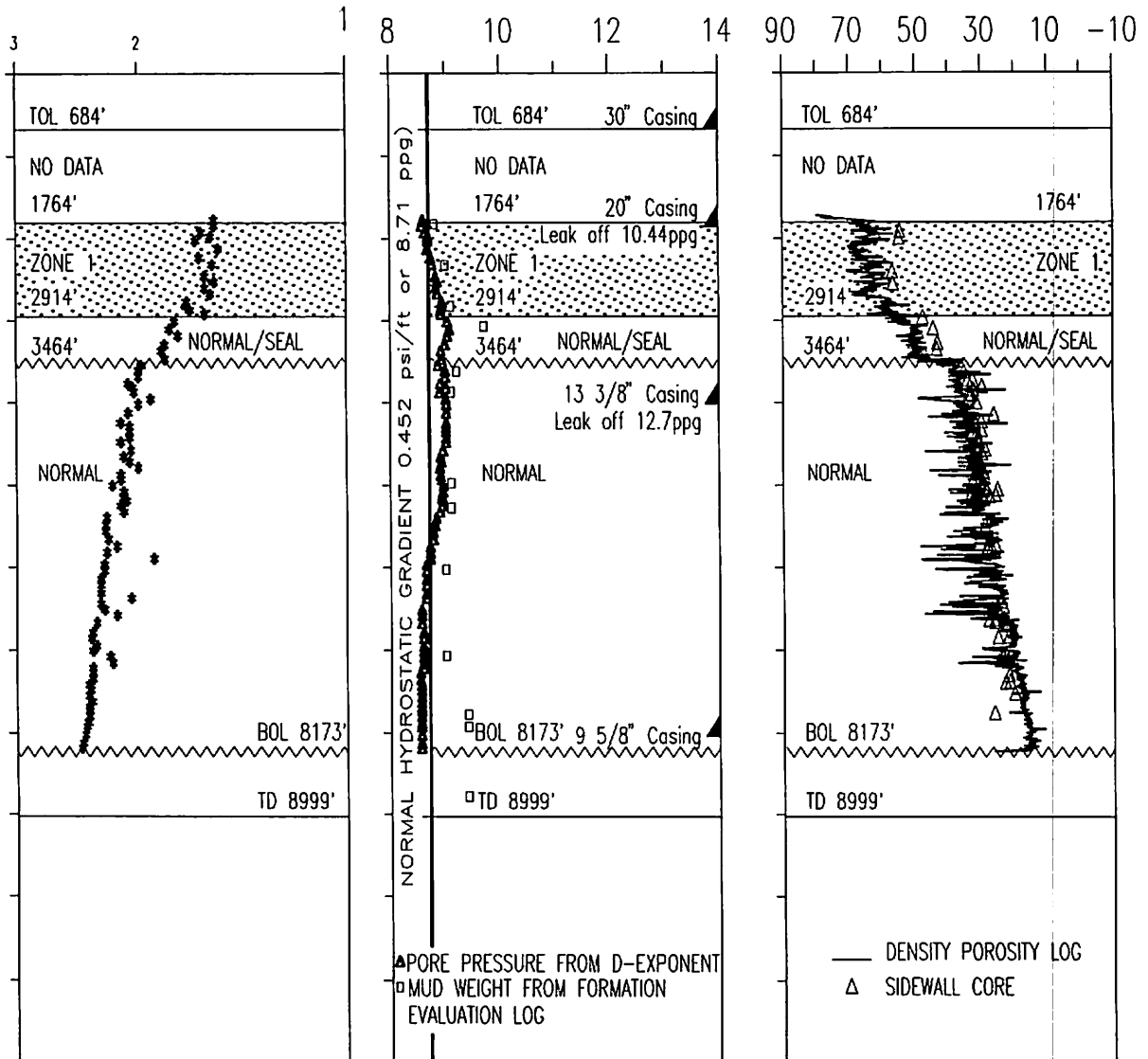
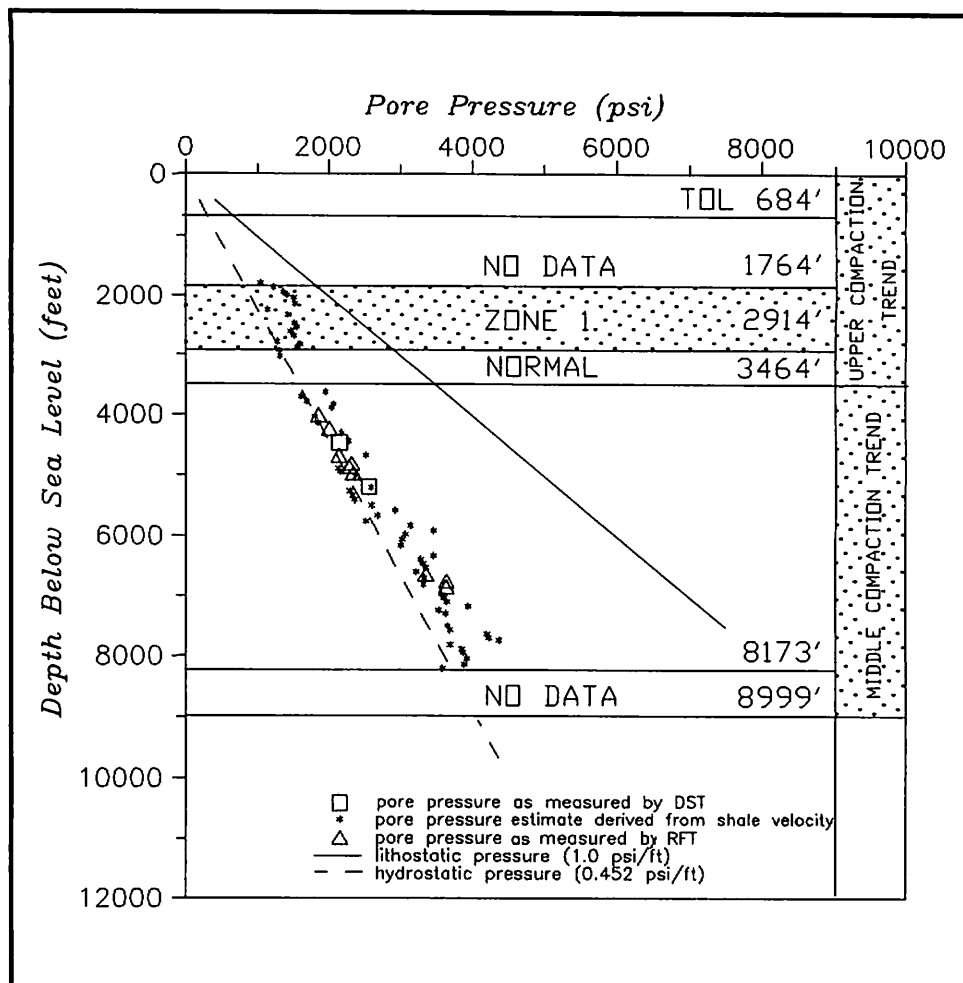


Figure 9. Pore pressure based on estimates derived from shale velocity by using pressure evaluation curves published by McClure (1977) and pore pressure measured by RFT and DST for the Amoco George No. 1 well.



In the overpressure zone, mud weights in the drilling column, as reported by the Exlog Formation Evaluation log, range up to 9.7 ppg (fig. 8) and were consistently less than the pore pressures estimated by shale travel times (fig. 9). The well from 1,764 to 2,915 ft was evidently drilled in an underbalanced condition.

ARCO Packard No. 1 Well

The ARCO Packard No. 1 well was drilled approximately 70 miles west-northwest of the ARCO COST No. 1 well (fig. 2). The Packard well is situated on an isolated basement high that occurs on the northwest flank of the Pinnacle Island subs basin (fig. 3). Neogene uplift of the basement folded the overlying Tertiary marine strata.

Overpressure zone 1 is present between 1,834 and 3,364 ft (fig. 10). Zone 1 occurs in layered marine strata of clay, claystone, siltstone, and minor amounts of gravel and sand that are of late Miocene to early Pliocene age (Core Laboratories, Inc., 1985c; Micropaleo Consultants, Inc., 1985b). Zone 1 occurs within the upper compaction trend. The base of the upper compaction trend lies at 3,614 ft and appears as a sharp break on all three wireline logs (fig. 10). Shale bulk density within zone 1 typically ranges between 1.55 and 1.87 g/cm³. The bulk density immediately below 3,614 ft

ranges between 2.03 and 2.37 g/cm³ and falls on or near a normal compaction trend down to a depth of 11,239 ft.

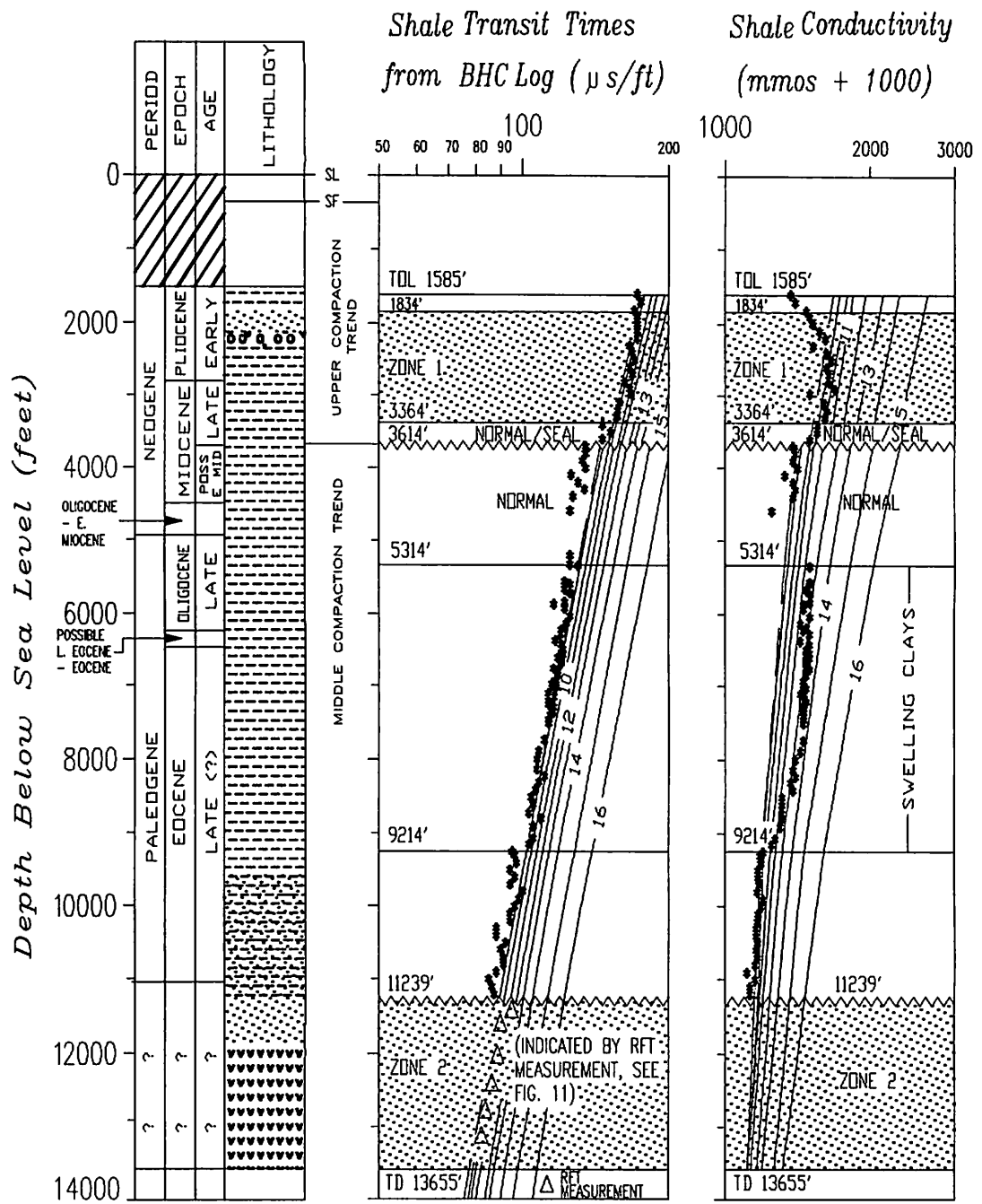
The presence of a lithologic change is suggested by low conductivity values above 2,400 ft (fig. 10). Bulk density data also suggest the presence of a "higher" density material above 1,834 ft. The final well report of Exlog (1985c) describes this section of the well as encountering 80 to 90 percent clay and claystone, interbedded with gravels, siltstones, and minor amounts of sand, all of early Pliocene age. The Formation Evaluation log describes the gravels as being gray, unconsolidated, volcanic pebbles with minor amounts of metavolcanics, quartz, and pyrite minerals. The siltstones, firm and slightly to moderately calcareous, are interbedded with claystones. These claystones are soft and hydrated, with trace amounts of pyrite, mica, and fossil fragments.

Zone 1 pore pressures range from 9.5 to 11.5 ppg EMW (0.488 to 0.591 psi/ft) and average 10.0 ppg EMW (0.514 psi/ft) (fig. 10). This is consistently higher than the normal pressure gradient of 8.71 ppg EMW (0.452 psi/ft) (Sherwood, 1984). DST measurements were not performed in the well, and there were no successful RFT measurements in zone 1. Bottom-hole circulating mud pressures were consistently normal or near normal until the depth of 11,239 ft, where mud pressures increased significantly in response to a lithology change to a sandstone and volcanic ash and tuffs (fig. 10). Mud weights reported on the Formation Evaluation log (fig. 10) were significantly less than what would be needed to balance the pore pressures indirectly calculated by the shale travel times for zone 1 (fig. 11).

Abnormally high conductivity values were measured between the depths of 5,314 and 9,214 ft (fig. 10). There were no corresponding responses in either the travel time data or the bulk density data. The final well report (Exlog, 1985c) describes this section as dominantly massive clay and claystone. These lithologies are typically 60 to 70 percent, but can be up to 100 percent, of the section. The clay is light to medium gray, soft to spongy, sticky, well hydrated, slight to very soluble. Calcite fragments are common, fossil fragments were observed, and trace pyrite is present. Interbedded siltstone and sandy siltstone form the remainder of the section.

Sidewall cores from the same section of the well sampled an olive-gray-black mudstone that is soft to firm, slightly silty, micaceous, calcareous, and moderately hydrated. Below 9,130 ft, sidewall core samples are gray, massive, muddy siltstones that are soft to firm and slightly calcareous.

The apparent anomalous shale conductivities are believed to be a response to the presence of abundant swelling clays of the montmorillonite group. Montmorillonite clays are indicated on the logs by high thorium and low potassium concentrations (inferred



86 feet from Kb to mean sea level. Water depth is 541 feet.

Figure 10. Geologic time scale, lithology, wireline-log information, and pore pressures of the ARCO Packard No. 1 well.

Shale

Bulk Density (g/cm^3) Pore Pressure (ppg EMW) Porosity (%)

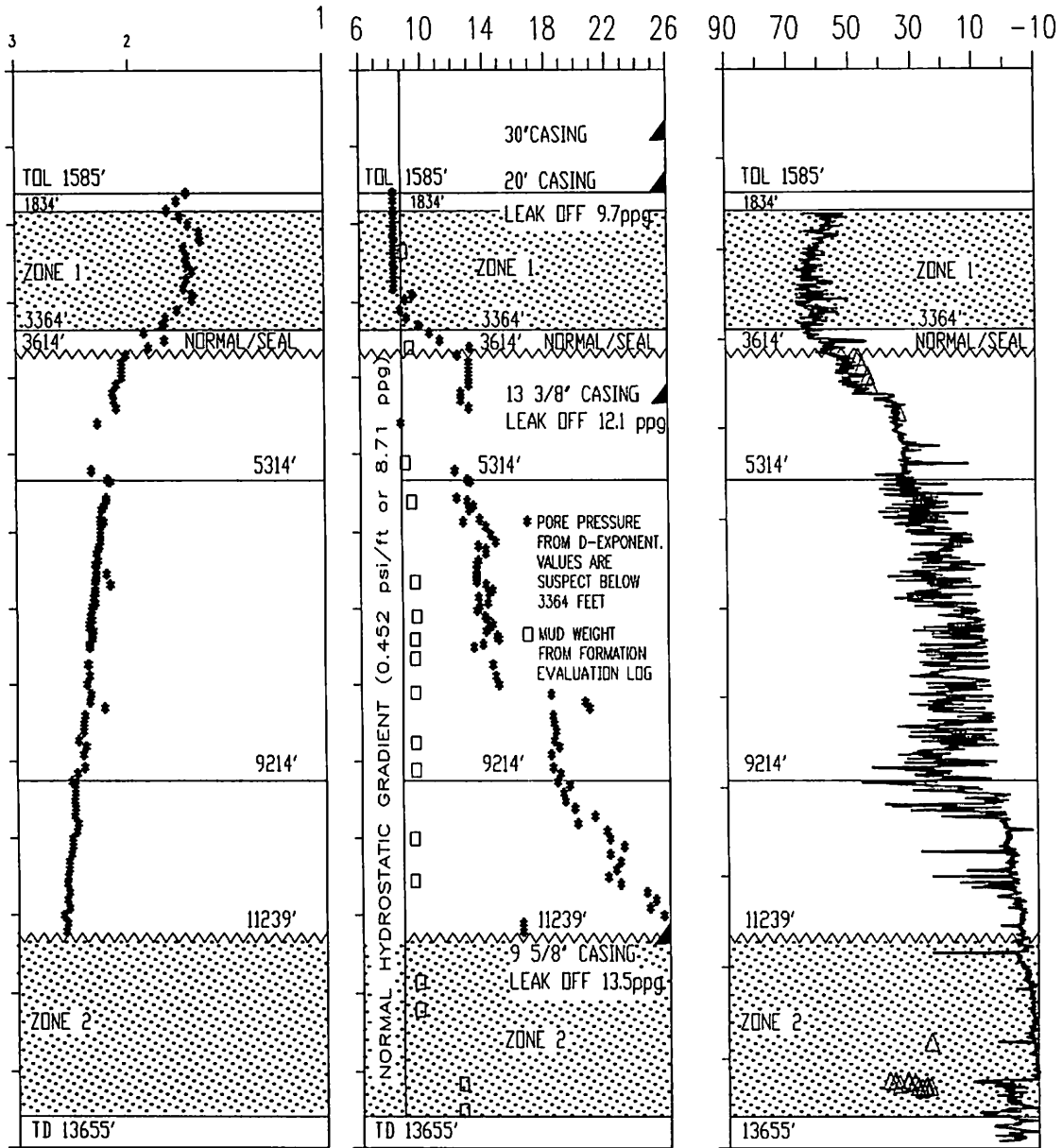
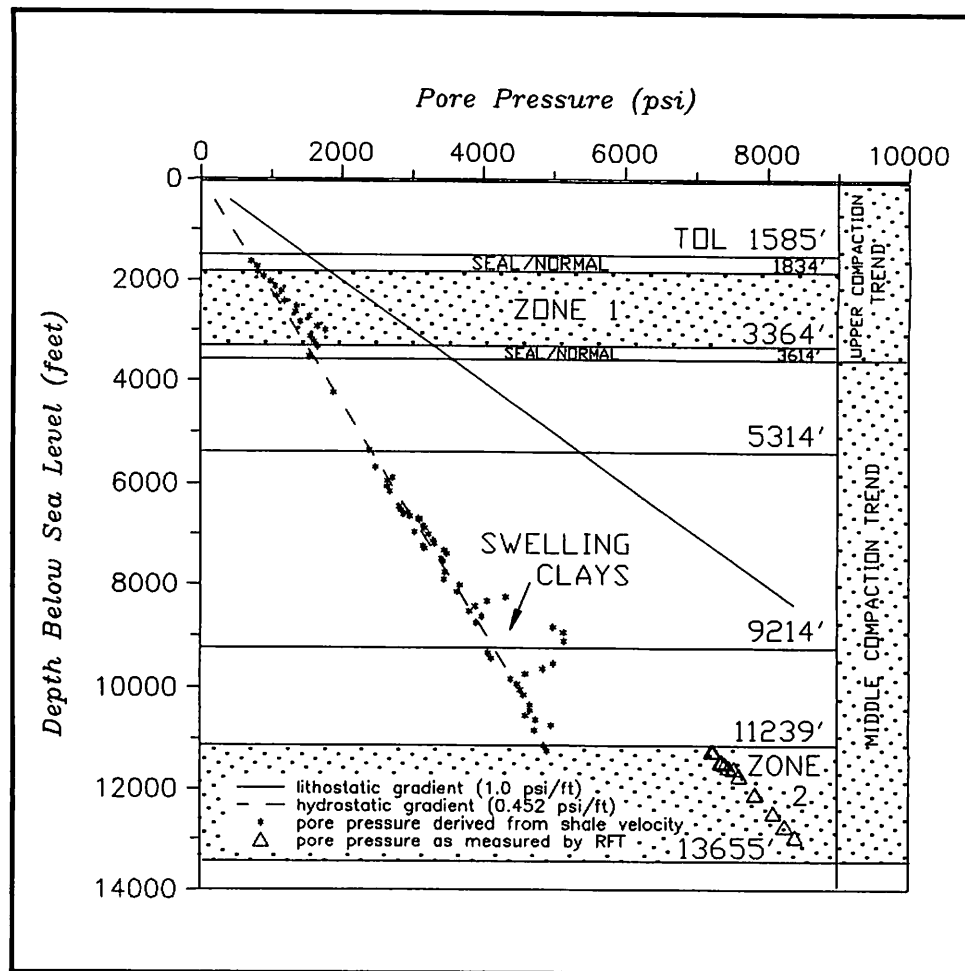


Figure 11. Pore pressure based on estimates derived from shale velocity by using pressure evaluation curves published by McClure (1977) and pore pressure measured by RFT for the ARCO Packard No. 1 well.



from the PEF and natural gamma ray spectrometry logs) that form a hyperbolic pattern on a K-Th crossplot. The absorption of water (hydration) was commonly observed throughout this section both on the Exlog Formation Evaluation log and on the sidewall core descriptions. Ruhovets and Fertl (1982) describe the montmorillonite (smectite) group as having the greatest capacity to absorb water and also the highest cation exchange capacity. The presence of montmorillonite clays also increases the conductivity of shales.

Zone 2 abnormal pressures extend from 11,239 ft to TD at 13,655 ft. In this interval, shale transit time and conductivity data were not analyzed for pore pressure because the lithology (nonmarine volcanoclastics) is inappropriate for analysis (fig. 10) (McClure, 1977; Core Laboratories, Inc., 1985c; Micropaleo Consultants, Inc., 1985b). However, RFT measurements in this interval were abnormally high, averaging 11.9 ppg EMW (0.612 psi/ft) (fig. 11). These RFT measurements verify formation pressures suggested by elevated bottom-hole circulating mud pressures (up to 13.0 ppg EMW) (fig. 10). D-exponent values are suspect because values immediately above the 11,239-foot level are erroneously recorded at pressures of up to 25.9 ppg EMW (fig. 10). The data available did not indicate a possible source for these erroneous calculations.

Exxon Redwood No. 1 Well

The Exxon Redwood No. 1 well was drilled approximately 35 miles northwest of the ARCO COST No. 1 well (fig. 2). The Redwood No. 1 well is situated on a fault-bounded basement high that trends northwestward and forms part of the ridge that separates the Pinnacle Island and Pervenets subbasins (fig. 3). Tertiary uplift at the basement high folded the overlying layered marine strata.

Overpressure zone 1 is present between 1,779 and 3,364 ft (fig. 12). Conductivity and bulk density data indicate a lithologic change above 1,969 ft, a change which may extend to the top of the log at 802 ft. Zone 1 lies within the upper compaction trend, which extends down to 3,914 ft.

Zone 1 occurs in layered marine strata of dominantly green-gray clays that are hydrated, sticky, and are interbedded with minor amounts of sandstone and siltstone. The sequence is early to late Pliocene in age (Micropaleo Consultants, Inc., 1985c). Zone 1 occurs within the upper compaction sequence. The bottom of this sequence at 3,914 ft is a sharp break on all three wireline logs (fig. 12). Shale bulk density within the upper compaction sequence typically ranges between 1.50 and 1.82 g/cm³, values which are similar to zone 1 bulk densities (1.57 to 1.80 g/cm³). Immediately below 3,914 ft, values range between 2.05 and 2.35 g/cm³; and bulk density continues to fall on or near a normal compaction trend down to a depth of 7,844 ft.

Low conductivity values from the top of the log (802 ft) to 1,969 ft reflect a more permeable (sandier) section (fig. 12). This more permeable section includes the top 190 ft of zone 1. Lithologic descriptions of cuttings identify this section as slightly calcareous to noncalcareous, micromicaceous mudstone (Geochem Laboratories, Inc., 1985). The Exlog Formation Evaluation log describes the same late Pliocene and early Pleistocene section as being interbedded with very fine-grained sandstones and slightly hydrated, sticky clays.

Zone 1 pore pressures range from 9.0 to 13.5 ppg EMW (0.463 to 0.694 psi/ft) and average 10.6 ppg EMW (0.545 psi/ft). This is consistently higher than the normal pressure gradient of 8.71 ppg EMW (0.452 psi/ft) (Sherwood, 1984). RFT measurements taken below zone 1 between the depths of 4,070 and 4,391 ft indicate a near-normal pressure gradient of 9.02 ppg EMW (0.464 psi/ft) (fig. 13). DST measurements were not performed in the well. Bottom-hole circulating mud pressures were not available. Mud weights reported on the Exlog Formation Evaluation log (fig. 12) for zone 1 were significantly less than what would be needed to balance the pore pressures indirectly calculated by the shale travel times (fig. 12).

Anomalously high conductivity values ranging from 400 to 556 mhos were measured between the depths of 4,814 and 5,514 ft and between 6,114 and 6,514 ft (fig. 12). There are correspondingly

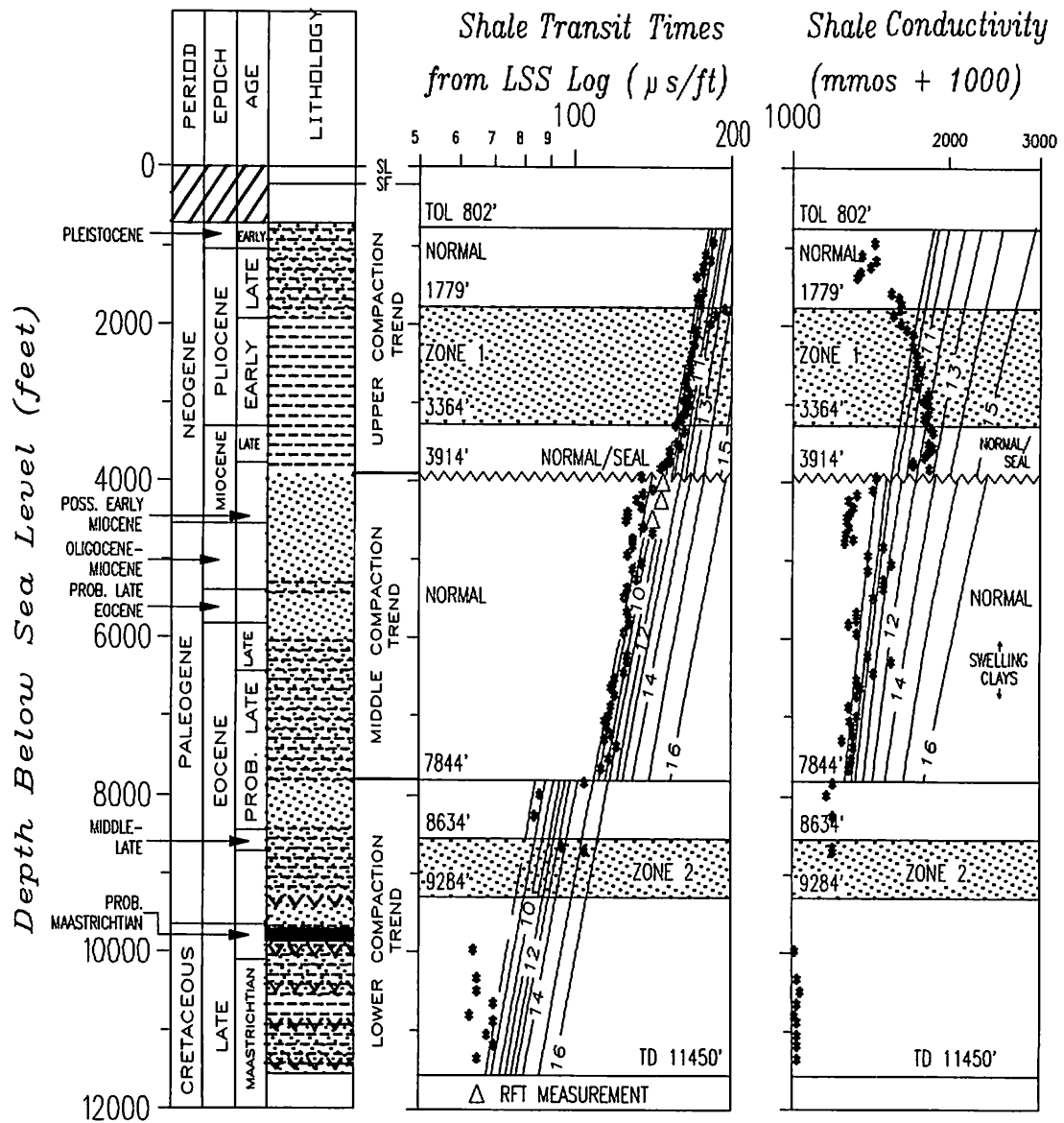


Figure 12. Geologic time scale, lithology, wireline-log information, and pore pressures of the Exxon Redwood No. 1 well.

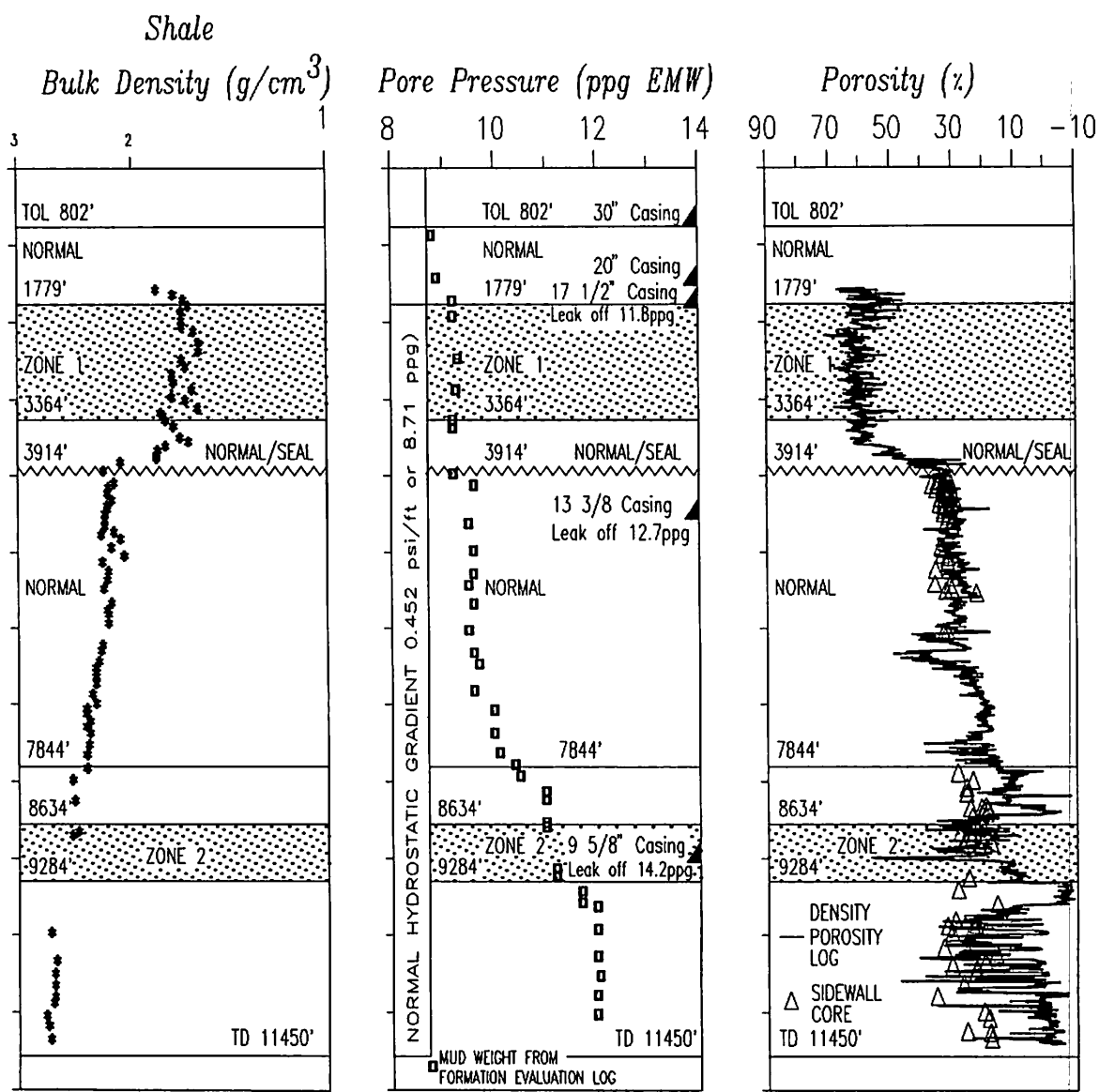
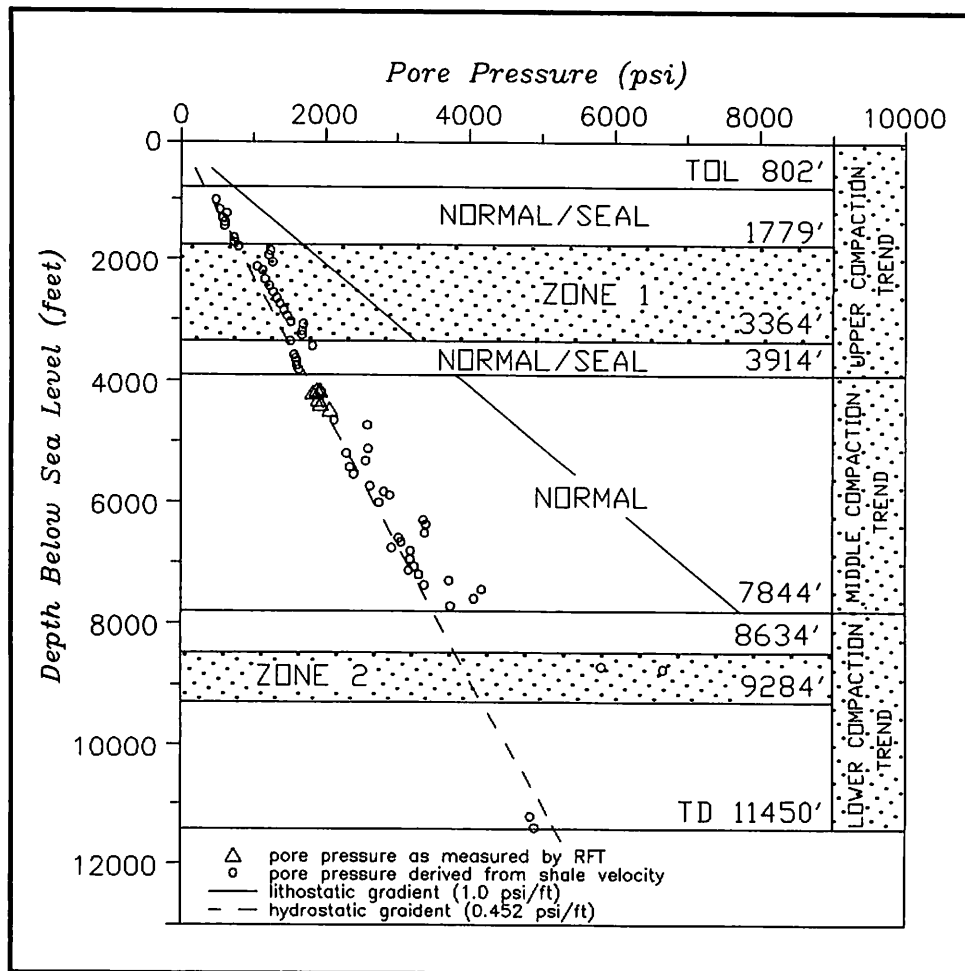


Figure 13. Pore pressure based on estimates derived from shale velocity by using pressure evaluation curves published by McClure (1977) and pore pressure measured by RFT for the Exxon Redwood No. 1 well.



small responses in the travel time and bulk density data. The anomalous values between 4,814 and 5,514 ft appear to be a response to lithology—a sandy claystone was identified in the interval. The anomalous section between 6,114 and 6,514 ft appears to be a zone of swelling clays, as signified by washout on the caliper log, variable but lower densities, high conductivities, and little or no change in the travel time data. The Exlog Formation Evaluation log describes this lower anomalous section as being dark-brown, soluble, slightly hydrated, sticky clay and shale. Sidewall core descriptions identify this same interval as sandstone and glauconite (Core Laboratories, Inc., 1985d). The PEF and the natural gamma ray spectrometry logs were used to identify these swelling clays as members of the montmorillonite group.

Overpressure zone 2 lies between 8,634 and 9,284 ft. Zone 2 is within the lower compaction trend, which ranges from 7,844 to 11,450 ft. This part of the well penetrated late Eocene sandstones; middle and late Eocene neritic shales, siltstones, and sandstones; Late Cretaceous and Eocene nonmarine volcanics, coals and interbedded sandstones and siltstones; and Late Cretaceous marine volcanoclastic sandstones and siltstones (Core Laboratories, Inc., 1985d; Micropaleo Consultants, Inc., 1985c).

Zone 2 is indicated by two abnormally high pressure values of 13.2 and 15.0 ppg EMW (0.678 psi/ft and 0.771 psi/ft) at 8,634 and 8,694 ft. These abnormally high pressures are believed to represent the middle and late Eocene shales that the well penetrated between 8,634 and 9,284 ft. RFT and DST measurements were not made within this interval. D-exponent values were not available.

Exxon Redwood No. 2 Well

The Exxon Redwood No. 2 well is located 6 miles north-northeast of the Exxon Redwood No. 1 well and 37 miles northwest of the ARCO COST No. 1 well (fig. 2). The No. 2 well drilled the northeast flank of the same basement high that the No. 1 well drilled (fig. 3). Abnormal pressures are present between 1,475 and 3,774 ft (zone 1), and between 7,439 ft and TD at 11,484 ft (zone 2) (figs. 14 and 15).

Zone 1, which occurs within the upper compaction trend, involves marine strata of clay, siltstones, and minor amounts of sandstones that are of late Miocene to late Pliocene age (Micropaleo Consultants, Inc., 1985d). Shale bulk density as reported by the FDC log was not available. Conductivity values range between 454 and 833 mmos (fig. 14).

Transit time data suggest that abnormal pressure extends up to the top of available data at 1,475 ft. Above 3,000 ft, however, the Pliocene section becomes sandier, a lithologic change which is reflected in low conductivity values (from 454 to 741 mmos) (fig. 14). Transit times from the LSS log did not indicate the high velocities traditionally associated with sands, however. The Exlog Formation Evaluation log describes the uppermost section of the well as consisting of medium- to fine-grained sands that are interbedded with gray, soft, hydrated clays and calcite-cemented, firm, clay-rich siltstones.

Between the base of zone 1 at 3,774 ft and the bottom of the upper compaction sequence at 4,014 ft is a normally pressured section that has the appearance of overcompaction. The bottom of the upper compaction sequence is a sharp break on all three wireline logs (fig. 14).

Zone 1 pore pressures range from 8.7 to 11.0 ppg EMW (0.447 to 0.565 psi/ft) and average 10.0 ppg EMW (0.514 psi/ft), as estimated by shale transit times. These values are typically higher than the normal pressure gradient of 8.71 ppg EMW (0.452 psi/ft) (Sherwood, 1984), and higher than the pressure gradient of 8.60 ppg EMW (0.442 psi/ft) measured by the RFT between 4,706 and 4,707 ft in the normally pressured section below zone 1 (fig. 15).

A second overpressured section, zone 2, is indicated between the depths of 7,439 ft and TD at 11,484 ft (fig. 14). Zone 2 encompasses a 4,045-foot section of flat-lying, possible middle

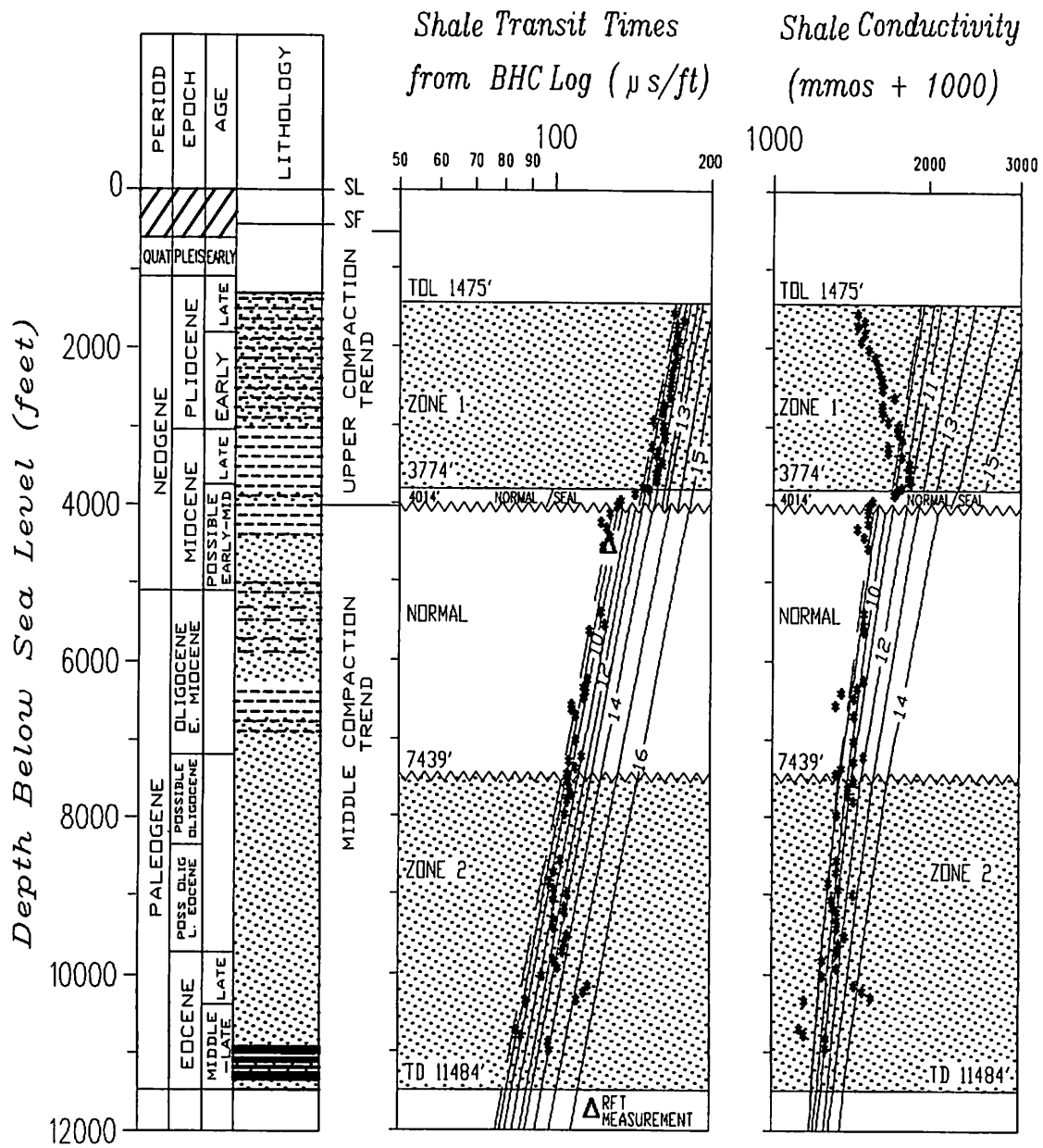


Figure 14. Geologic time scale, lithology, wireline-log information, and pore pressures of the Exxon Redwood No. 2 well.

Shale
 Bulk Density (g/cm^3) Pore Pressure (ppg EMW)

Porosity (%)

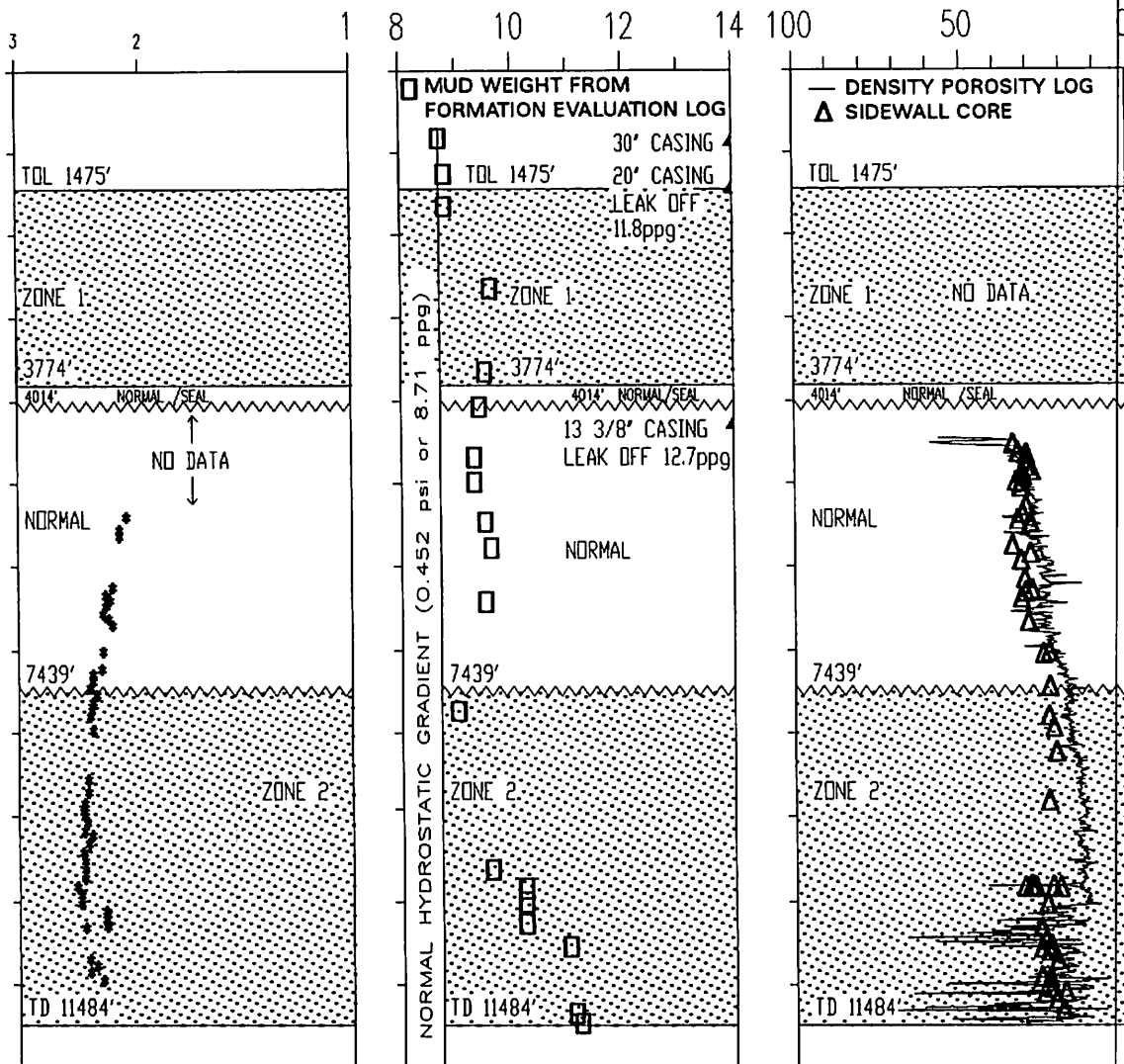
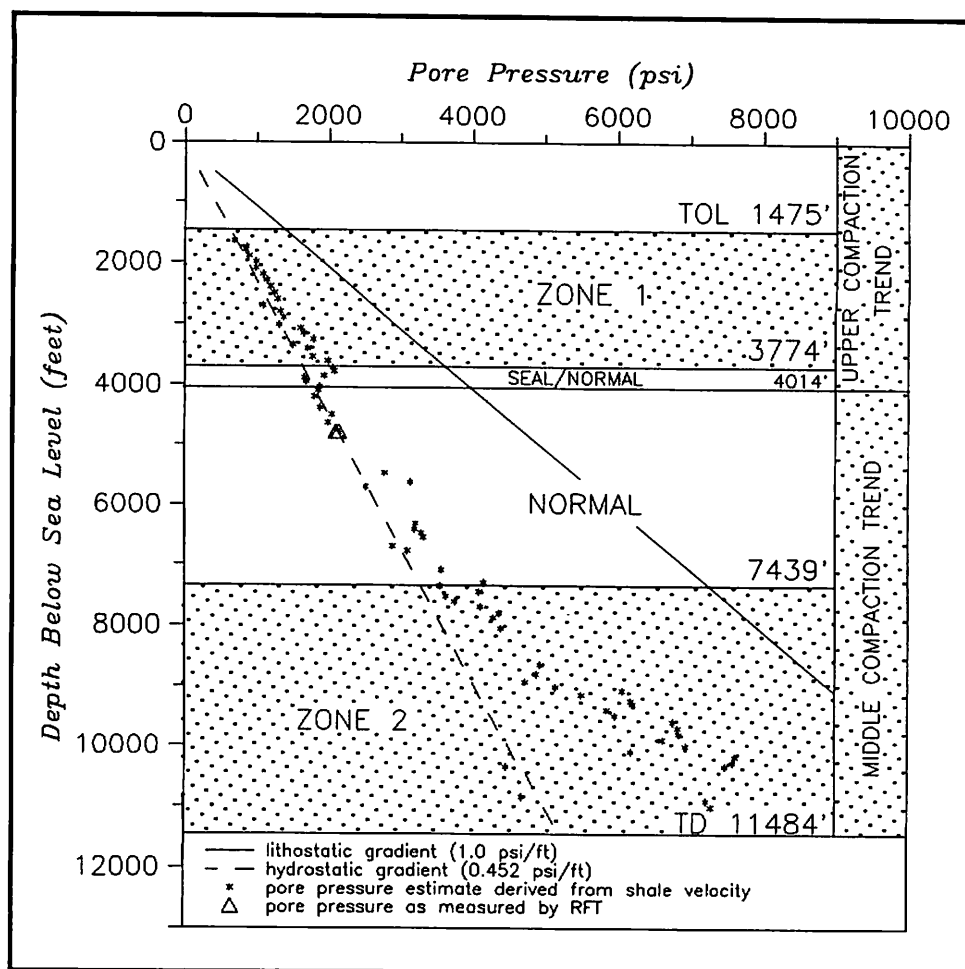


Figure 15. Pore pressure based on estimates derived from shale velocity by using pressure evaluation curves published by McClure (1977) and pore pressure measured by RFT for the Exxon Redwood No. 2 well.



Eocene to Oligocene, middle bathyal to middle neritic, clay-rich, calcareous siltstone that is interbedded with soft, sticky, gray clay. Near the bottom of the section are minor amounts of interbedded fine-grained sandstones and coals (Micropaleo Consultants, Inc., 1985d). Zone 2 has no distinct bulk density contrast with the strata above 7,439 ft, while bulk density for strata below 11,014 ft was not available. The top of zone 2 is tentatively placed at 7,439 ft, based on the consistent gradual deviation of both the travel time and conductivity data to the right of the 8.71-ppg EMW curve.

Pore pressures in zone 2 range from 9.5 to 15.2 ppg EMW (0.488 to 0.781 psi/ft). No RFT or DST measurements were taken, and no d-exponent calculations made. The Exlog Formation Evaluation log did, however, report elevated mud weights of up to 11.2 ppg (fig. 14).

Amoco Nancy No. 1 Well

The Amoco Nancy No. 1 well was drilled approximately 68 miles southeast of the ARCO COST No. 1 well (fig. 2). The Nancy well is situated on an isolated basement high that occurs on the southeast flank of the Pinnacle Island subbasin (fig. 3). Tertiary uplift of the basement folded the overlying layered marine and nonmarine strata.

The original hole extended to 8,021 ft below sea level, and a sidetrack was initiated at 6,964 ft and extended to 8,622 ft below sea level. Data below 7,314 ft in the sidetrack were not evaluated because the lithology consists of nonmarine volcanoclastics, coals, sandstones, and siltstones.

Two zones of overpressuring are present. Zone 1 extends from 1,650 to 3,514 ft. Travel time data indicate that abnormal pressure extends up to the top of available data at 1,650 ft. Zone 2 extends from 5,514 ft to below the bottom of usable data at 7,314 ft (fig. 16).

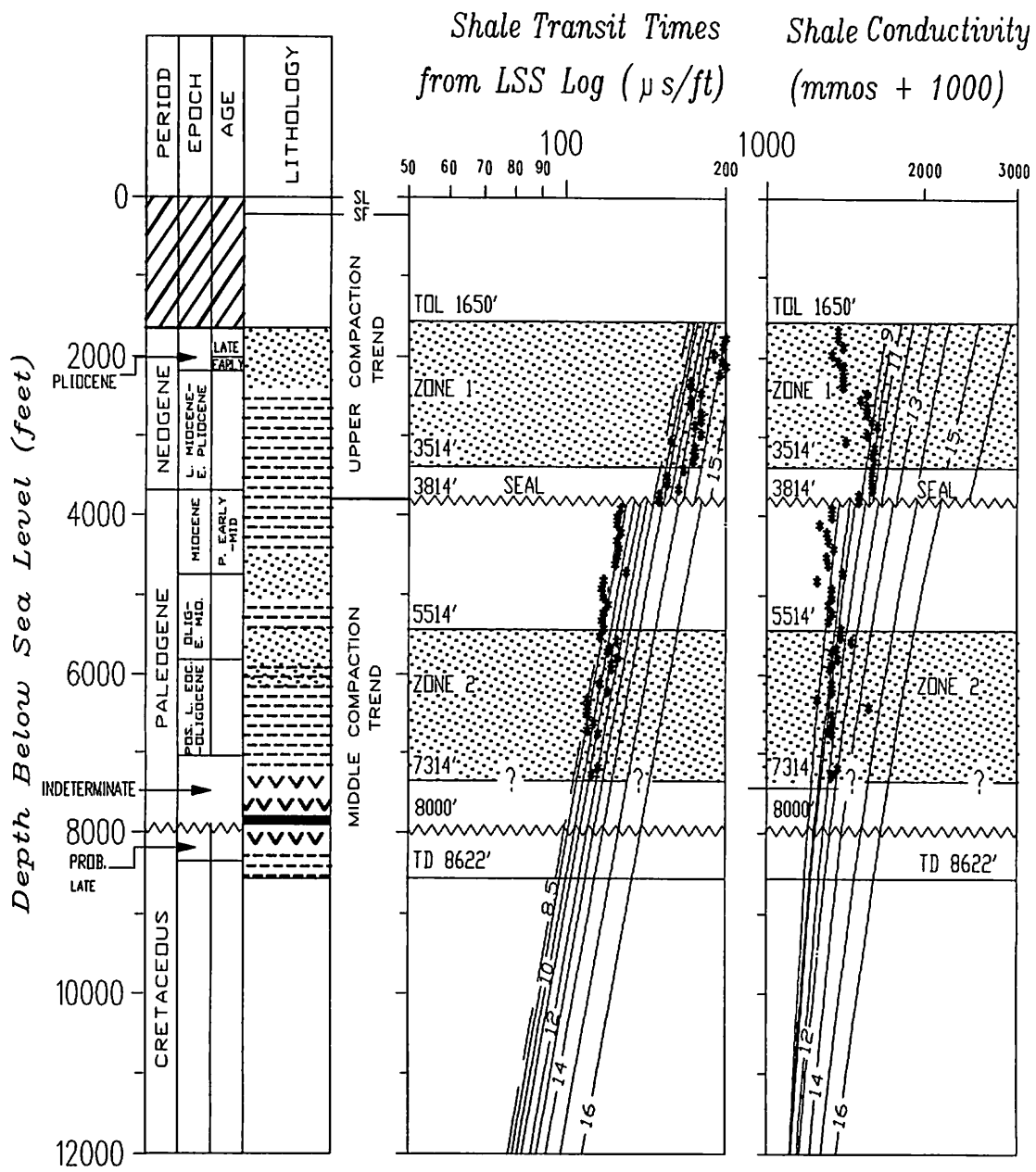
The lower half of zone 1, between 2,364 and 3,514 ft, occurs in layered marine claystone, with minor amounts of siltstone, sandstone, and limestone, of late Miocene to early Pliocene age (Core Laboratories, Inc., 1985e; Micropaleo Consultants, Inc., 1985e). The claystone is light to medium gray, soft, soluble, and hydrated. Conductivity values for the lower half of zone 1 typically range from 417 to 625 mmos.

The upper half of zone 1, between 1,650 to 2,364 ft, has lower conductivity values, indicating a lithologic section of increased permeability due to higher sand content (fig. 16). This section is mainly clay and sand, with trace amounts of limestone and volcanic fragments, of early to late Pliocene age (Exlog, 1985d). The clay, which composes 60 to 90 percent of the lithology, is dark gray to gray green, very soft, soluble, hydrated and locally calcareous. The medium- to coarse-grained sand was unconsolidated and sorted, and makes up 20 to 40 percent of the lithology (Core Laboratories, Inc., 1985e).

Zone 1 occurs within the upper compaction sequence. The bottom of the upper compaction sequence is a sharp break on all three wireline logs (fig. 16). Within zone 1, shale bulk density typically ranges between 1.63 and 1.95 g/cm³ (fig. 16). Bulk density ranges between 2.05 and 2.23 g/cm³ immediately below the upper compaction sequence, and falls on, or near, a normal compaction trend down to a depth of 5,514 ft.

Zone 1 pore pressures range from 10.5 to 14.3 ppg EMW (0.540 to 0.735 psi/ft) and average 13.2 ppg EMW (0.678 psi/ft), as estimated by shale travel times (fig. 17). This is higher than the normal pressure gradient of 8.71 ppg EMW (0.452 psi/ft) (Sherwood, 1984). No DST or RFT measurements were taken. Elevated d-exponent values were also found within zone 1 (fig. 16).

Zone 2 encompasses a 609-foot section of flat-lying, Oligocene to early Miocene, fine-grained sandstones deposited in an outer neritic to upper bathyal setting; and a 1,191-foot section of flat-lying, possible Eocene to Oligocene claystone and siltstone deposited in an upper to middle bathyal setting (Core Laboratories, Inc., 1985e; Micropaleo Consultants, Inc., 1985e). The base of zone 2 probably extends below 7,314 ft. This is suggested by mud weights in this



86 feet from Kb to mean sea level. Water depth is 452 feet.

Figure 16. Geologic time scale, lithology, wireline-log information, and pore pressures for the Amoco Nancy No. 1 well.

Shale
Bulk Density (g/cm³)

Pore Pressure (ppg EMW)

Porosity (%)

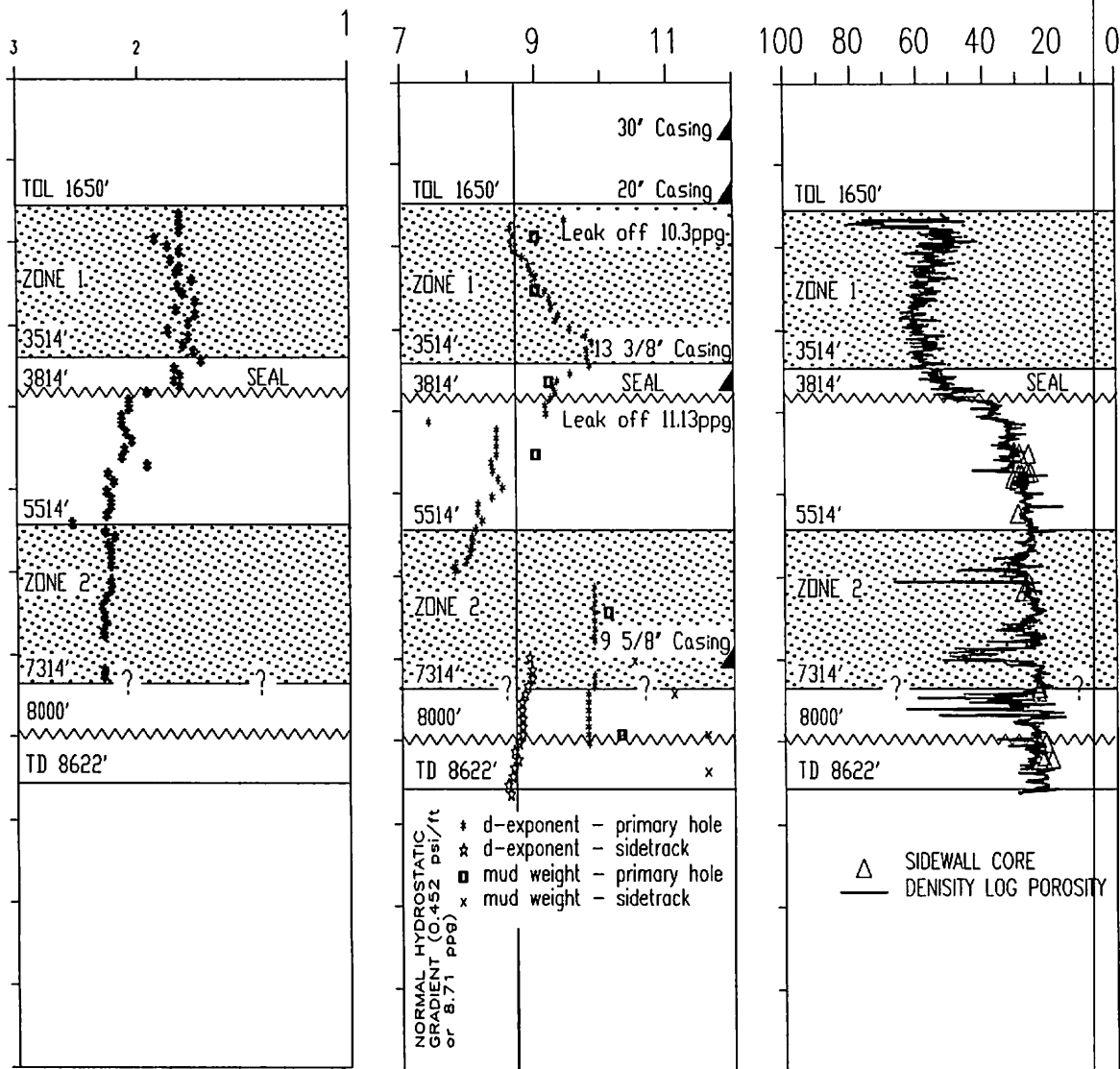
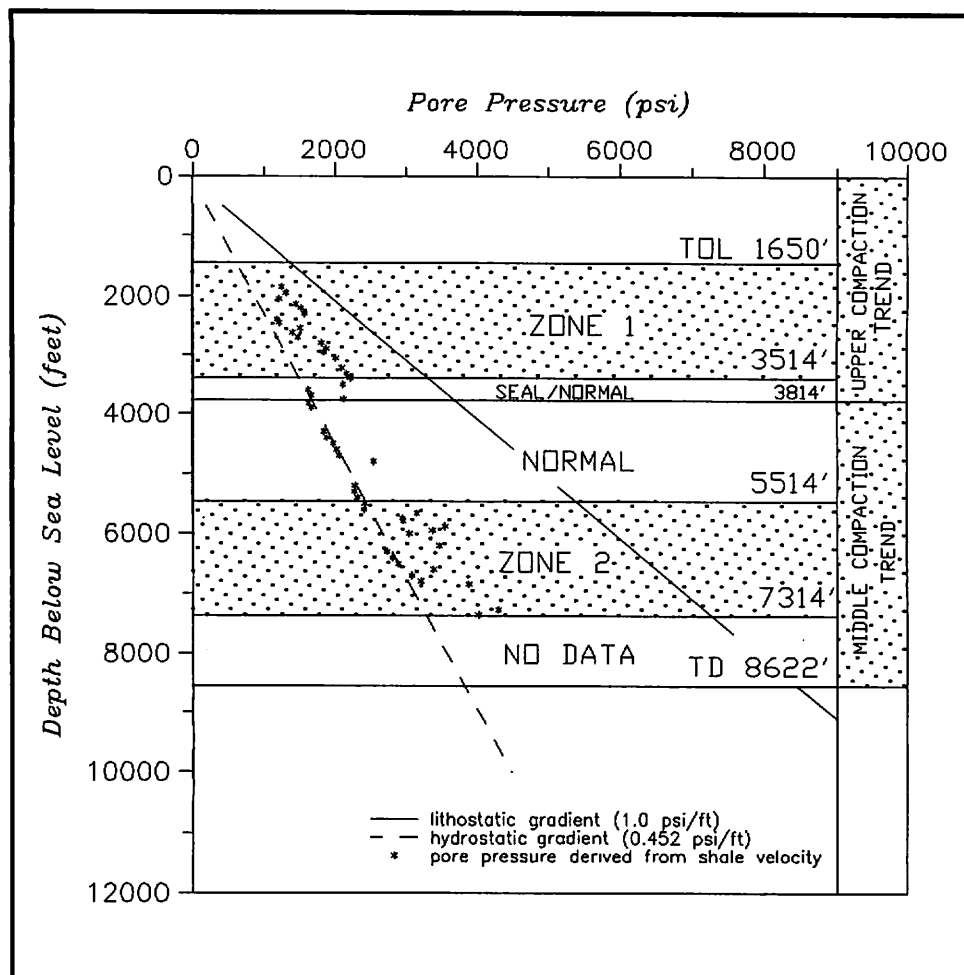


Figure 17. Pore pressure based on estimates derived from shale velocity by using pressure evaluation curves published by McClure (1977) for the Amoco Nancy No. 1 well.



part of the hole as high as 11.6 ppg (fig. 16). In addition, d-exponent data for the primary hole indicate overpressured conditions below 6,014 ft. D-exponent data for the sidetrack hole, however, indicate near normal conditions below 6,964 ft.

Amoco Misha No. 1 Well

The Amoco Misha No. 1 well was drilled approximately 50 miles southwest of the Exxon Redwood No. 1 well and 85 miles west-southwest of the ARCO COST No. 1 well (fig. 2). The Misha well is situated on an outer-shelf-break ridge that trends northwestward and separates the Pinnacle Island subbasin to the northeast from a small isolated half-graben to the southwest (fig. 3). Tertiary uplift of the ridge folded the overlying layered marine and nonmarine strata.

Abnormal pressure is present between 1,434 and 3,084 ft (zone 1), and between 4,469 and 4,989 ft (zone 2) (fig. 18).

Zone 1 occurs in layered marine strata, dominantly clay, with minor amounts of sand, silt, and coal, of late Miocene to late Pliocene age (Core Laboratories, Inc., 1985f; Micropaleo Consultants, Inc., 1985f). The clay is gray to gray green, soft to occasionally firm, amorphous and hydrated. The sand is coarse grained, angular, and

consists of clear quartz, glauconite, amber calcite, and minor amounts of volcanic tuff, lithic fragments, fossil fragments, and pyrite. The silt is gray and soft, sandy in places. Shale bulk density within zone 1 typically ranges between 1.63 and 1.85 g/cm³ (fig. 18). The bulk density ranges between 2.05 and 2.17 g/cm³ immediately below 3,904 ft, and falls on or near a normal compaction trend down to a depth of 4,469 ft. Conductivity values range between 435 and 625 mmos (fig. 18).

Transit time data suggest that abnormal pressure extends up to the top of available log data at 684 ft; however, the conductivity and density data indicate a lithology change between 684 and 2,014 ft. The presence of this lithologic unit is most apparent in the conductivity data, where an increase in sand content probably results in the lower conductivities (fig. 18). The BHC log does not indicate a lithologic change, but the bulk density data do suggest higher densities of 1.90 to 1.95 g/cm³ between 684 and 1,434 ft.

Lithologic descriptions of the well were not available above 1,697 ft. Between 1,697 and 2,014 ft, the well penetrated gray-green, fine-grained sandstones and siltstones with stringers of calcite and glauconite, pyrite, and shell fragments, as described by the Exlog Formation Evaluation log.

Zone 1 pressures range from 9.2 to 11.7 ppg EMW (0.473 to 0.601 psi/ft) and average 10.6 ppg EMW (0.545 psi/ft), as estimated by shale travel times (fig. 18). Calibration of the McClure curves was accomplished by setting the appropriate curve equal to the RFT measurement at a specific depth. This correlation is shown on figure 19 where the pore pressure derived from shale travel times is equal to the pore pressure as measured by the RFT. Zone 1 pressures are higher than the normal pressure gradient of 8.71 ppg EMW (0.452 psi/ft) (Sherwood, 1984).

Zone 2, which lies between 4,469 and 4,989 ft, encompasses, from top to bottom, a 225-foot section of middle to late Eocene claystone that is gray, soft to firm, generally noncalcareous, and contains minor amounts of sand and silt; an 80-foot section of early to middle Eocene, very fine to fine-grained sandstone composed of quartz grains and lithic volcanic fragments; and a 215-foot section of unconsolidated sand consisting of quartz grains and lithic volcanic fragments (Core Laboratories, Inc., 1985f; Micropaleo Consultants, Inc., 1985f).

Both the top and bottom of zone 2 occur as sharp breaks on all three wireline logs (fig. 18). Within zone 2, shale bulk densities average 1.90 g/cm³, in contrast to densities of 2.05 to 2.17 g/cm³ above the zone and 2.15 to 2.25 g/cm³ below. Shale conductivities within the zone range between 555 and 667 mmos, in contrast to 303 to 385 mmos above and 250 to 333 mmos below. Abnormal pressures as high as 15.5 ppg EMW (0.797 psi/ft) were calculated using the

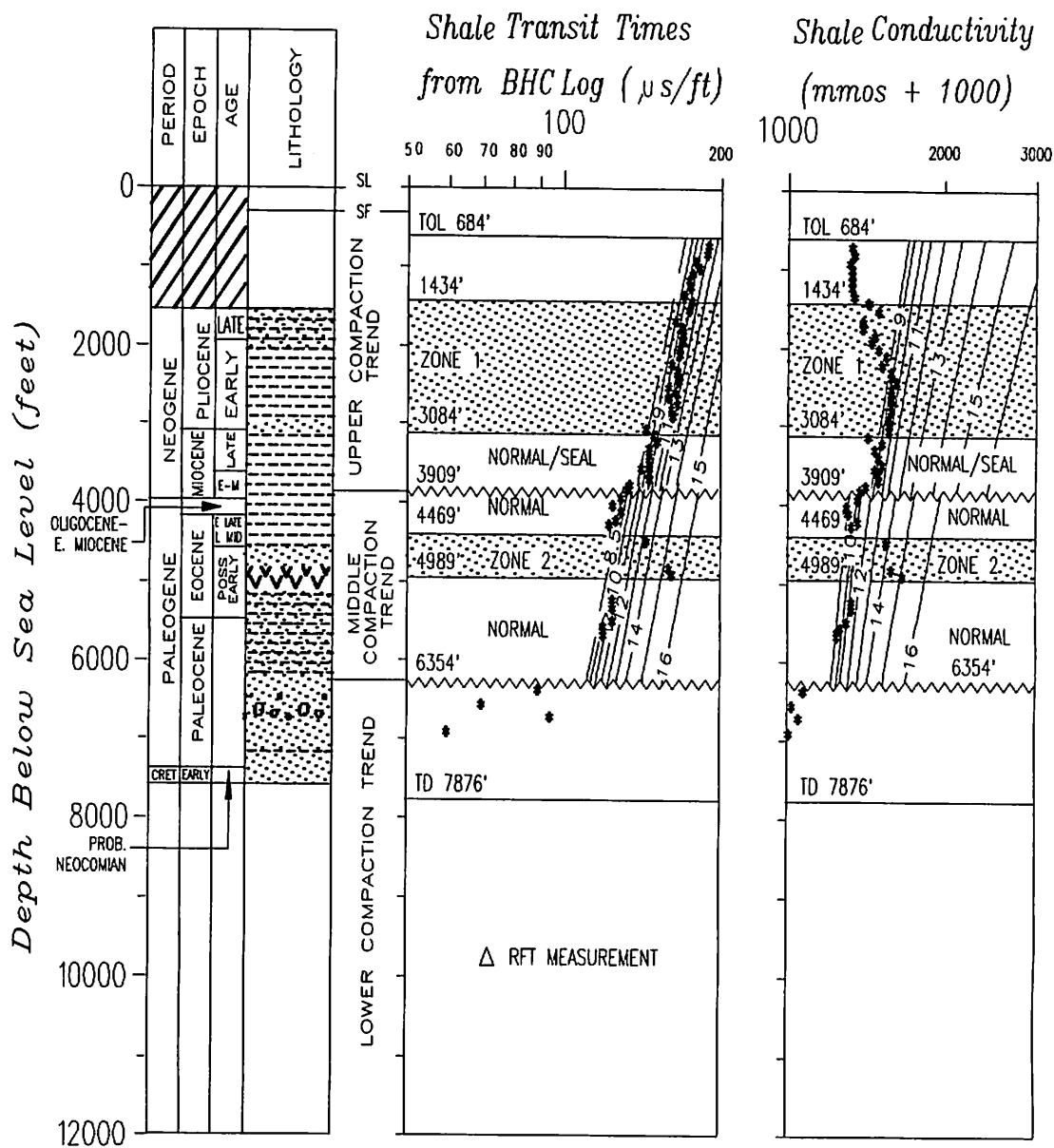


Figure 18. Geologic time scale, lithology, wireline-log information, and pore pressures for the Amoco Misha No. 1 well.

Shale

Bulk Density (g/cm³)

Pore Pressure (ppg EMW)

Porosity (%)

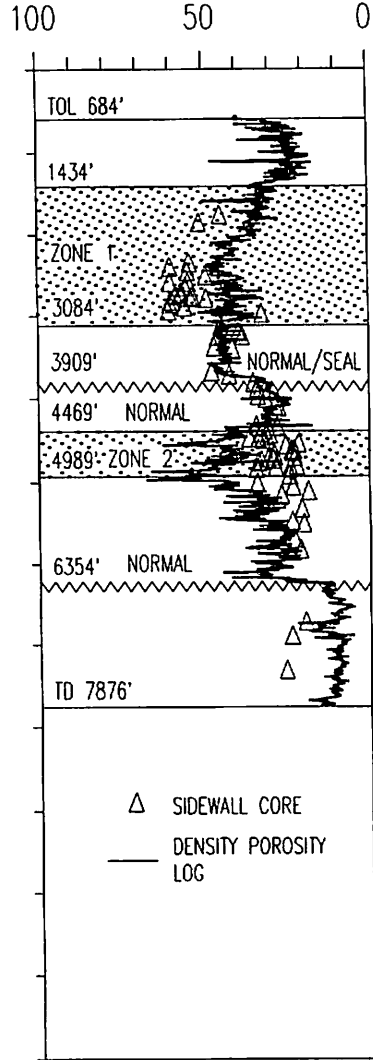
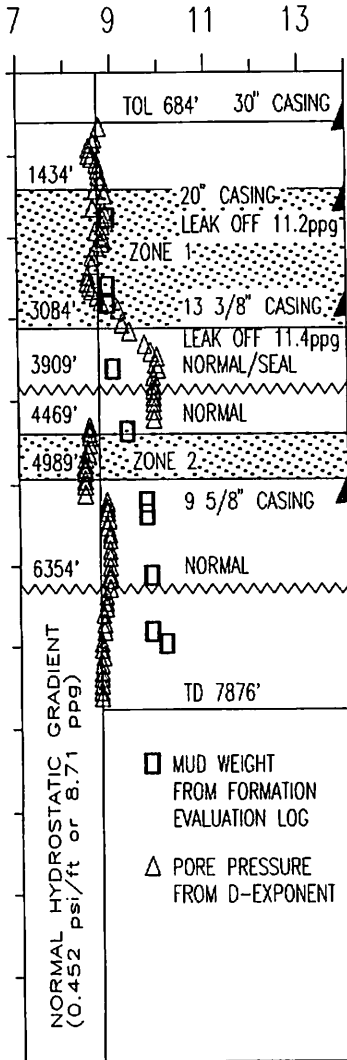
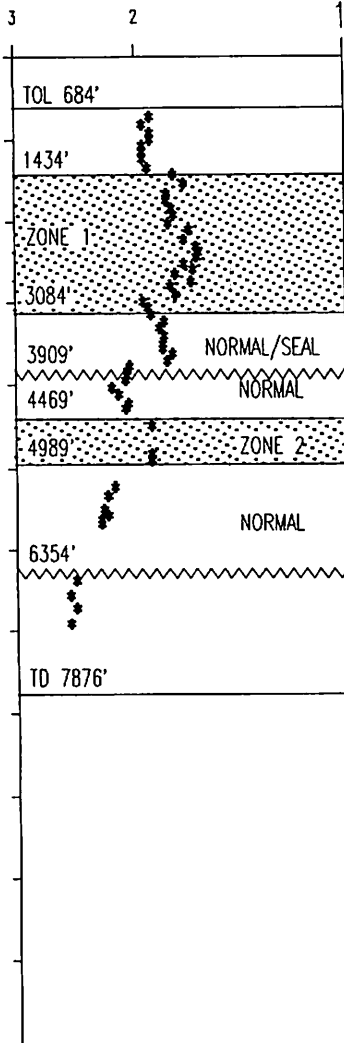
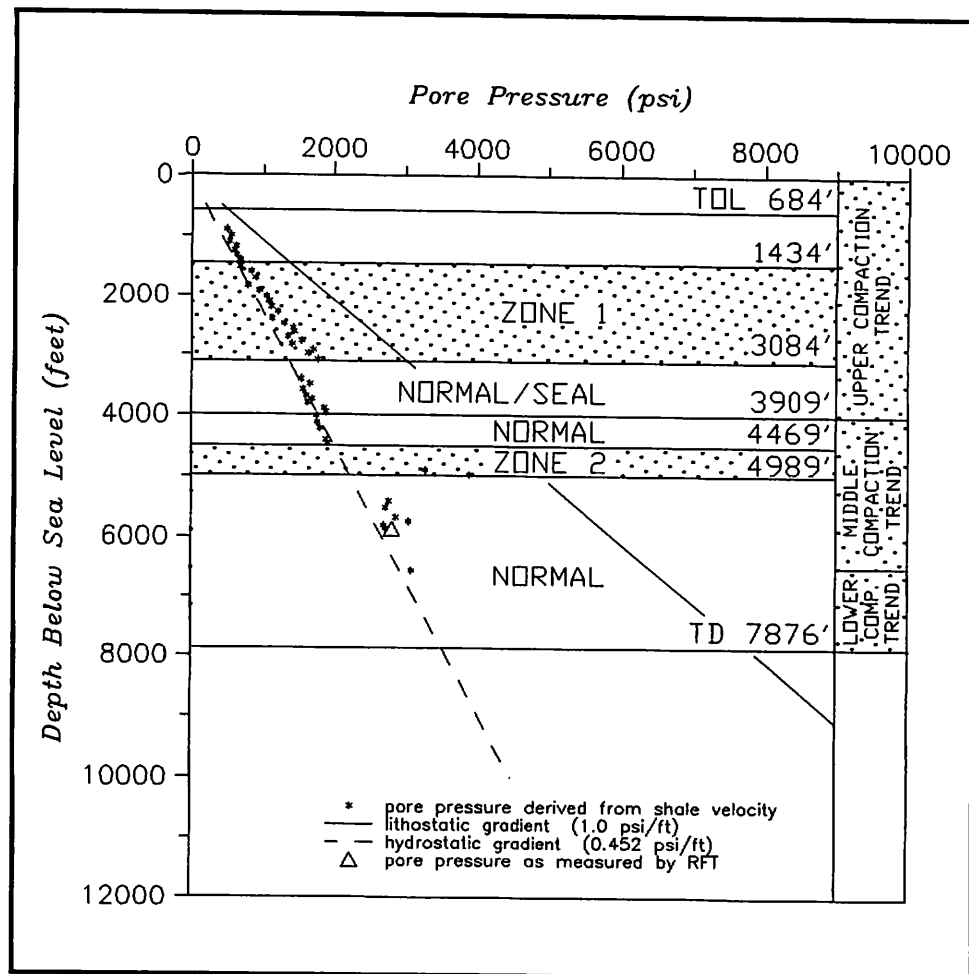


Figure 19. Pore pressure based on estimates derived from shale velocity by using pressure evaluation curves published by McClure (1977) and pore pressure measured by RFT for the Amoco Misha No. 1 well.



McClure curves (1977). Zone 2 was drilled using a mud weight of 9.3 ppg (0.478 psi/ft).

The overpressuring associated with zone 2 apparently does not extend below 4,989 ft because an RFT measurement of 9.5 ppg EMW was taken at 5,777 ft.

Between the depths of 6,354 and 7,876 ft, the well penetrated sandstones, volcanic sandstones, and conglomerates, which are not conducive to analysis (McClure, 1977; Core Laboratories, Inc., 1985f). This sequence lies within the lower compaction trend and appears overcompacted in travel time, conductivity, and shale bulk density data. Mud weights as high as 10.1 ppg were reported in this section (fig. 18), although d-exponent data suggested normal pore pressures.

Amoco Danielle No. 1 Well

The Amoco Danielle No. 1 well was drilled 45 miles north of the ARCO COST No. 1 well and 40 miles northeast of the Exxon Redwood No. 1 well (fig. 2). The Danielle well is situated on an isolated basement high that trends east-west and forms part of the border between the Navarinsky and Pervenets subbasins (fig. 3). The basement high formed as a compressional ridge in the Paleogene and

grew throughout the Tertiary. Overlying marine strata of Neogene age are folded.

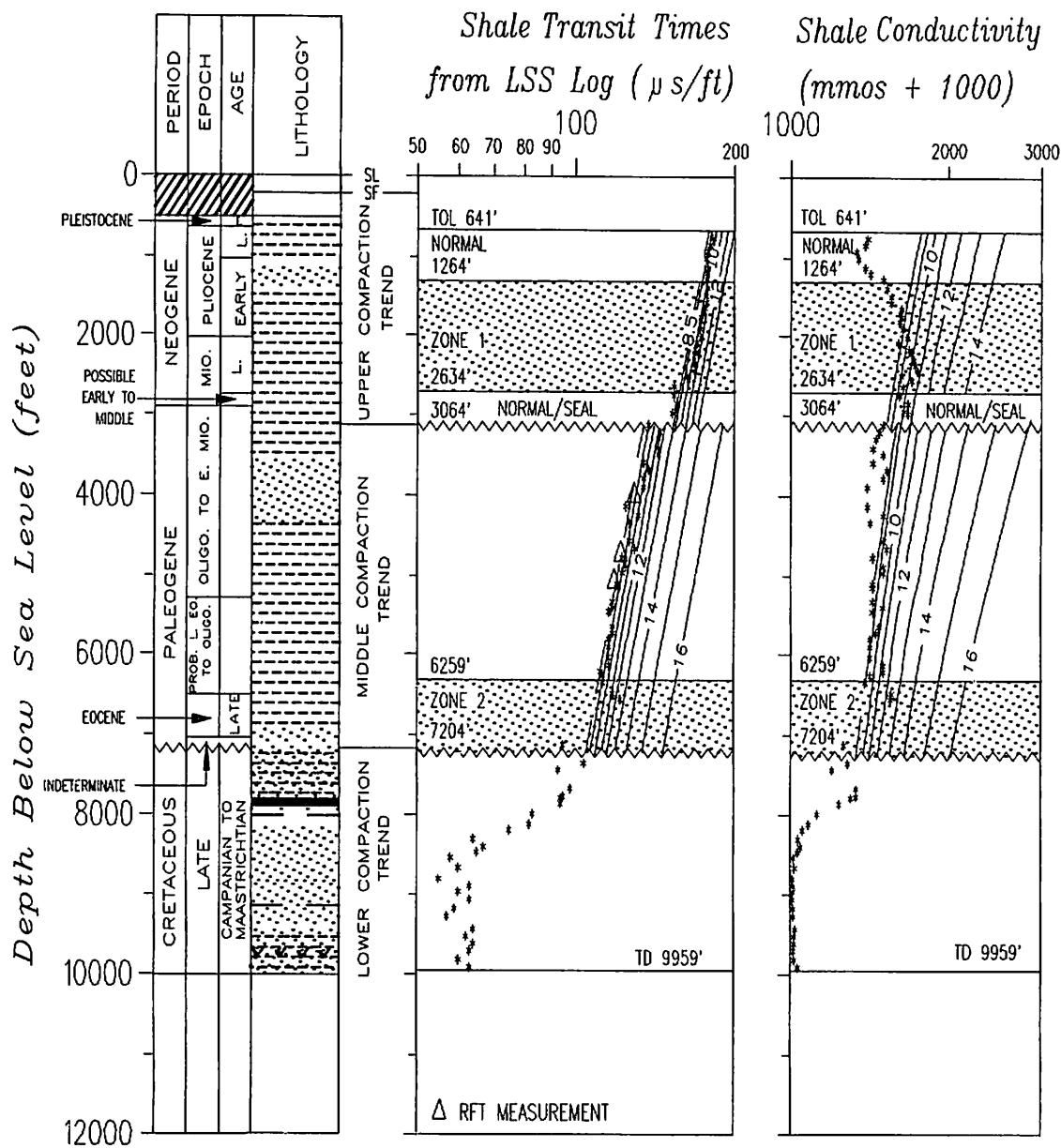
Abnormal pressure is present between 1,264 and 2,634 ft (zone 1), and between 6,259 and 7,204 ft (zone 2) (fig. 20).

Zone 1 occurs in marine silty or sandy claystones of late Miocene to early Pliocene age. The claystones contain up to 80 percent medium- to dark-gray clay; the proportion of clay decreases to 50 percent below 2,559 ft (Core Laboratories, Inc., 1985g; Exlog, 1985f). Siltstone stringers above 2,064 ft are dark brown, very hard, siliceous, and contain quartz and pyrite veins. The bottom of zone 1 is a sharp break on the conductivity and sonic logs and a transitional boundary on the bulk density log (fig. 20). Shale bulk density typically ranges between 1.6 and 1.93 g/cm³ within zone 1, and falls at or near a normal compaction trend below 3,039 ft. Conductivity values range between 625 and 741 mmos (fig. 20).

A distinct sandier section above 1,649 ft is most apparent in the conductivity data, where sands result in low conductivity values (fig. 20). This more permeable section is characterized by a depletion of the abnormal pore pressures due to a more porous, sandier sequence. The bulk density data do suggest higher densities of up to 1.95 g/cm³ near the top of the log (TOL). Between 1,134 and 1,464 ft, the well encountered a continuous medium-gray, very calcareous, well-sorted, fine-grained sand section.

Zone 1 pressures range from 9.2 to 11.7 ppg EMW (0.473 to 0.601 psi/ft) and average 10.5 ppg EMW (0.540 psi/ft), as estimated by shale travel times (fig. 21). This is higher than the normal pressure gradient of 8.71 ppg EMW (0.452 psi/ft) (Sherwood, 1984). Calibration of the McClure curves was accomplished by setting the appropriate curve equal to the RFT measurements at specific depths. Unfortunately, no RFT measurements were taken within the upper compaction sequence of zone 1. This correlation is shown on figure 20.

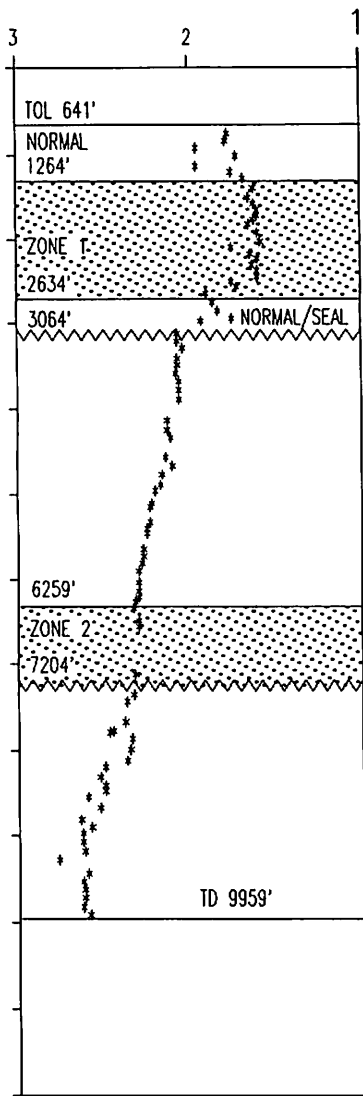
Zone 2, which lies between 6,259 and 7,204 ft, consists dominantly of clay, with siltstone and sandstone interbeds and minor, thin limestone lenses. The sequence is late Eocene through Oligocene in age, except for the bottom 180 ft, which is of indeterminate age. The clay is brown, soft, and noncalcareous. The siltstone is gray to gray-brown, firm, massive, and noncalcareous. The sandstone is fine to coarse grained, poorly sorted, with a calcareous matrix. The top of zone 2 is a moderately sharp break on sonic and resistivity logs (fig. 20). Within the zone, shale transit times range between 113 and 122 μ s/ft, in contrast with transit times below the zone of 95 to 104 μ s/ft. Conductivities within the zone range between 263 and 556 mmos, in contrast with conductivities of 417 to 455 mmos above the zone and 200 to 333 mmos below.



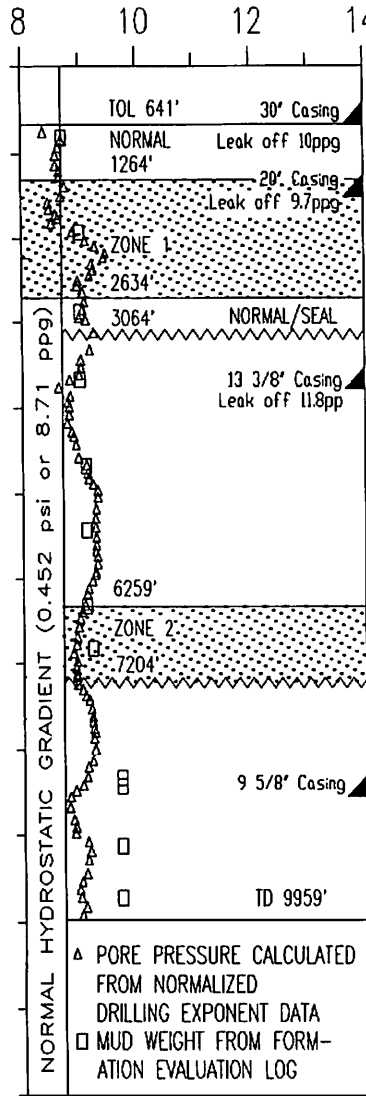
86 feet from Kb to mean sea level. Water depth is 393 feet.

Figure 20. Geologic time scale, lithology, wireline-log information, and pore pressures for the Amoco Danielle No. 1 well.

Shale
Bulk Density (g/cm^3)



Pore Pressure (ppg EMW)



Porosity (%)

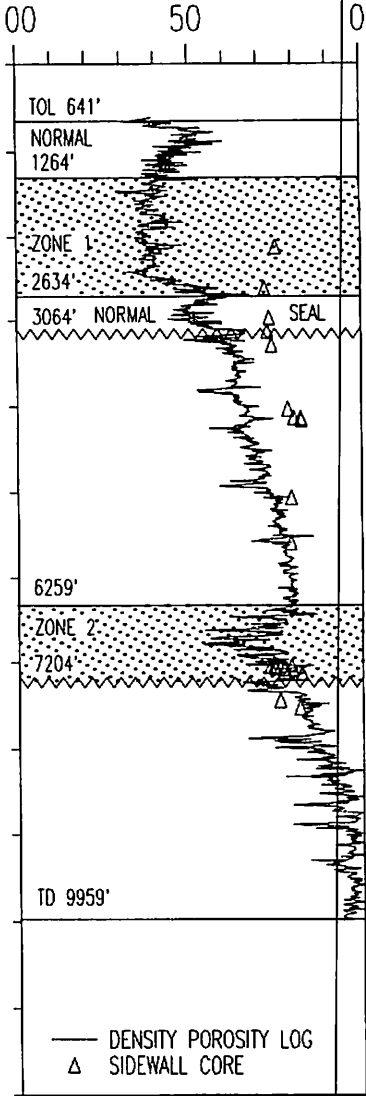
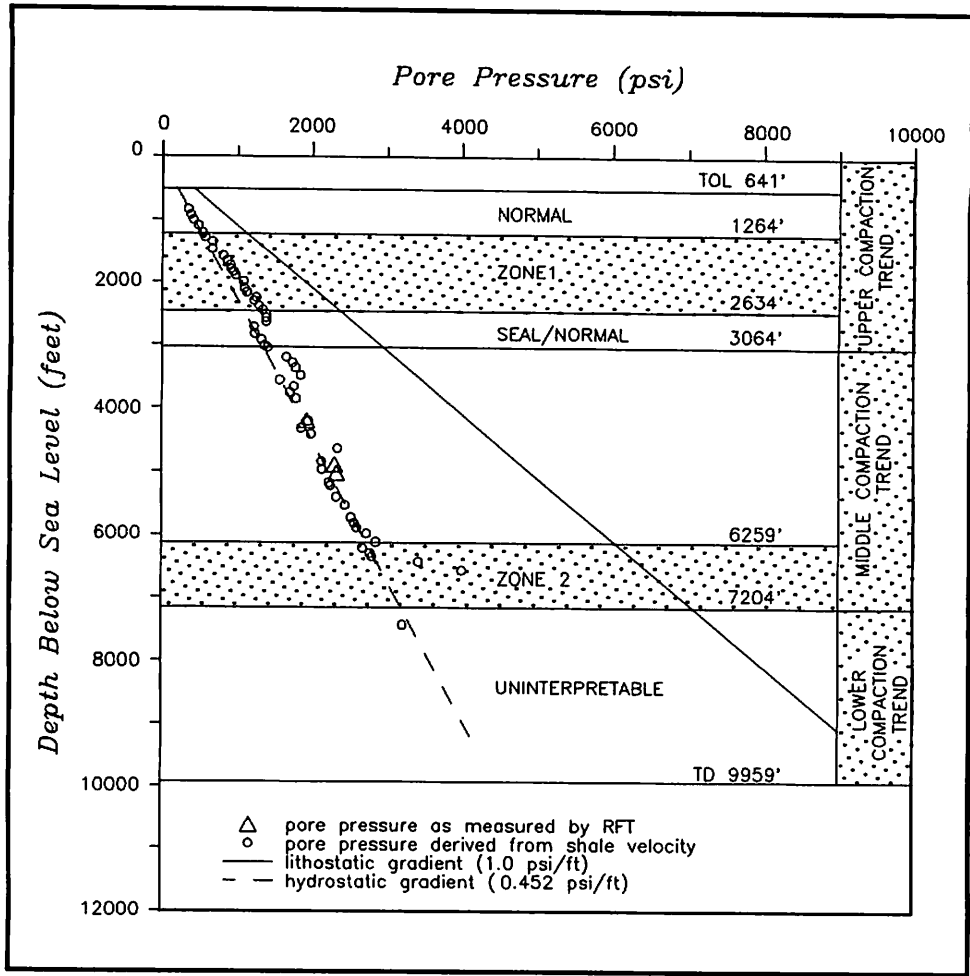


Figure 21. Pore pressure based on estimates derived from shale velocity by using pressure evaluation curves published by McClure (1977) and pore pressure measured by RFT for the Amoco Danielle No. 1 well.



Abnormal pressures as high as 12 ppg EMW (0.617 psi/ft) were derived indirectly from shale velocity analysis (fig. 21). No RFT or DST measurements were taken within zone 2.

5 Compaction History

The reduction of porosity and the increase in density which accompany compaction follow systematic but nonlinear trends as the depth of burial increases. These compaction trends will extend unbroken throughout a sedimentary column unless interrupted by unconformities or faults. Multiple compaction trends may be present due to a complex history of tectonic movements.

The pressure evaluation techniques of McClure (1977) apply to a single compaction sequence. Ignoring changes in the compaction history will lead to mislocation of pressure evaluation curves and to an overestimation of abnormal-pressure zones. To improve pressure analysis in this study, shale pressure plots, well stratigraphy and lithology, and known basin history were utilized to identify three compaction trends in the Navarin basin shale. The upper, middle, and lower trends are commonly bounded by unconformities associated with uplift and probably major erosional episodes. Exceptions to this association occur in the Exxon Redwood No. 1 well (fig. 12) and the Amoco Nicole No. 1 well (fig. 6). Other diastems are present but do not appear to materially affect the compaction histories. Table 2 lists the depth intervals and stratigraphic ages for each compaction trend in all the wells.

For all wells except Exxon Redwood Nos. 1 and 2, the upper compaction trend extends from the seafloor and includes strata ranging from Recent to late Miocene in age. In the Redwood No. 1 well, the upper compaction trend extends into possible early Miocene strata, whereas in the Redwood No. 2 well, it extends into possible early to middle Miocene strata. In all wells, the strata within the upper compaction trend typically consist of clays that are overlain by sandy mudstones and fine-grained sandstones.

The upper compaction trend is bounded at the base by a possible early to late Miocene regional unconformity that resulted from uplift and possible erosion throughout the basin. The unconformity truncates basement highs at the margins of the individual subbasins and correlates to a disconformity or paraconformity in the middle of the subbasins.

The middle compaction trend embraces strata from late Miocene to Late Cretaceous in age. The strata involved are dominantly fine-grained marine clastics with sandstone interbeds. The boundary

between the middle and lower compaction trends in most wells is a middle Eocene regional unconformity that represents the breakup of the Navarin outer continental shelf and the formation of the subbasins that became depositional centers throughout most of the Tertiary (fig. 3). In the wells, this unconformity typically represents middle Eocene bathyal mudstones resting on Paleocene nonmarine strata or Cretaceous marine and nonmarine clastics. However, in three wells (table 2), the middle compaction trend extends down into Paleocene or Cretaceous rocks.

The lower compaction trend appears to involve a section of marine volcanic-rich clastics, which are as young as probable late Eocene and, in the ARCO COST No. 1 well, as old as Campanian; and a section of nonmarine clastics and coals, which are as old as Maastrichtian in the Exxon Redwood No. 1 and Amoco Danielle No. 1 wells.

Table 2. Characteristics of compaction trends.

Compaction Trend	Well Name and Operator	Depth (feet)*		Age of Strata Involved
		Top	Bottom	
UPPER	ARCO COST No. 1	432	3,755	Pleistocene - l. Miocene
	AMOCO George No. 1	480	3,464	l. Pleistocene - l. Miocene
	ARCO Packard No. 1	541	3,614	e. Pliocene - l. Miocene
	EXXON Redwood No. 1	483	3,914	e. Pliocene - poss. e. Miocene
	EXXON Redwood No. 2	481	4,014	e. Pleistocene - poss. e.-m. Mio.
	AMOCO Nancy No. 1	452	3,814	l. Pleistocene - m. Miocene
	AMOCO Misha No. 1	473	3,909	(?) - e. Miocene
	AMOCO Danielle No. 1	393	3,064	e. Pleistocene - Olig.-e. Miocene
	AMOCO Nicole No. 1	443	3,785	Pleistocene - m. Miocene
MIDDLE	ARCO COST No. 1	3,755	15,215	l. Miocene - L. Cretaceous
	AMOCO George No. 1	3,464	8,999 TD	l. Miocene - L. Cretaceous
	ARCO Packard No. 1	3,614	13,655 TD	l. Miocene - l. Eocene(?)
	EXXON Redwood No. 1	3,914	7,844	poss. e. Miocene - l. Eocene
	EXXON Redwood No. 2	4,014	11,484 TD	poss. e.-m. Mio. - m.-l. Eocene
	AMOCO Nancy No. 1	3,814	8,622 TD	e. Miocene - L. Cretaceous
	AMOCO Misha No. 1	3,909	6,354	e.-m. Miocene - Paleocene
	AMOCO Danielle No. 1	3,064	7,204	Olig.-e. Miocene - l. Eocene
	AMOCO Nicole No. 1	3,785	10,430	poss. e.-m. Mio. - L. Cretaceous(?)
LOWER	ARCO COST No. 1	15,215	16,315 TD	Maastrichtian - Campanian
	EXXON Redwood No. 1	7,844	11,450 TD	l. Eocene - L. Cretaceous
	AMOCO Misha No. 1	6,354	7,876 TD	Paleocene - E. Cretaceous
	AMOCO Danielle No. 1	7,204	9,959 TD	L. Cretaceous
	AMOCO Nicole No. 1	10,430	10,945 TD	L. Cretaceous(?)

*Measured depth below mean sea level.

6 Pore Pressures and Present-Day Stress Directions and Magnitudes

The state of in situ stress is calculated in an approximate way by utilizing leak-off pressures, which are routinely measured in wells. When measured leak-off pressures are combined with integrated density data and calculated hydrostatic pressures, not only the relative magnitude, but also the disposition (vertical versus horizontal) of the three major stress axes can be discovered. This can be extrapolated to inferences about tectonic regime, although actual compass orientations of stress axes cannot be determined. In addition, inferences about microfracture porosity and permeability development can be made using the computed magnitudes of the stresses. The occurrence of microfracture porosity and permeability will in turn have implications for the maintenance of abnormal pressures within the sedimentary section.

It is customarily assumed that all three axes of earth stress are oriented either vertically or horizontally; that is, one parallels the line of gravitational attraction. Therefore, overburden stress (S_v), determined by integrating a density log from a well, is equated to one of the three principal stresses. The other two stress directions are horizontal, but in unknown directions.

The minimum horizontal compressive stress (S_{HMIN}) is equated to the leak-off pressures (P_1) measured over short open-hole intervals (Ervine and Bell, 1987). Leak-off tests record pressures required to fracture shales or other impermeable rocks and are listed for each well on the figure depicting geologic time scale, lithology, wireline log information, and pore pressure. The maximum horizontal compressive stress (S_{HMAX}) is related to leak-off pressure and hydrostatic pressure (P_0) measured over the same interval by the equation:

$$S_{HMAX} = 2P_1 - P_0$$

Table 3 summarizes the stress analysis for each of the wells and lists the magnitude and orientation of the maximum and minimum principal stress axes.

Two tectonic regimes exist within the Navarin basin and are delimited by this stress analysis method. One regime has the principal stress directed vertically, an orientation associated with normal-fault tectonics. The other regime has principal and minor

Table 3. Results of stress analysis for each well. An asterisk indicates the possibility of microfracture development (differential stress equals one-half to two-thirds the stress at ultimate failure, or SH_{MIN}). Question mark indicates suspect data.

Well Name and Operator	Depth (feet) Below Sea Level	P_o (psi)	SH_{MIN} (psi)	SH_{MAX} (psi)	S_v (psi)	Stress Orientation	Differential Stress (psi)	Differ'l Stress divided by SH_{MIN}
ARCO Packard No. 1	1,574	687	785	883	1,143	σ_1 vert., σ_3 horz.	98	0.12
	4,512	2,018	2,806	3,594	2,620	σ_1 horz., σ_3 horz.	788	0.28
	11,328	4,949	7,628	10,307	9,997	σ_1 horz., σ_3 horz.	2,679	0.35
ARCO COST No. 1	1,423	636	797	985	1,042	σ_1 vert., σ_3 horz.	188	0.24
	4,913	2,205	3,244	4,283	3,820	σ_1 horz., σ_3 horz.	1,034	0.32
	12,749	7,208	10,159	18,290	11,528	σ_1 horz., σ_3 horz.	8,131	0.80*
AMOCO Misha No. 1	1,711	791	984	1,177	1,209	σ_1 vert., σ_3 horz.	193	0.20
	3,140	1,452	1,839	2,266	2,262	σ_1 vert., σ_3 horz.	427	0.23
AMOCO Nicole No. 1	1,586	692	864	1,036	1,028	σ_1 horz., σ_3 horz.	172	0.20
	3,844	1,778	2,390	3,002	2,695	σ_1 horz., σ_3 horz.	612	0.26
AMOCO Nancy No. 1	1,709	1,148	905?	662?	1,212	σ_1 vert., σ_3 horz.	550?	0.61*?
	4,099	1,791	2,318	2,845	3,020	σ_1 vert., σ_3 horz.	527	0.23
AMOCO Danielle No. 1	642	330	330	330	333	σ_1 vert., σ_3 horz.	0	0.00
	1,465	790	730?	670?	952	σ_1 vert., σ_3 horz.	282?	0.39?
	3,828	1,869	2,322	2,775	2,803	σ_1 vert., σ_3 horz.	453	0.20
EXXON Redwood No. 1	1,534	710	975	1,240	1,127	σ_1 horz., σ_3 horz.	265	0.27
	4,043	1,872	2,556	3,240	2,227	σ_1 horz., σ_3 horz.	684	0.27
	9,014	5,093	6,581	8,069	7,825	σ_1 horz., σ_3 horz.	1,488	0.23
EXXON Redwood No. 2	1,544	675	936	1,197	—	—	261	0.88
	4,543	1,985	2,966	3,830	—	—	864	0.29
	9,084	5,510	6,630	7,750	—	—	1,120	0.17
AMOCO George No. 1	1,729	1,022	928	1,116	1,289	σ_1 vert., σ_3 horz.	188	0.20
	3,925	2,017	2,455	2,893	2,935	σ_1 vert., σ_3 horz.	438	0.18

Abbreviations: P_o , hydrostatic pressure; SH_{MIN} , minimum horizontal stress; SH_{MAX} , maximum horizontal stress; S_v , overburden, or vertical, stress; Differential Stress (also Differ'l Stress), $SH_{MAX} - SH_{MIN}$.

stresses directed horizontally, an orientation associated with strike-slip tectonics.

Figure 22 maps stress states as determined from Navarin basin wells. A central zone of horizontally directed stresses (the strike-slip regime) trends northwestward across the entire basin. This zone corresponds to the central Navarin wrench fault, independently interpreted from structural mapping as a fundamental strike-slip tectonic element of the basin.

Abnormal pore pressures influence the development of microfractures, which in turn may drain excess pore fluids and limit the extent of the overpressuring. Microfractures near or intersecting the wellbore are indirectly inferred by wireline logs such as the Schlumberger Fracture Index log. However, when these less frequently acquired logs are not available, stress evaluation can be used as an alternative method of predicting microfracture occurrences.

Brace (1968) found that microfractures only develop when the differential stress magnitude—the difference between S_{HMAX} and S_{HMIN} —reaches one-half to two-thirds the stress at ultimate failure. In this report, it is assumed that the ultimate failure stress is approximated by the fracture gradient measured in the wellbore and is equal to the minimum horizontal compressive stress (S_{HMIN}) (table 3). With this criterion for microfracture development, only two wells (ARCO COST No. 1, Nancy No. 1) showed evidence for fracturing to be present. In both wells, fracturing would occur within an overpressure zone, and drainage of the pore fluids along microfractures becomes plausible. The remainder of the wells showed little or no possibility of fracture permeability, which is one of the reasons abnormal pore pressures are ubiquitous.

To corroborate the results of the Brace (1968) method in the prediction of microfracture development, a proposition of Gretener (1981) is applied. Gretener states that when pore pressure (P_o) rises to a point where it equals overburden pressure (S_v), then a state of flotation exists and microfractures are sure to be generated. In a comparison of P_o and S_v on table 3, no wells were found to meet this condition. More specifically, microfractures are unlikely in the abnormal pore pressure zones of the ARCO COST No. 1 well and the Nancy No. 1 well, where microfractures are predicted by the Brace (1968) method.

The results of predicting microfracture development are inconclusive. Overall, stress conditions encountered by the wells, for the most part, appear not conducive to the generation of microfractures and the resulting fracture porosity and permeability. The apparent lack of fracture permeability bodes well for the development and maintenance of abnormal pressure conditions in the impermeable portions of the stratigraphic column. However, the

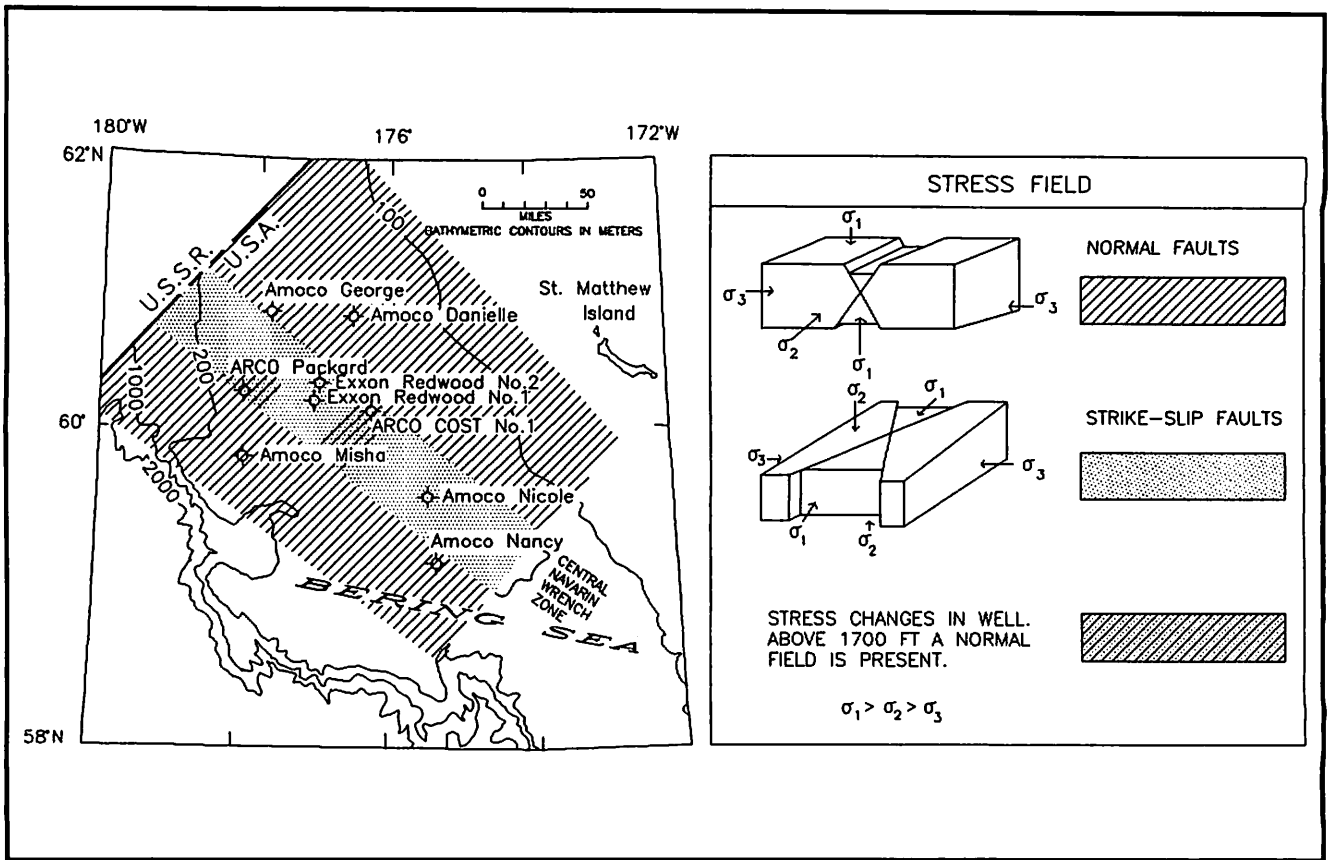


Figure 22. Current stress pattern of the Navarin continental shelf based on well pressure data.

deeper occurrence of the zone within the strike-slip regime implies some type of structural control. The exact form and extent at this juncture are undefinable.

7 Abnormal Pore Pressures and Shale Diapirism

The presence of a regional stratigraphic section prone to abnormal pore pressures will have an effect on the stability of the sediments, the movement of pore fluids (including oil and gas), and the structural disruption caused by present-day stresses. In the Navarin basin, a secondary effect of deep-seated abnormal pressures is the generation of shale diapirs. Shale diapirs result when overpressured, and therefore plastic, shale is destabilized by uneven overburden pressures and the diapir rises by piercing the overlying strata to reach a balanced hydrostatic environment (Gretener, 1981).

A middle Eocene to early Oligocene seismic sequence is identified by Turner and others (1985) as the source for shale diapirs in the northern Navarinsky subbasin (figs. 3 and 23). Basinwide well penetrations indicate that the sequence is everywhere made up of shale (fig. 23). These fine-grained materials are identified as being within overpressure zone 2.

Hedberg (1976) suggested that methane formation in organic-rich shales might enhance their instability. The presence of an unsampled gas plume over the flank of a shale diapir in the Navarinsky subbasin (Carlson and Marlow, 1984) may suggest gas-enhanced diapirism. At the ARCO COST No. 1 well, the source (diapiric) sequence lies within the oil window and contains kerogen suitable for wet-gas generation.

The diverging stratal surfaces of this seismic sequence indicate continuous, rapid sedimentation. Rapid sedimentation dilutes organic content but increases the likelihood of preservation of trapped organic matter by enhancing anoxic conditions near the seafloor (Anstey, 1977).

Diapiric movement occurred no later than middle Miocene (fig. 23). Eventually, the diapirs were truncated by an erosional surface, the middle Miocene unconformity (horizon A, fig. 23).

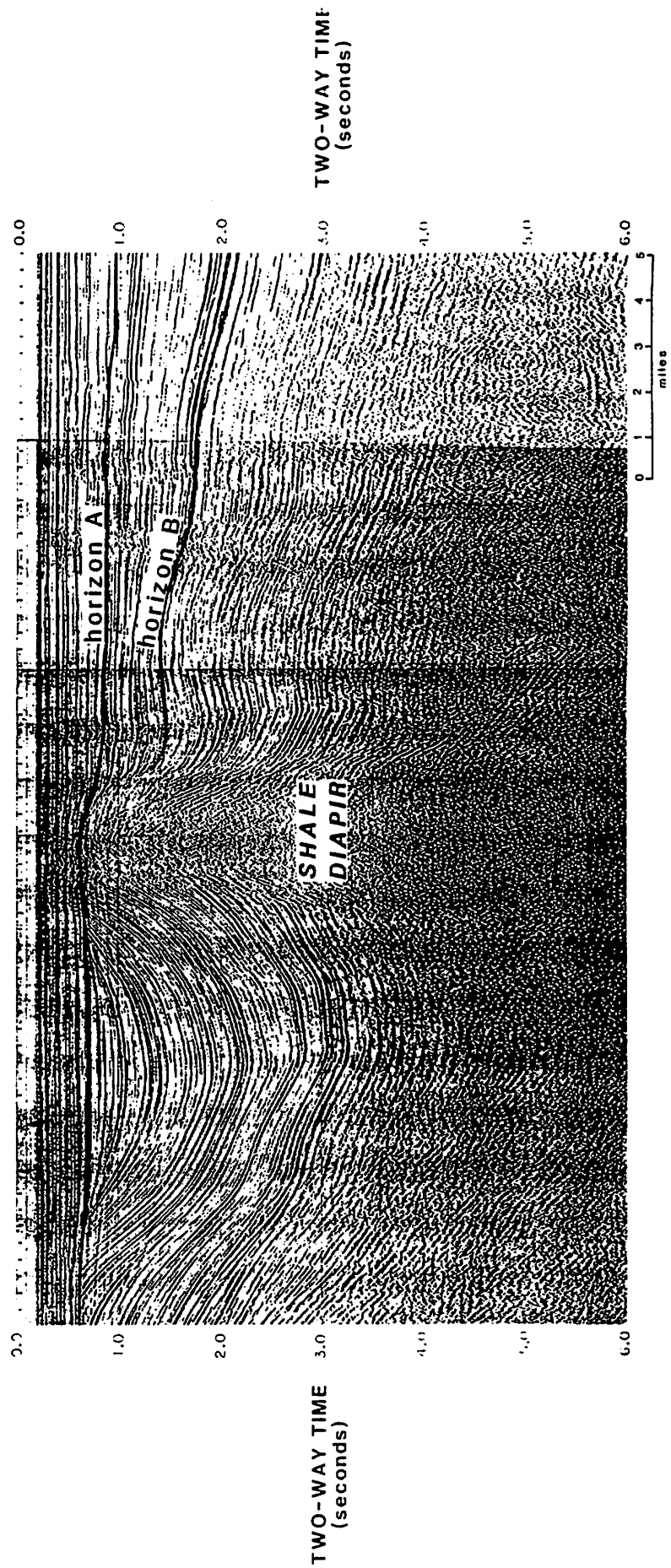
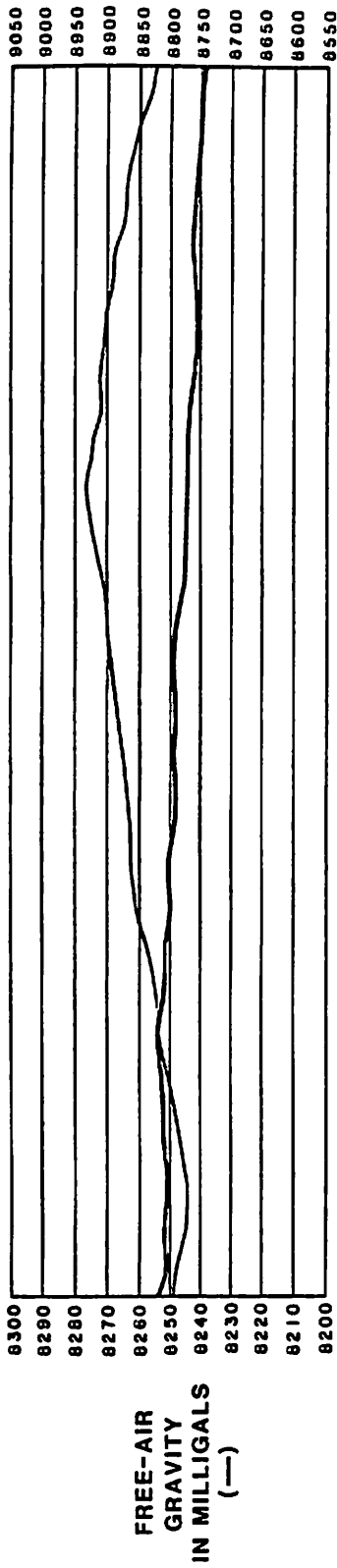


Figure 23. Seismic profile, free-air gravity profile, and filtered magnetics profile of a shale diapir (adapted from Turner and others, 1985). Location of seismic profile is shown on figure 3.

8 Mechanisms of Abnormal-Pressure Production and Maintenance

Mechanisms for producing overpressure are of two types: (1) mechanisms that produce excess head throughout the sedimentary section (such as fossil pressure and tectonic compression); and (2) mechanisms that involve impedance of flow of "excess" fluids from a source layer.

Most overpressure systems recognized in sedimentary basins such as the Navarin involve source-layer mechanisms. Common mechanisms for development of excess water in a source layer are: compaction disequilibrium, thermal expansion of pore fluids ("aquathermal" effects), and diagenetic processes that alter the volume of pores or pore fluids.

Overpressure Zone 1

In all nine wells, a shallow occurrence of abnormal pressure, termed zone 1, lies within a late Miocene to late Pliocene section of diatom-rich clays that are drained by calcareous sands and clays above and are sealed by a cemented, impermeable section below. Pressures within zone 1 range between 8.7 and 14.5 ppg EMW (0.447 and 0.745 psi/ft). The top of zone 1 ranges in depth from 1,264 to 2,415 ft below sea level, and the zone averages 1,500 ft in thickness.

Table 4 characterizes abnormal-pressure zone 1 for all wells used in this study. Similarities for this zone across all wells include:

- the age of the involved section
- the depth of overpressuring
- the lithology of the section
- the presence of a reduced porosity section immediately below the abnormal-pressure zone
- the presence of a permeable section above the zone
- the temperature at the base of the abnormal-pressure zone

Table 4. Characteristics of abnormal-pressure zone 1.

Well Name and Operator	Location on Well Log (feet)			Age	Sediment Type	Bulk Density (g/cm ³)	Conductivity range (mmhos)	Pressures (ppg)		Lowest Stratigraphic Occurrence of Identifiable Siliceous Microfossils (feet)	Temp. at Bottom of Lower Seal (°F)
	Top	Bottom	Base of Bottom Seal*					Range	Average		
ARCO Cost No. 1	2,415	3,425	3,755	l. Miocene- e. Pliocene	diamt mdst + ooze	1.65-1.75	1,250	9.0-10.7	10.0	3,631	125
EXXON Redwood No. 1	1,779	3,364	3,914	e. Pliocene- l. Pliocene	clay	1.50-1.82	606-869	9.0-13.5	10.6	3,854	120
EXXON Redwood No. 2	1,475	3,774	4,014	l. Miocene- l. Pliocene	clay	—	454-833	8.7-11.0	10.0	3,894	122
ARCO Packard No. 1	1,834	3,364	3,614	l. Miocene- e. Pliocene	claystone	1.55-1.87	500-690	9.5-11.5	10.0	3,794	90
AMOCO George No. 1	1,764 (TOL**)	2,914	3,464	l. Miocene- e. Pliocene	claystone	1.55-1.85	625-800	9.0-14.5	12.0	3,514	93
AMOCO Danielle No. 1	1,264	2,634	3,064	l. Miocene- e. Pliocene	claystone	1.60-1.93	606-725	9.2-11.7	10.5	3,064	101
Amoco Misha No. 1	1,434	3,084	3,909	l. Miocene- l. Pliocene	clay	1.63-1.85	500-625	9.2-11.7	10.6	3,844	82
Amoco Nancy No. 1	1,650	3,514	3,814	l. Miocene- e. Pliocene	claystone	1.63-1.95	333-625	10.5-14.3	13.2	3,844	112
Amoco Nicole No. 1	2,155	3,785	3,785	l. Miocene- e. Pliocene	radiolarian shale	1.59-1.72	455-617	8.5-11.0	10.6	3,817	123

*Base of bottom seal and of upper compaction trend.
**Top of log.

Figure 25 (page 67) is a northeast-southwest geologic cross section of the Navarin basin through four wells. Correlation of paleontologic tops, unconformities, and major facies changes (marine and nonmarine) are displayed. The cross section clearly illustrates the stratigraphic position of overpressure zone 1. The position is a result of the source-layer mechanism envisioned for the formation of zone 1 and the lithologic features producing the top and bottom seals required for the maintenance of the excess pore pressures.

The depth and physical characteristics of this overpressure zone suggest that the high pore pressures result from the same dual mechanisms that Sherwood (1984) inferred for this zone in the ARCO COST No. 1 well, that is, pore space reduction and increased pore water volume consequent to silica diagenesis. Pore space reduction is due to the collapse of the structural framework as a result of clay particle realignment and silica dissolution. Excess pore water originates from opal dissolution and mechanical compaction of clays.

The primary mechanism of generating excess pore pressure in zone 1 is probably the mechanical dewatering of clays as a consequence of compaction-related pore volume reduction. These processes are part of the "first-stage" dewatering as defined by Burst (1969). In the first-stage of dewatering, pore waters and excess interlayer waters are expelled in response to compaction and the reduction of pore space. The total water content is commonly reduced from 70-80 percent to 30 percent. This expulsion of fluids occurs within the first few thousand feet of burial. A bulk density increase from 1.32 to 1.95 g/cm³ is observed to accompany this expulsion of water in sediments of the Gulf of Mexico. After this initial dewatering, little additional pore water can escape because of reduced porosity and permeability.

A second mechanism of pore reduction in zone 1 is a collapse of pore walls due to dissolution of abundant diatoms or other siliceous microfossils (Sherwood, 1984). In addition, some water is added to pore fluids by the two-phase transformation of opal-A (biogenic material) to opal-CT, and opal-CT to quartz. This two-phase transformation commences between the temperatures of 102 and 120 °F, and may result in a porosity reduction of 15 to 30 percent (Powers, 1967). In the Navarin basin, the base of abnormal-pressure zone 1 is associated with temperatures ranging from 82 to 125 °F (average, 109 °F). A porosity reduction of 20 percent is associated with the base of zone 1.

At all locations, siliceous microfossils are present above the base of abnormal-pressure zone 1 but are depleted or absent immediately below the base. The results of dissolution are seen on the scanning electron photomicrograph of the diatom *Coscinodiscus marginatus* taken from 3,360 ft in the Amoco Danielle No. 1 well (fig. 24, next page). The photomicrograph shows the surface detail obscured by

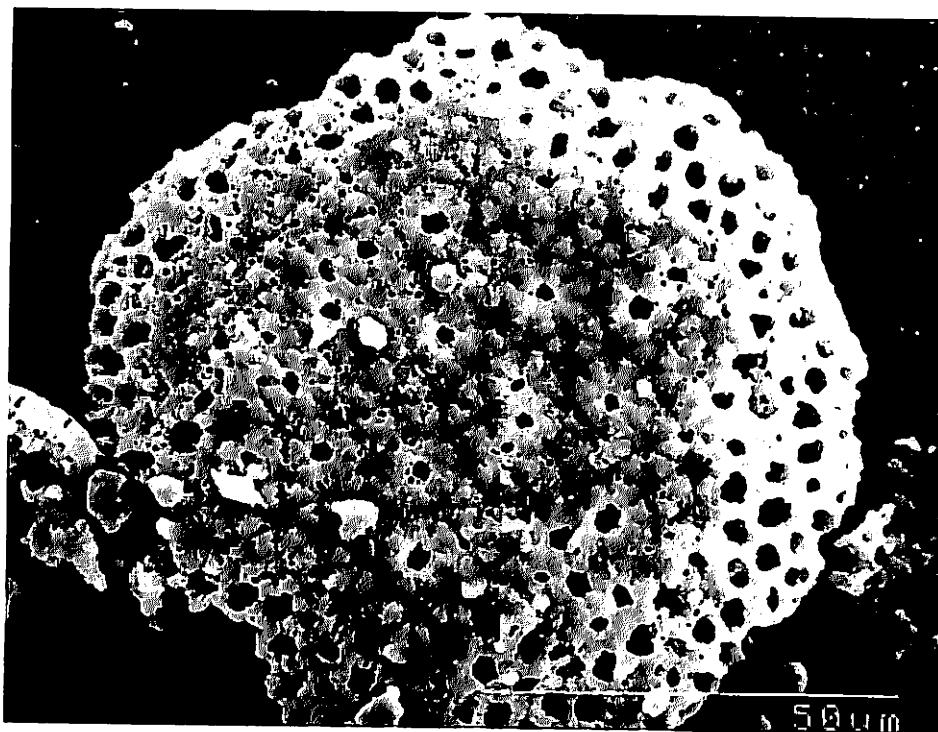


Figure 24. Scanning electron microscope photomicrograph of the diatom Coscinodiscus marginatus magnified 1,000 times.

precipitation of silica, the rounding of the pore edges, and the general destruction of the diatom. The fossils are presumed absent because of dissolution in a hostile thermal environment. The disappearance of fossils is associated with the disappearance of opal and the appearance of authigenic quartz and clay minerals. In the ARCO COST No. 1 well, dissolution of opal-A biogenic material is the dominant diagenetic process within abnormal-pressure zone 1. Below the zone, authigenic silica and clay minerals are observed to fill pores and restrict flow.

The clays in abnormal-pressure zone 1 feature porosities of up to 60 percent. Below zone 1, clays feature porosities of only 40 percent. This reduction in porosity resulted in the formation of a bottom seal immediately below overpressure zone 1. This bottom seal is required to maintain the negative pressure gradient at the bottom of zone 1. The existence of these negative pressure gradients is suggested by the log data but has not been confirmed by direct measurements anywhere in the basin.

Table 4 (page 64) compares the depths for the lowest occurrence of identifiable siliceous microfossils and the bottom seal for zone 1 in each well. The error in identification of the lowest fossil occurrence is ± 90 ft, reflecting sampling and processing intervals

(Olson, personal commun., 1990). On average, the lowest occurrence of siliceous microfossils occurs within 76 ft of the base of the seal which floors zone 1, which is also the bottom of the upper compaction trend. This coincidence suggests that the disappearance of the fossils is related to silica diagenesis, which is in turn linked to the overpressure phenomenon.

No "cap rock" forms the upper limit for abnormal-pressure zone 1. Instead, the uppermost part of zone 1 at each well occurs at a basinwide facies transition into early to late Pliocene sandy mudstones and sandstones (with increased porosities and permeabilities). Evidently, these permeable rocks act as a drainage layer and thereby form the upper limit of abnormal-pressure zone 1.

Overpressure Zone 2

Overpressure zone 2 is found in deep parts of eight of the nine Navarin basin wells (table 5). Pressures within zone 2 range between 9 and 16 ppg EMW (0.463 and 0.822 psi/ft). The top of zone 2 ranges in depth from 4,469 to 11,239 ft below sea level. The magnitude of overpressuring in zone 2 is unrelated to the depth of its occurrence. Zone 2 involves chiefly Oligocene and Eocene rocks, although Paleocene and Cretaceous rocks are involved in some parts of the basin. The Amoco George No. 1 well was the only well that did not encounter overpressure zone 2. The position of overpressure zone 2 is depicted on a northeast-southwest geologic cross section of the Navarin basin (fig. 25).

The cause of this deeper zone of abnormal pressure is less rigorously documented than for zone 1. Sherwood (1984) attributed overpressure zone 2 in the ARCO COST No. 1 well to entrapment of water expelled from clays into pores during illitization of smectites.

This mechanism was originally described by Burst (1969). The process is basically a thermally driven desorption of water from clay crystal lattices into intergranular pores (Powers, 1967). The water is thought to require 40 to 50 percent more volume when expelled than it did when locked in the clay crystal lattice. This expulsion of structural water is accompanied by a rearrangement of the crystal lattice and is part of the conversion of expandable clays or smectites to illites. Illitization is observed over a temperature range of 200 to 300 °F, with a critical temperature of 221 °F for transformation (Burst, 1969). Burst (1969) noted that this transformation is accompanied by a bulk density increase of 1.96 to 2.28 g/cm³.

Table 5 compares the depth of the 200-°F isotherm to the depth of overpressure zone 2 for each well. For all wells identified as lying within a strike-slip tectonic regime, the 200-°F isotherm lies above or within overpressure zone 2. In these wells, the thermal conditions are appropriate for smectite dehydration in overpressure zone 2. In contrast, for the three wells that lie within a normal-fault tectonic regime, zone 2 lies above the depth of the 200-°F isotherm (table 5).

Impermeable mudstones separate the 200-°F isotherm from the overlying zone 2. Indigenous smectite illitization cannot have caused the abnormal pore pressures in zone 2 in these wells.

The actual contribution of smectite dehydration to abnormal pore pressure is controversial and is denied by some researchers (Mann and Mackenzie, 1990). Colten-Bradley (1987), in fact, argues forcefully that smectite dehydration requires low pore pressure and a well-drained pore system. She points out that if abnormal pore pressures did develop, then conditions would favor rehydration and inhibit further dehydration of the smectite.

Abnormal pore pressures are often a consequence of compaction disequilibrium (Exlog, 1980). Equilibrium occurs when the balance between rate of burial (compaction) and rate of pore network drainage for a basin is maintained such that dewatering of the sediments is unimpeded and pore pressures remain hydrostatic. Compaction disequilibrium occurs when sediments are loaded at a rate exceeding the rate of dewatering, resulting in abnormal pore pressures. This process is believed to be the primary cause of the large overpressures seen in major basins in the North Sea, the Gulf of Mexico, Norway, and the Nile Delta (Mann and Mackenzie, 1990).

The stratigraphic setting of the Navarin basin promoted the development of compaction disequilibrium and the resultant overpressuring. Well data indicate that Paleogene sediments in the basin are a thick, monotonous sequence of impermeable, fine-grained clastics. These sediments filled a rapidly subsiding basin in which water depths progressively deepened with time (Turner and others, 1985). These dual characteristics of high sedimentation rate and impermeable fill provided the necessary conditions for compaction disequilibrium.

In a closed system with a geothermal gradient above 0.82 °F/100 ft, excess hydrostatic pressures can be generated by thermal expansion of pore fluids, or "aquathermal pressuring" (Barker, 1972). If sedimentary rocks become so hydrodynamically isolated (because of low permeabilities) that the mass and volume of the closed system are constant, then any rise in temperature will result in a rise in pressure which is larger than what would occur in the surrounding normally pressured area (Barker, 1972). The rise in pressure within this closed system is due to thermal expansion of pore fluids. The magnitudes of these aquathermal pressures are dependent on the depth of burial and the size of the isolated volume.

In four of the eight wells, sufficient data were available to calculate the aquathermal effect for overpressure zone 2 using the method of Barker (1972) (table 5). In these wells, aquathermal pressure could account for 15, 60, 92, and 100 percent, respectively, of the observed pressure anomaly.

In summary, zone 2 abnormal pressures in the Navarin basin are probably due to some combination of compaction disequilibrium, aquathermal pressure, and, to a lesser extent, smectite-to-illite transformation. Segregating the quantitative contributions of these processes is not possible. However, Barker (1972) does provide a quantitative method to evaluate the potential contribution from the aquathermal effect.

In the ARCO COST No. 1 well, Sherwood (1984) correlated a log-defined cap rock at the top of overpressure zone 2 with the presence of a "shale, light to medium gray, hard, silty, non- slightly-calcareous, with abundant fossils," and a carbonate content (calcite, ankerite, and siderite) of from 1.4 percent (at a depth of 8,639 to 8,649 ft) to 3.5 percent (at a depth of 9,402 to 9,430 ft).

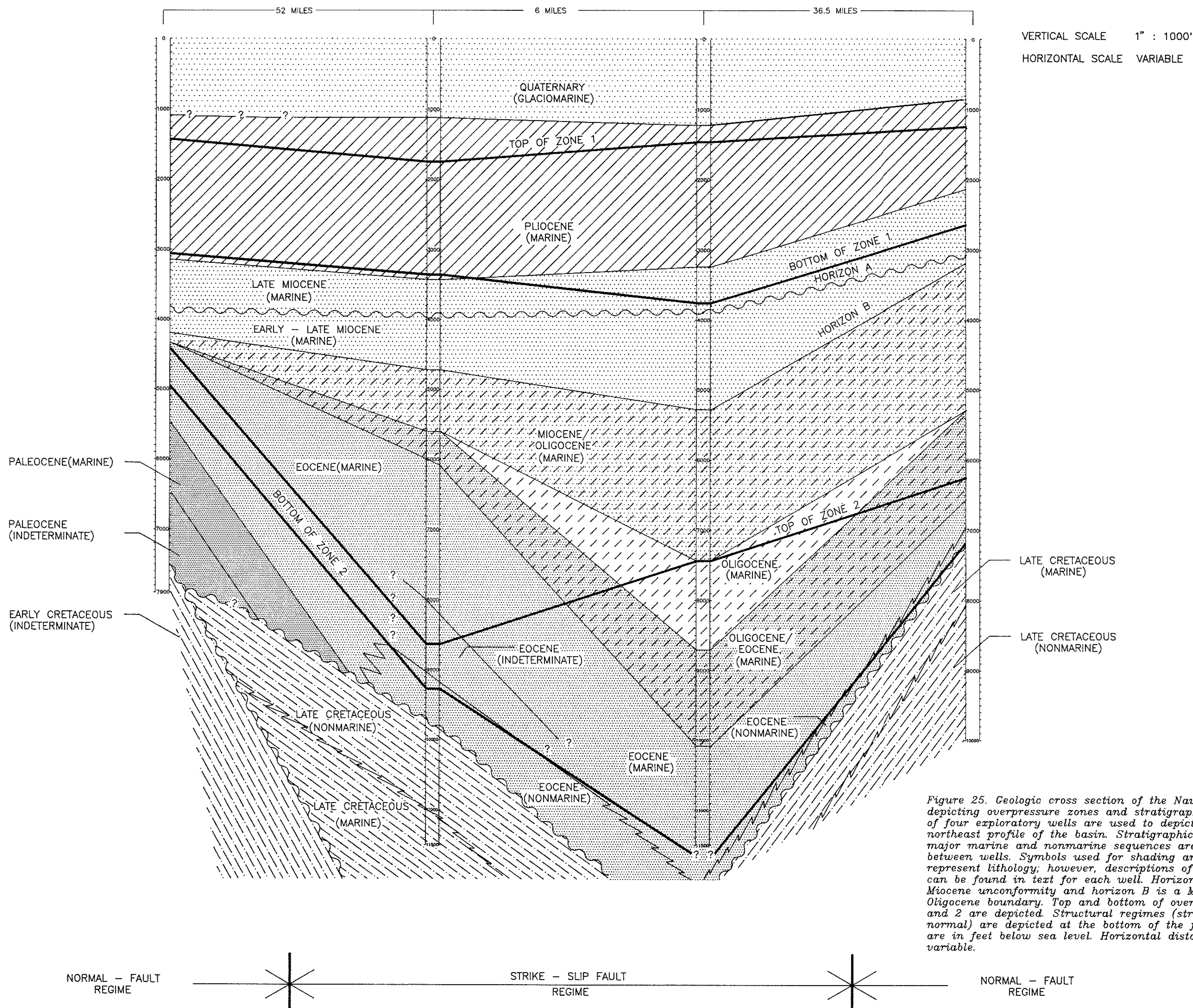
This cap rock is less well developed or absent in other parts of Navarin basin. In other parts of the basin, a relatively thick sequence of impermeable Oligocene claystone seals at varying levels the top of overpressure zone 2.

In wells where zone 2 is deep enough for illitization to occur, some sealing effects may result from Freed and Peacor's (1989) model for diminishment of permeability due to pore occlusion by authigenic illites. This may explain why the tops of overpressured zones commonly correspond worldwide to the onset of illitization (Colten-Bradley, 1987).

The top of overpressure zone 2 within the strike-slip zone (fig. 25) ranges from 7,065 to 11,239 ft. In contrast, the depth to the top of overpressure zone 2 within the normal-fault regime ranges from 4,469 to 6,259 ft (table 5). The systematic difference in depth to overpressure between the two structural regimes is intriguing. The depth contrast may reflect different depths for seals, which mark the depth to which open microfractures persist within the Tertiary section. This relationship cannot be proven at this juncture, however, since an analysis of compressive stresses calculated using well data reveals no evidence for microfracture porosity development in either tectonic regime.

The geologic cross section (fig. 25) illustrates the following features of overpressure zone 2:

- the top of zone 2 (a seal?) cuts across both time boundaries and lithologic facies (marine and nonmarine)
- the top of zone 2 deepens in the strike-slip regime
- the depth of the zone changes rapidly, especially between Redwood Nos. 1 and 2 wells



VERTICAL SCALE 1" : 1000'
 HORIZONTAL SCALE VARIABLE

Figure 25. Geologic cross section of the Navarin basin depicting overpressure zones and stratigraphy. Results of four exploratory wells are used to depict a southwest-northeast profile of the basin. Stratigraphic tops and major marine and nonmarine sequences are correlated between wells. Symbols used for shading are not meant to represent lithology; however, descriptions of lithology can be found in text for each well. Horizon A is a "middle" Miocene unconformity and horizon B is a Miocene--Miocene/Oligocene boundary. Top and bottom of overpressure zones 1 and 2 are depicted. Structural regimes (strike-slip, normal) are depicted at the bottom of the figure. Depths are in feet below sea level. Horizontal distances are variable.

NORMAL - FAULT REGIME

STRIKE - SLIP FAULT REGIME

NORMAL - FAULT REGIME

- the vertical extent of zone 2 is greatest where the sedimentation rates have been greatest (i.e., where the zone has been buried the deepest)
- the structure of the top of the zone mimics the structure at the Miocene–Miocene/Oligocene boundary (horizon B) in most areas

These observations suggest that the top of overpressure zone 2 was originally horizontal throughout the basin sometime prior to structuring of the Miocene–Miocene/Oligocene boundary (fig. 25). Overpressure zone 2 cuts across both time and facies boundaries inclined toward the basin axis. Overpressure zone 2 is attributed to compaction disequilibrium. Compaction disequilibrium is considered responsible for the zone because: (1) the shallowest occurrences of overpressure zone 2 (table 5: Misha No. 1, Danielle No. 1, and Nancy No. 1) presently lie above the 200-°F isotherm, ruling out smectite conversion, and (2) aquathermal pressuring of these same occurrences can account for only some fraction of the excess pressure (as seen in the Misha No. 1 well, where only 15 percent of excess pore pressure could be caused by aquathermal effects).

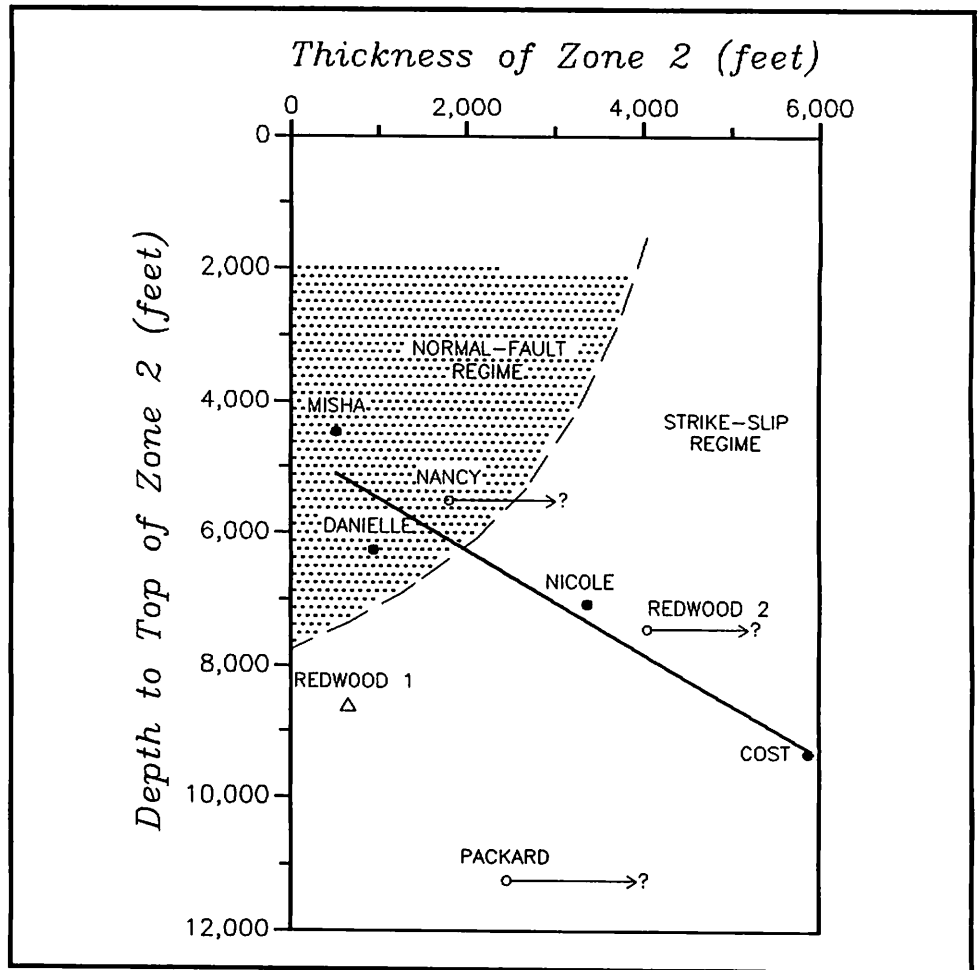
Subsequent burial of the overpressure zone augmented excess pore pressures by other processes such as illitization and aquathermal effects in some parts of the basin.

The cross-cutting relationship of overpressure and stratigraphy has been noted by Hunt (1990) in his study of deep overpressure zones throughout the world, including the Cook Inlet and North Slope of Alaska. In addition, Hunt (1990) characterizes deep overpressure zones as being compartmentalized, that is, the zone is not continuous but consists of individual compartments isolated by seals that prevent hydrodynamic communication with other overpressure zones or the overlying rock. The only evidence suggestive of pressure compartmentalization in the Navarin basin is the rapidly changing depth (1,195 ft) of the top of zone 2 which occurs over the 6-mile distance that separates the Exxon Redwood Nos. 1 and 2 wells. This significant change in elevation of zone 2 could indicate the isolation of individual compartments of overpressured pore fluids with depth throughout the basin.

Presently, the deepest occurrences of overpressure zone 2 are along the basin axis where most stratigraphic units achieve maximum thickness. Figure 26 depicts this relationship as a plot of present-day depth to top of zone 2 versus zone thickness. A linear relationship is drawn using only those wells that encountered the top of zone 2 in the middle compaction sequence and that also penetrated the bottom of the zone.

The role of structural geology in the evolution of abnormal pore pressure in the Navarin basin remains an enigma. Tectonic stress

Figure 26. Graph showing relationship between burial depth and thickness of overpressured zone 2. Solid circles are wells that penetrated the entire zone. Open circles are wells that only partially penetrated. Open triangle indicates a well that encountered the top of zone 2 in the lower compaction sequence and the bottom of the zone was also penetrated. A least-squares fit was made using only the solid circles.



state might control the depth of microfracture development, although this cannot be shown. However, zone 2 is consistently deeper in the part of the basin where a strike-slip regime prevails. This hints that stress-state may influence overpressure depth through some subtle control of microfractures and seal integrity.

Conclusions

By use of well-log information and direct pressure measurements, two zones of overpressuring were identified in eight of the nine Navarin basin wells. A shallow occurrence of abnormal pressure, termed zone 1, with pore pressures ranging up to 14.5 ppg EMW (0.745 psi/ft) (table 4, Amoco George No. 1), lies within a late Miocene to late Pliocene section of diatom-rich clays that are drained above by calcareous sands and clays and sealed below by a cemented, impermeable section. Dual mechanisms appear to have caused the overpressuring in zone 1: (1) pore reduction due to compaction and framework collapse of siliceous microfossil tests (in response to pressure-temperature conditions); and (2) the expulsion of water associated with mechanical dewatering and the dissolution of microfossil tests.

The deeper occurrence of abnormal pressure, termed zone 2, with pore pressures ranging up to 16 ppg EMW (0.822 psi/ft), lies within a Late Cretaceous to Oligocene-early Miocene section of clastics. Overpressure in zone 2 is probably caused by the combined effects of illitization, compaction disequilibrium, and aquathermal pressuring. Compaction disequilibrium is likely to be present, given the rapid accumulation of large volumes of impermeable fine-grained clastics in Navarin basin, but its impact on excess pore pressure development is unassessable. Illitization is a controversial mechanism for generating large pore pressures. Generally, the thermal regime and clay composition of the Paleogene section in the Navarin basin are appropriate for illitization to occur. Illitization was found to be less probable in the three wells (Amoco Nancy No. 1, Amoco Misha No. 1, Amoco Danielle No. 1) located in the normal-fault tectonic regime because of low geothermal gradients. In contrast, where analyzed, aquathermal pressuring can account for 15 to 100 percent of the excess pore pressures calculated.

Cap rock for zone 2 is a calcareous shale in the ARCO COST No. 1 well, whereas in all the exploratory wells a less definitive seal of impermeable Oligocene claystone is present. The magnitude of overpressure in zone 2 is not related to depth, but the vertical extent does increase with depth.

The depth to the top of zone 2 is greater in the strike-slip tectonic regime than in the normal-fault tectonic regime. Although not

proven, microfracture development which could be controlled by regional tectonics may account for the differences.

Diapirs in the northern flank of the Navarin basin are believed to be a side effect of zone 2 overpressuring.

References

- Anstey, N. A., 1977, Seismic interpretation - the physical aspects. Boston: International Human Resources Development Corporation.
- Barker, C., 1972, Aquathermal pressuring - role of temperature in development of abnormal-pressure zones. American Association of Petroleum Geologists Bulletin, v. 56, no. 10, p. 2068-2071.
- Brace, W. F., 1968, The mechanical effects of pore pressure on fracturing of rocks. Geological Survey of Canada Paper 68-52, p. 113-124.
- Bredehoeft, J. B., and Hanshaw, B. B., 1968, On the maintenance of anomalous fluid pressures, I: Thick sedimentary sequences. Geological Society of America Bulletin, v. 79, p. 1097-1106.
- Burst, J. F., 1969, Diagenesis of Gulf Coast clayey sediments and its possible relation to petroleum migration. American Association of Petroleum Geologists Bulletin, v. 53, p. 73-93.
- Carlson, P. R., and Marlow, M. S., 1984, Discovery of a gas plume in Navarin basin. Oil & Gas Journal, 2 April, v. 82, p. 157-158.
- Colten-Bradley, V. A., 1987, Role of pressure in smectite dehydration - effect on geopressure and smectite-to-illite transformation. American Association of Petroleum Geologists Bulletin, v. 71, no. 11, p. 1414-1427.
- Core Laboratories, Inc., 1985a, Core analysis report for Amoco Production Company Nicole No. 1. Dallas, Texas, 19 p.
- Core Laboratories, Inc., 1985b, Core analysis report for Amoco Production Company George Prospect OCS Y-0560. Dallas, Texas, 4 p.
- Core Laboratories, Inc., 1985c, Core analysis report for ARCO Packard Prospect, Bering Sea, Alaska. Dallas, Texas, 6 p.
- Core Laboratories, Inc., 1985d, Core analysis report for Exxon Company, U.S.A., OCS Y-0583 #1 exploratory, Navarin basin, Alaska. Dallas, Texas, 23 p.
- Core Laboratories, Inc., 1985e, Core analysis report for Amoco Production Company Nancy prospect original hole and sidetrack, Navarin basin field, offshore Alaska. Dallas, Texas, 14 p.
- Core Laboratories, Inc., 1985f, Sidewall core descriptions for Amoco Production Company Misha prospect. Dallas, Texas, 13 p.
- Core Laboratories, Inc., 1985g, Geochemical study of the No. 1 Danielle well, Navarin basin, for Amoco Production Company. Dallas, Texas, 116 p.
- Ervine, W. B., and Bell, J. S., 1987, Subsurface in situ stress magnitudes from oil-well drilling records - an example from the Venture area, offshore eastern Canada. Canadian Journal of Earth Science, v. 24, p. 1748-1759.
- Exlog (Exploration Logging of U.S.A., Inc.), 1980, Theory and evaluation of formation pressures - the pressure log reference manual. Applications Manual EL P/N 18792 MS-156. Sacramento, California, 63 p.

- Exlog (Exploration Logging of U.S.A., Inc.), 1985a, Final well report, Amoco Production Company Nicole prospect, OCS Y-0707 #1, Navarin basin, Bering Sea, offshore Alaska, July 7, 1985, to July 24, 1985. Sacramento, California.
- Exlog (Exploration Logging of U.S.A., Inc.), 1985b, Final well report, Amoco Production Company George prospect, OCS Y-0560 #1, Navarin basin, offshore Alaska, August 1985 to September 1985. Sacramento, California.
- Exlog (Exploration Logging of U.S.A., Inc.), 1985c, Final well report, ARCO Packard prospect, OCS Y-0586 #1, Navarin basin, offshore Alaska, August 1985 to October 1985. Sacramento, California.
- Exlog (Exploration Logging of U.S.A., Inc.), 1985d, Final well report, Amoco Production Company Nancy prospect, OCS Y-0719 #1, Navarin basin, Bering Sea, offshore Alaska, October 11, 1985, to November 18, 1985. Sacramento, California.
- Exlog (Exploration Logging of U.S.A., Inc.), 1985e, Final well report, Amoco Production Company Misha Prospect, OCS Y-0673 #1, Navarin basin, Bering Sea, offshore Alaska, August 31, 1985, to October 2, 1985. Sacramento, California.
- Exlog (Exploration Logging of U.S.A., Inc.), 1985f, Final well report, Amoco Production Company Danielle Prospect, OCS Y-0639 #1, Navarin basin, Bering Sea, offshore Alaska, June 19, 1985, to August 3, 1985. Sacramento, California.
- Fertl, W. H., 1976, Abnormal formation pressures. *Developments in Petroleum Science*, 2 ed. New York: Elsevier, 382 p.
- Foster, Jr., J., 1990, Pore-pressure plot accuracy increased by multiple trend lines. *Oil & Gas Journal*, 7 May, v. 88, p. 100-108.
- Freed, R. L., and Peacor, D. R., 1989, Geopressured shale and sealing effect of smectite to illite transition. *American Association of Petroleum Geologists Bulletin*, v. 73, no. 10, p. 1223-1232.
- Geochem Laboratories, Inc., 1985, Results of geochemical analyses on one hundred ninety-two (192) cuttings and cores from OCS-Y-0599 no. (well A) - geochem job no. 3147. Houston, Texas.
- Gretnener, P. E., 1981, Pore pressure - fundamentals, general ramifications, and implications for structural geology (revised). *American Association of Petroleum Geologists Educational Course Note Series #4*, 131 p.
- Hedberg, H. D., 1976, Relation of methane generation to under-compacted shales, shale diapirs and mud volcanoes. *American Association of Petroleum Geologists Bulletin*, v. 58, p. 661-673.
- Hein, J. R., Scholl, D. W., Barron, J. A., Jones, M. G., and Miller, J., 1978, Diagenesis of late Cenozoic diatomaceous deposits and formation of the bottom-simulating reflector in the southern Bering Sea. *Sedimentology*, v. 25, p. 155-181.
- Hottman, C. E., and Johnson, R. K., 1965, Estimation of formation pressures from log-derived shale properties. *Journal of Petroleum Technology* (June 1965), p. 717-722.
- Hottman, C. E., Smith, J. H., and Purcell, W. R., 1979, Relationship among earth stresses, pore pressure, and drilling problems, offshore Gulf of Alaska. *Journal of Petroleum of Technology*, v. 31, no. 11, p. 1477-1484.
- Hunt, J. M., 1990, Generation and migration of petroleum from abnormally pressured fluid compartments. *American Association of Petroleum Geologists Bulletin*, v. 74, no. 1, p. 1-12.

- Isaacs, C. M., Pisciotto, K. A., and Garrison, R. E., 1983, Facies and diagenesis of the Miocene Monterey Formation, California: A summary. *In* Siliceous deposits in the Pacific region, A. Ikjima, J.R. Hein, and R. Seiver, eds. *Developments in Sedimentology*, no. 36. New York: Elsevier, p. 247-282.
- Jorden, J. R., and Shirley, O. J., 1966. Application of drilling performance data to overpressure detection. *Journal of Petroleum Technology*, v. 18, p. 1387-1394.
- Mann, D. M., and Mackenzie, A. S., 1990, Prediction of pore fluid pressures in sedimentary basins. *Marine and Petroleum Geology*, v. 7, p. 55-65.
- McClure, L. J., 1977, Drill abnormal pressure safely. Manual for a short course offered by the author. Houston.
- Micropaleo Consultants, Inc., 1985a, Amoco OCS-Y-0560 No. 1 George prospect, Navarin basin, Bering Sea, Alaska, biostratigraphic report. Encinitas, California, 3 oversized charts, 35 p.
- Micropaleo Consultants, Inc., 1985b, ARCO OCS-Y-0586 No. 1 Packard prospect, Navarin basin, Bering Sea, Alaska, biostratigraphic report. Encinitas, California, 3 oversized charts, 44 p.
- Micropaleo Consultants, Inc., 1985c, Exxon OCS-Y-0599 No. 1, Redwood prospect no. 1, Navarin basin, Bering Sea, Alaska, biostratigraphic report. Encinitas, California, 53 p.
- Micropaleo Consultants, Inc., 1985d, Exxon OCS-Y-0583 No. 1, Redwood prospect no. 2, Navarin basin, Bering Sea, Alaska, biostratigraphic report. Encinitas, California, 3 oversized charts, 44 p.
- Micropaleo Consultants, Inc., 1985e, Amoco OCS-Y-0719 No. 1, Nancy prospect original hole and sidetrack, Navarin basin, Bering Sea, Alaska, biostratigraphic report. Encinitas, California, 1 oversized chart, 41 p.
- Micropaleo Consultants, Inc., 1985f, Amoco OCS-Y-0673, Misha prospect, Navarin basin, Bering Sea, Alaska, biostratigraphic report. Encinitas, California, 46 p.
- Powers, M. C., 1967, Fluid-release mechanisms in compacting marine mudrocks and their importance in oil exploration. *American Association of Petroleum Geologists Bulletin*, v. 51, no. 7, p. 1240-1254.
- Rehm, W. A., and McClendon, R., 1971, Measurement of formation pressure from drilling data. *American Institute of Mechanical Engineers*, 46th AIME Fall Meeting, New Orleans, October, SPE 3601.
- Ruhovets, N., and Fertl, W. H., 1982, Volumes, types, and distribution of clay minerals in reservoir rocks based on well logs. *SPE/DOE Unconventional Gas Recovery Symposium of the Society of Petroleum Engineers*, Pittsburgh, May 16-18, SPE/DOE 10796, p. 67-87.
- Sherwood, K. W., 1984, Abnormal formation pressure. *In* Geological and operational summary: Navarin basin ARCO COST No. 1 well, Bering Sea, Alaska, R. F. Turner (ed.). U.S. Minerals Management Service OCS Report MMS 84-0031, p. 167-192.
- Turner, R. F., Martin, G. C., Flett, T. O., and Steffy, D. A., 1985, Geologic report for the Navarin Basin Planning Area, Bering Sea, Alaska. U.S. Minerals Management Service OCS Report MMS 85-0045, 156 p.

As the Nation's principal conservation agency, the Department of the Interior has responsibility for most of our nationally owned public lands and natural resources. This includes fostering the wisest use of our land and water resources, protecting our fish and wildlife, preserving the environmental and cultural values of our national parks and historical places, and providing for the enjoyment of life through outdoor recreation. The Department assesses our energy and mineral resources and works to assure that their development is in the best interest of all our people. The Department also has a major responsibility for American Indian reservation communities and for people who live in Island Territories under U.S. Administration.

